Online entrapment of epitope-containing peptides from integrins using immobilized antibodies

Sunniva Furre Amundsen

Thesis for the Master's Degree in Chemistry
Sixty ECTS Credits

Department of Chemistry
Faculty of Mathematics and Natural Sciences

UNIVERSITY OF OSLO

May 2018

II

Online entrapment of epitope-containing peptides from integrins using immobilized antibodies

Sunniva Furre Amundsen

Thesis for the Master's Degree in Chemistry

60 ECTS Credits

Department of Chemistry

Faculty of Mathematics and Natural Sciences

University of Oslo

2018

IV

Abstract

Integrins constitute a group of dimer proteins where some are associated with cancer and metastasis, making them potential biomarkers. Detection of integrins can be challenging due to the high complexity of biological samples and often only low amounts of sample is available. Utilizing the high specificity between an antibody (AB) and the peptide it binds to (epitope), a peptide from a digested target protein can be extracted before analysis. In this work, a mass spectrometry (MS)-based method was developed for online detection of integrin derived peptides. Integrin analytes were α3β1 and αVβ5, which are both associated with cancer and metastasis, and αVβ1 was included as a negative control. Sensitivity and specificity was ensured using commercially available ABs (available for the integrin chains αV, β1 and β5) for entrapment of an epitope-containing integrin peptide, followed by detection using nano-liquid chromatography (LC)-MS. The approach was successful regarding the αV chain, enabling detection in cell samples from brain cancer. The approach was not successful for the other integrin chains, due to either inefficient AB-trapping or other sample-preparation related issues. The implication is that an online AB monolithic column can be used for selective sample clean up for the detection of peptides from integrins. However, sample preparation steps, such as digestion, are crucial and a method that works for one integrin chain does not necessarily work for a different chain.

Preface

The work presented in this thesis was performed at the Bioanalytical Chemistry group at the Department of Chemistry at the University of Oslo from August 2016 to May 2018.

I would like to thank my supervisors for all their help, support and guidance throughout my work; Associate Professor Steven R.H. Wilson, PhD candidate Henriette Engen Berg, Dr. Hanne Røberg-Larsen and Professor Elsa Lundanes. Especially Henriette, for all her help and guidance with the nanopump, protein digestion and cells. I would also like to thank Christine Olsen for teaching me how to make monoliths, and Dr. Ole Kristian Brandtzæg for all his help with monoliths, immobilization, and trapping of peptides. Thank you to Inge Mikalsen for all his help with the pumps and ferrules, to Dr. Helle Malerød for her advice regading deglycosylation, to Professor Lèon Reubsaet for his advice regarding BLAST and to Associate Professor Nikolina Sekulic for her help with Pymol.

A big thanks to PhD candidate Frøydis Sved Skottvoll for all her support and friendship, and for helping me with western blot. And also to the Cell signalling unit at Rikshospitalet for letting me use their space and equipment for western blotting. I would also like to thank everyone from the bioanalytical chemistry group, for being a great and fun group of people. Especial thanks to Stian Kjønnås Solheim and Ramneet Kaur Kular for their friendship during the entire course of my studies.

Lastly, I want to give a huge thanks to my family, especially my parents, for all their love, support and care throughout my studies.

Sunniva Furre Amundsen

Oslo, May 2018

Abbreviations

Abbreviation	Meaning
AB	Antibody
ABC	Ammonium bicarbonate
AC	Alternating current
ACN	Acetonitrile
AGC	Automatic gain control
AIBN	α-α'-Azoisobutyronitrile
BCA	Bicinchoninic acid
BIS-TRIS	2-Bis (2-hydroxyethyl) amino-2-(hydroxymethyl)propane-1,3-diol
BLAST	Basic local alignment search tool
BSA	Bovine serum albumin
C-terminus	Carboxyl-terminus
CRM	Charged residue model
DC	Direct current
dd/MS/MS	Data-dependant tandem mass spectrometry
DDA	Data-dependent acquisition
DMF	Dimethylformamide
DNA	Deoxyribonucleic acid
DPPH	2,2-Diphenyl-1-picrylhydrazyl
DTT	Dithiothreitol
ECL	Enhanced chemilumiscense
ECM	Extracellular matrix
EDMA	Ethylene dimethacrylate
EDTA	Ethylenediaminetetraacetic acid

EIC	Extracted ion chromatogram
ESI	Electrospray ionization
FA	Formic acid
FASP	Filter-aided sample preparation
GBM	Glioblastoma multiforme
GE	Gel electrophoresis
HCD	Higher-energy collisional dissociation
HPLC	High performance liquid chromatography
HSA	Human serum albumin
IAM	Iodoacetoamide
ID	Inner diameter
IEM	Ion evaporation model
Ig	Immunoglobulin
IgG	Immunoglobulin G
IUPAC	International union of pure and applied chemistry
LC	Liquid chromatography
m/z	Mass-to-charge
MA	Mass analyser
mAB	Monoclonal antibody
MOPS	3-Morpholinopropane-1-sulfonic acid
MP	Mobile phase
MS	Mass spectrometry
MS/MS	Tandem mass spectrometry
N-terminus	Amino-terminus
NL	Normalized level
OD	Outer diameter

PAGE	Polyacrylamide gel electrophoresis
PDB	Protein data bank
PEEK	Polyetheretherketone
PM	Plasma membrane
PNGase F	Peptide N-glycosidase F
PRM	Parallel reaction monitoring
RP	Reversed phase
Rpm	Rounds per minute
SDS	Sodium dodecyl sulfate
SEM	Scanning electron microscope
SP	Stationary phase
SPE	Solid phase extraction
TBS	Tris buffered saline
TBS-T	Tris buffered saline in polyoxyethylene (20) sorbitan monolaurate ("Tween")
TICC	Total ion current chromatogram
t_R	Retention time
VDMA	2-Vinyl-4,4-dimethyl azlactone
WB	Western blot
γ-MAPS	3-(Trimethoxysilyl)propylmethacrylate

Definitions

Acquired and copied from

[1]   Cammack, R., T. Atwood, P. Campbell, H. Parish, A. Smith, F. Vella, and J. Stirling, *Oxford Dictionary of Biochemistry and Molecular Biology*. 2nd edition. 2006, Oxford University Press (Acessesd on 01.05.18).

[2]   Harris, D.C., *Quantitative chemical analysis*. 8th ed. 2010, New York: Freeman (p.GL9-GL20).

[3]   Petsko, G.A. and D. Ringe, *Protein structure and function*. Primers in Biology. 2004, London: New Science Press (p.2 and p.52).

[4]   International Union of Pure and Applied Chemistry (IUPAC) Gold Book. https://goldbook.iupac.org/ (Acessed on 02.05.18).

*   Definition made by the author.

Term	Definitions
Activity (in biochemistry)[1]	"The natural or normal functioning of an enzyme, hormone, inhibitor or other agent"
Affinity[1]	"Chemical attraction; the tendency of a chemical substance to combine with, bind to, or dissolve in other chemical substances."
Gradient elution[2]	"Chromatography in which the composition of the mobile phase is progressively changed to increase the eluent strength of the solvent."
In silico[1]	"Made to occur by means of a computer."
In situ*	Procedure performed on site.
In vivo[1]	"Occurring or made to occur within a living organism."
Inhibitor[1]	"Any substance that inhibits an enzymatic reaction."
Ligand[3]	"Small molecule or macromolecule that recognizes and binds to specific site on macromolecule."

Offline*	Procedure performed manually and separately from the analysis system.
Online*	Procedure performed in automated fashion, directly coupled to the analysis system.
Protease[1]	"Enzyme that catalyses the hydrolysis of peptide bonds in a protein."
Residue[3]	"The basic building block of a polymer (…). In proteins, the residues are the amino acids"
Sensitivity[4]	"The slope of a calibration curve."
Signature peptide*	Amino acid sequence which is found in no other protein.
Selectivity (in analytical chemistry)[2]	"Capability of an analytical method to distinguish analyte from other species in the sample."
Specificity (in biochemistry)[1]	"The degree to which an association between two molecular units may be considered unique."

Table of contents

1 Introduction

1.1 Cancer and metastasis

An important part of a cell's division process is the replication of its genetic information, the deoxyribonucleic acid (DNA). If this process, or the process of DNA repair, is unsuccessful, it can lead to a mutation in the new cell. If a cell accumulates several genetic mutations, it can start an abnormal and uncontrolled division that results in a localized growth, called a tumour. The increase in tumour cells, which leads to tumour growth, is called proliferation. When the tumour cells possess the ability to invade surrounding tissue normally inhabited by other cells, the tumour is said to be malignant, or cancerous. This tumour will disturb the normal function of the tissue it invades [1]. A difference between cancerous cells and healthy cells is their protein expression. Proteins that aid in e.g. cell death are underexpressed in cancerous cells compared to healthy ones. Proteins that contribute to e.g. cell survival, proliferation or migration are overexpressed in cancer cells [2, 3]. When cancerous cells migrate away from the primary tumour site and create a new tumour, this is called metastasis. This secondary tumour is then made up of cells from the primary tumour, and not cells from where this tumour is located [4, 5]. Metastasis is found to be the cause of most cancer related deaths [6-8]. Starting cancer treatment early can constrain the tumours chance of spreading. This is an important reason a higher chance of survival is associated with early detection of the cancer [9-11]. Detection of cancerous tumour and metastasis can be done through biomarkers, which are biomolecules that can distinguish cancer cells from healthy cells.

1.1.1 Biomarkers

A biomarker is a molecule found in body fluids or tissues that can be used to detect or measure a biological processes, disease or progress of a treatment [12]. There is a large interest in biomarkers for diagnosing, predicting and understanding both cancer and metastasis [13-15]. By development of accurate and sensitive methods for detection of biomarkers associated with cancer, the disease be diagnosed earlier, increasing the chance of survival. Such methods should be robust and inexpensive to make them trustworthy and viable options for hospitals [9, 16]. *Figure 1* illustrates how biomarkers are used. Blood [17], urine [18] or tissue [19, 20] are

examples of sample matrices, where different compounds that can be used as biomarkers are found, for example proteins (e.g. for diagnosing prostate cancer [21] or breast cancer [22]).
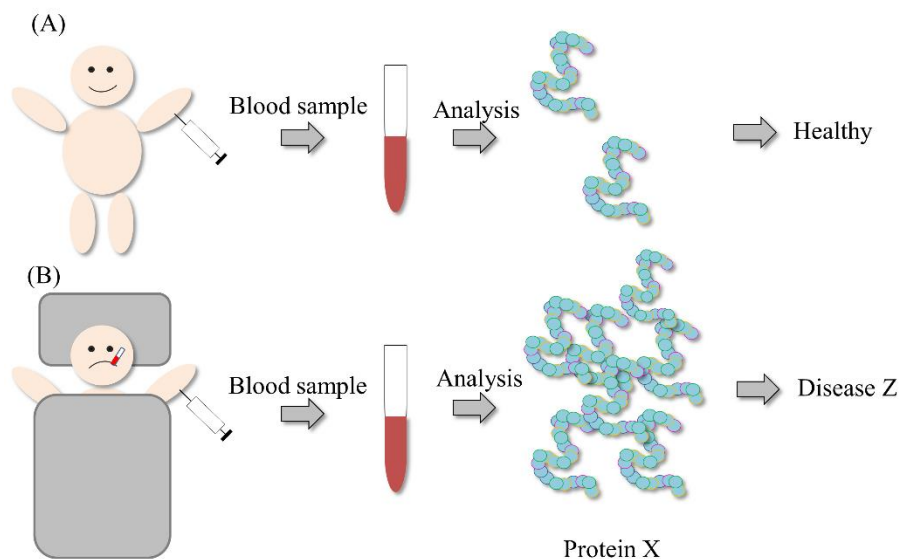
Figure 1: An example of how a biomarker is used. *A healthy person has a certain amount of Protein X (A), while an increase in the amount of Protein X will cause a person to be ill with disease Z (B). If the difference in Protein X can be measured or detected from a blood sample, it can be used as a biomarker for disease Z.*

1.2 Proteins

Proteins are biological polymers encoded by DNA, and are made up of one or more chains of amino acid residues. There are 20 different natural amino acids. Each amino acid can be denoted using a 3-letter code or a single letter code [23], which is given in **Appendix 7.1**. How the amino acids are located in a sequence determines how a protein will fold in physiological conditions. The amino acids are held together via peptide bonds (***Figure 2***), creating a repetitive protein backbone. It is the different side chains on the amino acid residues that generate the great variability of protein structures found in the human body. Side chains can be non-polar or polar, acidic or basic. Different functions in the human body rely on different proteins and a cell's composition of proteins will affect its behaviour [1].
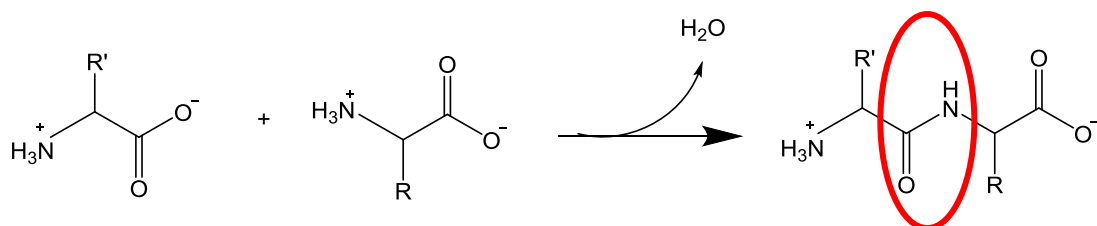
Figure 2: Peptide bond formation. *The circle indicates the peptide bond between two amino acid residues. R and R' represents arbitrary side chains.*

2

1.2.1 Membrane proteins

There is a variety of proteins found in the plasma membrane (PM) of the cell. The PM is a lipid bilayer that encloses the cell from its exterior surroundings, the extracellular space. This space is filled with extracellular molecules, making the extracellular matrix (ECM). Molecules in the PM supervises the exchange of molecules and signals between a cell and another cell, or between a cell and the ECM, and it allows growth and movement of a cell. Some of the proteins found in the PM are transmembrane, meaning they extend across the entirety of the membrane [1]. *Figure 3* illustrates such a protein. The domain of the protein within the hydrophobic PM will also be hydrophobic. A common feature for membrane proteins is that their extracellular domains are glycosylated, meaning they carry one or more sugar groups. This is a type of post-translational modification, which affects a how a protein will fold, its stability and function [24].
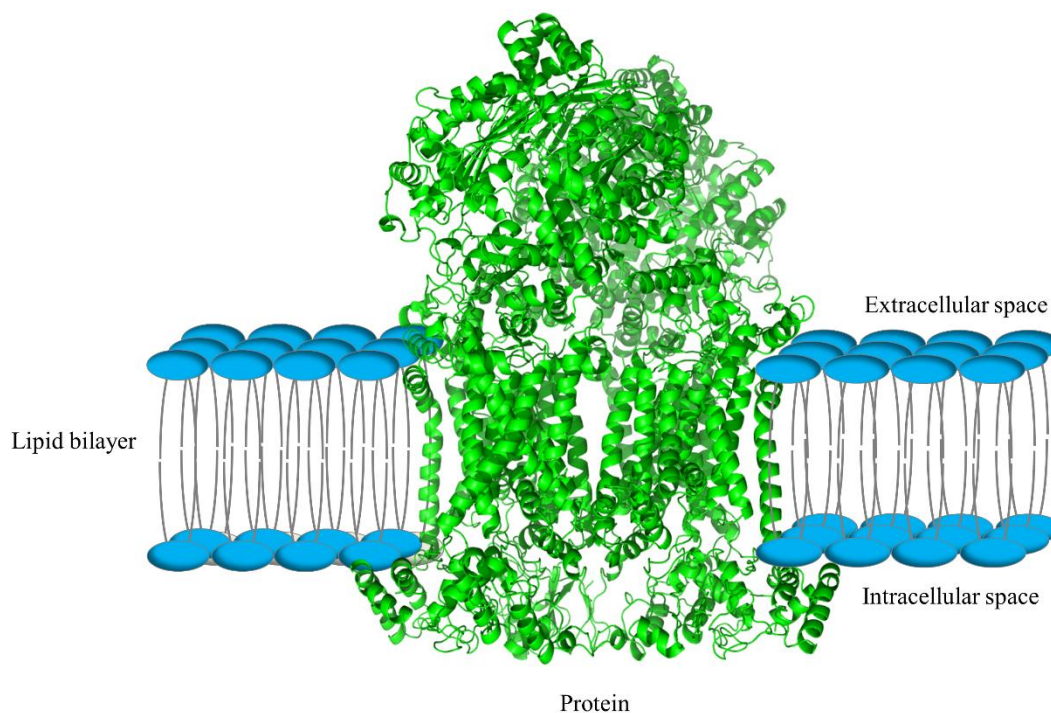
Figure 3: A transmembrane protein. An example of how a transmembrane protein is located within the lipid bilayer that make up the PM. Image made from Protein data bank (PDB) ID 1BGY [25] using Pymol software. Adapted from [26]

Membrane proteins are important for communication in between cells, and between a cell and the ECM [24]. For this reason, some membrane proteins have a role in proliferation and metastasis, and therefore are proteins that can be expressed differently between cancerous and healthy cells. An important group of transmembrane proteins is integrins, which connects the ECM to the cell [1].

1.2.2 Integrins

Integrins are glycosylated transmembrane proteins [27] found in many different cells [28]. They are heterodimeric proteins, consisting of one α- and one β-chain non-covalently bonded. There are 18 α-chains and 8 β-chains, which are made up of about 1000 and 800 amino acids each, respectively. The two chains combine to make up 24 different integrins in humans, which are shown in *Figure 4*. These 24 have various binding properties and distribution, but overlaps in traits do occur between different integrins [28].
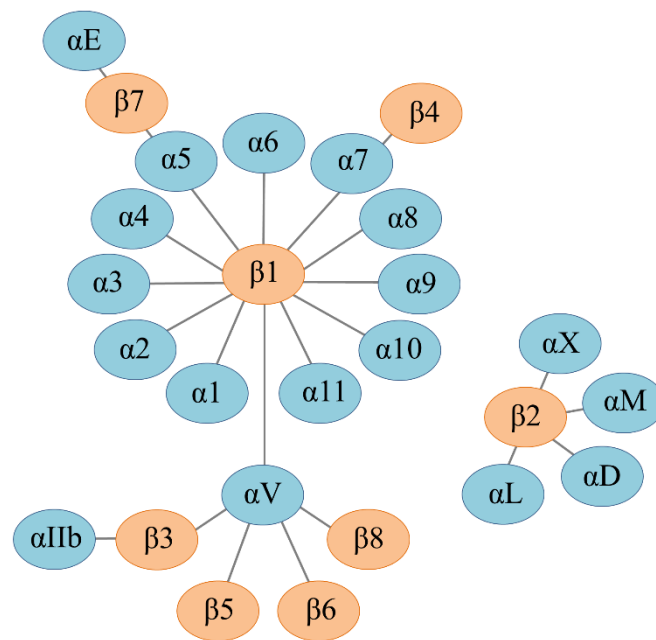
Figure 4: The 24 integrins found in humans. *The different combinations of one α and one β chains making up the 24 integrins found in humans. Adapted from [28].*

Integrins are signal receptors that bind to ligands in the ECM and are involved in a variety of cell processes like cellular communication, proliferation, migration and survival. Integrins have two conformations, called the "active" (or "open") and the "inactive" (or "bent") conformations (*Figure 5*). In the inactive conformation, the extracellular domain is bent, with the extracellular ligand binding site directed towards the PM. An integrin goes into its active conformation through ligand binding, at either its intracellular- or extracellular domain [28]. Most of an integrin (about 93% of its total amino acids) is located in the extracellular space, 3% is in the PM and 4% is intracellular [29, 30].
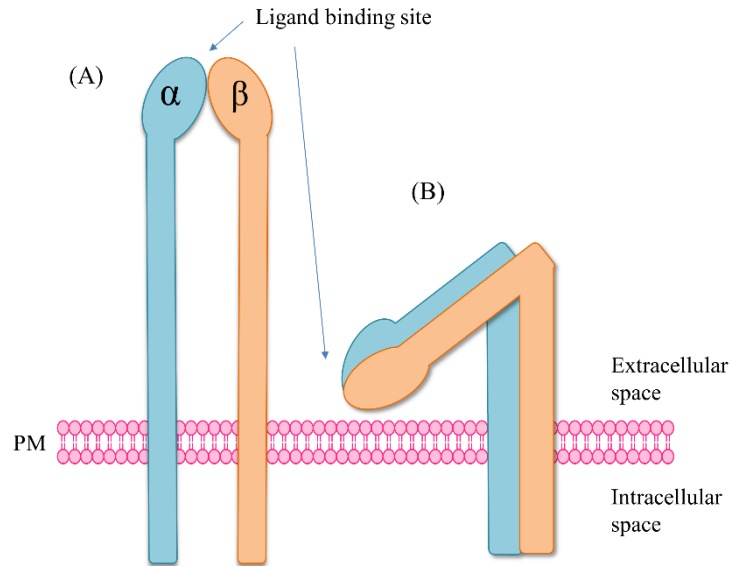
Figure 5: An integrin in the PM. *A: the active, outstretched conformation. B: the bended, inactive conformation. Adapted from [28].*

Integrins can through their role in cellular processes be a contributor to the progression and metastasis of cancer [31]. It follows that some integrins show different expression between healthy cells and cancerous cells [32], and some have also been found to be indicators of potential metastasis sites (***Table 1***). It should be noted that this is not a comprehensive list, and the role of integrins in cancers is still being researched.

Table 1: *Examples of integrins related to various types of cancer, and if this integrin is associated to metastasis of the cancer to a particular site in the body.*

Integrin	Cancer type	Associated metastasis site
α3β1	Expressed in most tumour cells [33]	
α6β4	Breast	Lung [34]
α9β1	Colon [33]	
αVβ3	Melanoma [33]	Lymph node [35]
	Breast	Bone [36, 37]
	Prostate	Bone [38]
	Pancreatic	Lymph node [39]
	Glioblastoma multiforme (GBM) (brain cancer) [40]	
αVβ5	GBM [40]	Liver [34]
	Breast [41]	
	Lung cancer [42]	Bone [37]
αVβ6	Cervical [43]	
	Colon [44]	
	Prostate [45]	

Hence, integrins are targets in cancer-drugs and therapies [46, 47], and have the potential to work as biomarkers for cancers and metastasis.

1.3 Proteomics

Proteomics is the study of the proteome, which is the proteins expressed in a cell, tissue or biological system at a given time [48]. When the focus is on one or more specific proteins in the system (e.g. integrins), the term "targeted proteomics" is used [49]. The purpose of a targeted proteomic study can be examining the proteins interactions or function in a system or the proteins's role as a biomarker (e.g. [21]). Various analysis techniques are used in proteomics, and the two most common methods are western blot (WB) and mass spectrometry (MS)–based proteomics. MS can be used for both targeted and untargeted proteomic studies. WB, like many other targeted proteomic techniques, use antibodies (ABs) to interact with a target protein.

1.3.1 Antibodies

ABs, also called immunoglobulins (Ig), are proteins produced by cells of the immune system as a response and defence mechanism to a foreign substance. The AB recognizes and binds to specific target molecules, called antigens. Antigens can be various molecules, e.g. proteins. The binding between the AB and the antigen can be a marker for destruction or block the antigens functionality. The most abundant, and simplest, AB is a Y-shaped molecule, called immunoglobulin G (IgG) [50]. In *Figure 6* the basic structure of an IgG is shown. It is made up of two "heavy" polypeptide chains and two "light" polypeptide chains. The largest part of the AB is constant between all ABs, whilst the region at the outer ends vary greatly. It is at these two regions the AB will create a specific binding site to the antigen [24]. This site is called the "paratope", whilst the site of the antigen that binds is called the "epitope" [51]. Hydrogen bonding, electrostatic- and hydrophobic interactions all contribute when an AB and an antigen bind [52].
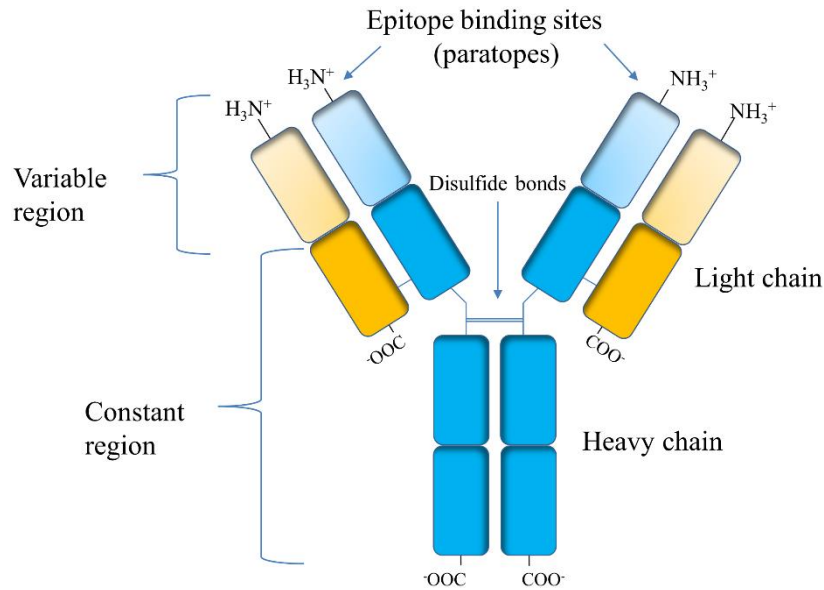
Figure 6: An IgG AB. *An AB is made up of four polypeptide chains, two identical heavy chains that each are covalently bonded through a disulfide bridge to identical light chains. It has a constant region, which is identical between IgGs, and a variable region. It is in this last region where an epitope will bind, and the amino acid sequence in this part of an AB varies between ABs. Adapted from [24].*

Some ABs recognizes linear epitopes, others a conformational epitope. A linear epitope is a group of sequential amino acids, usually between 5-15 amino acids long. A conformational epitope will consist of amino acids that are close together in space from how the protein is folded in physiologically conditions [51]. Polyclonal ABs are ABs that recognise multiple epitopes on a specific antigen, whilst monoclonal antibodies (mABs) will only bind to one specific epitope of an antigen. This trait comes from the fact that mABs are produced by clones of one unique parent cell [53], while polyclonal ABs are secreted by different cell lineages. Both types of ABs are utilized in various fields like therapy, diagnostics and in the study of proteins (e.g. WB).

1.3.2 Western blot

WB is a semi-quantitative technique for targeted proteomics that utilizes the binding between an AB and a target protein for detection. Denatured proteins in a sample are first separated from one another through gel electrophoresis before binding to ABs [54]. In targeted proteomics, selectivity is important. In western blot, selectivity is achieved by first a separation of the proteins in a sample based on size and then the high specificity of binding between a target protein and an AB.

Gel electrophoresis, immunolabeling and visualization

Gel electrophoresis (GE) is the separation of molecules by an electric field applied to a gel.

Charged molecules in this gel will move through the gel and the speed at which they move is dependent on their size and charge. This movement creates bands of proteins through the gel. These bands can be transferred, or "blotted" to a membrane. ABs specific to any protein of interest is then introduced onto the membrane and bind to their target protein (***Figure 7***). This AB is referred to as the primary AB. For detection, a secondary AB which can bind to the primary AB and carry a substrate able to produce a detectable signal (e.g by creating a chemiluminescent signal) can be used [55]. This is called WB.

Figure 7: The concept of WB. *The target protein is transferred to a membrane after GE, and a primary AB will attach. A secondary AB, specific for the primary AB attaches and holds a group that is able to create a detectable signal.*

1.3.3 Antibody specificity

WB, and other AB based proteomic methods, relies on the AB being specific towards its intended protein and that no other protein will bind to it. However, cross reactivity does occur and ABs made in separate batches can show a difference in performance and specificity. This has led to what has been referred to as a "reproducibility crisis" [56]. So despite WBs ability to provide good sensitivity, the inaccuracy that can arise from potential cross reactivity of ABs can create a need for a more reliable analytical method. The reliability issues [57, 58] and the challenge for automation of WB can give need for different analysis techniques. An alternative method, which does not rely on AB specificity, is fully quantitative and more easily automated, is MS-based proteomics [59].

1.4 Mass Spectrometry

In an MS, ions are identified by their mass-to-charge ratios (*m/z*). First, gaseous ions from an ion source enters the ion optics where electrodes guide them into a mass analyser (MA). Here, the ions are separated based on their *m/z* values. Different MS-instruments obtain this separation through different methods. Examples of MS-instruments are; time-of-flight, quadrupole, ion trap and Orbitrap [60]. The detected *m/z* values give rise to a mass spectrum, which gives the intensity of the ion signal against the measured *m/z*-value.

An important aspect of an MS is the mass accuracy, which is how close a measured value lies to the true value. Another important feature of MS is how well it can distinguish between close *m/z* values. Mass resolution is given in Equation 1, and is defined by IUPAC as "the observed *m/z* value divided by the smallest difference Δ*m/z* for two ions that can be separated".

$$R = \frac{m/z}{\Delta m/z} \hspace{4cm} (1)$$

Mass resolving power is, as given by IUPAC "a measure of the ability of a mass spectrometer to provide a specified value of mass resolution" [61].

Protein samples are complex with many different compounds that can be close in mass. Because of this, together with the low amounts often available from biological samples, proteomics will benefit from a MS with a high resolution. A high resolution instrument often used in proteomics is a hybrid instrument combining a linear ion trap (quadrupole) and an orbital ion trap (Orbitrap) [62, 63]. Such an instrument is in this work is called a Q-Orbitrap (commercially it is known as the Q Exactive Hybrid Quadrupole-Orbitrap MS).

1.4.1 The Orbitrap

In the Q-Orbitrap (***Figure 8***), ions from an ion source are transported into a quadrupole MA via ion optics. The quadrupole is made up of four parallel electrode rods. Two rods opposite one another creates a "pair" that will have the same potential. A direct current (DC) and alternating current (AC) is applied between one pair, whilst an opposite DC and AC is applied between the other, creating an oscillating electric field. For specific values of AC and DC, only ions of a particular *m/z* value will obtain a stable trajectories through the rods [64]. So at a given point in time, only ions of one *m/z* value passes through the quadrupole and all other ions in the MA

at that time are lost. Over a time window, the quadrupole is set to pass through a range of masses (mass range). From the quadrupole, the ions are sent to an ion-trap, which consists of four electrodes with a radio frequency field. The electrodes are curved in the shape of a "c", giving rise to its name; the C-trap. The ions are tapped by the radio frequency field, and relaxed through collision with nitrogen gas, before they are injected into the Orbitrap. The purpose of the C-trap is to inject the ions into the Orbitrap in one small packet with appropriate kinetic energy [63]. In MS mode, they are sent directly into the Orbitrap MA from the C-trap for separation and detection. With tandem MS (MS/MS) mode they are fragmented in a collision cell prior to detection.

The orbital ion trap (Orbitrap) is the second MA, in which the ions are separated and detected. It is a high resolution MA where ions are trapped by an electrostatic field between a central and an outer electrode. This field causes the ions to orbit around and along the axis (axial oscillation) of the central electrode. Ions are detected via an image current. This is an opposing current, which is induced in the outer electrode when ions oscillate from one half of the Orbitrap to the other. The current is due to attraction between the ions and electrons in the outer electrodes. Axial oscillation is dependant to the *m/z* value of the ion, so ions with different *m/z* values will induce image current with different frequencies. The observed signal will be the sum of all current frequencies from all the different *m/z* values in the Orbitrap. Through a Fourier transformation, this detected signal is decomposed into its component frequencies. A mass spectrum can be generated from these frequencies since, as mentioned, the axial oscillation frequency is *m/z* dependant [60, 65].
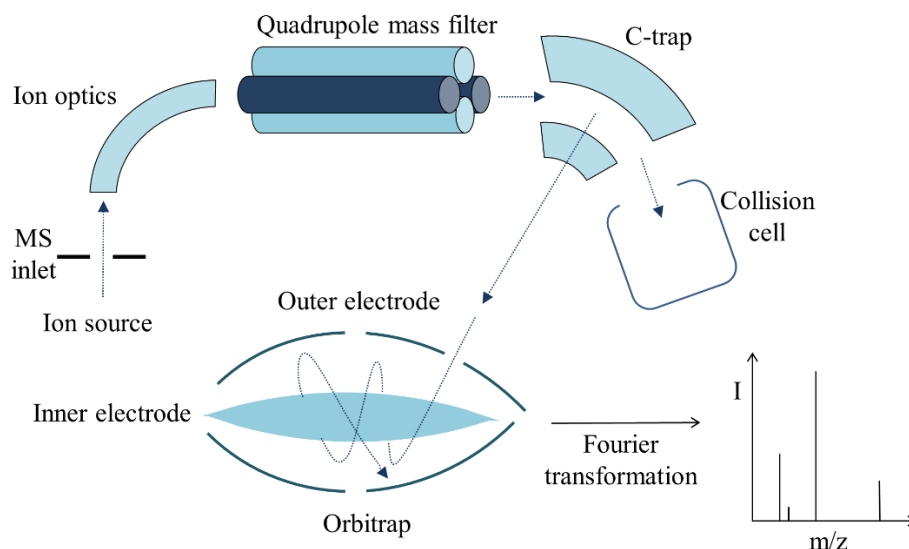
Figure 8: The central parts of the Q-Orbitrap. Ions from an ion source are guided into the quadrupole through an ion beam guide. The m/z values allowed through the quadrupole are guided to a C-trap. From here, they are either injected into the Orbitrap directly, or fragmented in the collision cell and sent back into the C-trap and the fragment ions are injected into the Orbitrap for separation and detection. Adapted from [60].

1.4.2 Tandem mass spectrometry

MS/MS is a process in which a specific *m/z* value, a precursor ion, is "selected" and fragmented into several product ions that is detected [61], this can be achieved by coupling two MAs in series (e.g. a quadrupole and an Orbitrap). The selectivity achieved from an MS/MS method can lead to an increase in the sensitivity, as fewer ions that can create background noise will be detected [66]. When operating the Q-Orbitrap in MS/MS mode, the ions are transferred from the C-trap to a higher-energy collisional dissociation (HCD) cell where the ions are fragmented via collisions with nitrogen gas. The fragments are sent back to the C-trap and injected into the Orbitrap for detection [67].

MS measures ions in the gas phase. It is therefore necessary to implement an interface (an ion source) to convert the analytes in a liquid biological sample into gaseous ions before entering the MS. In proteomics, the electrospray ionization (ESI) interface is often used.

1.4.3 Electrospray ionization

ESI is a soft ionization technique, meaning little fragmentation of the ions occurs before they enter the MS. It is used when the analytes are polar and can be ionized by adjusting the pH in the solvent [68-70]. Usually in MS, the detected signal will be proportional to mass flow

(number of molecules per unit time) i.e. MS is a mass sensitive detector. However, when using ESI the MS acts as a concentration sensitive detector [71].

In ESI, the liquid sample enters a capillary where a high voltage (e.g. 2-3 kV) is applied at the end. By having the analytes charged when they enter the capillary this voltage will cause a gathering of ions at the end of the outlet creating a Taylor cone. In "positive mode" this is achieved by the applied voltage and the analytes both being positively charged. A highly charged jet will emerge from the cone tip, and break up into droplets due to repulsion between charges [68]. In *Figure 9* the mechanism of formation of gaseous ions in the ESI is shown. There are two different theories regarding this formation; the charged residue model (CRM) regarding macromolecules [72] and the ion evaporation model (IEM) for small compounds [73]. In the CRM model, the droplets will undergo fission that continues until only droplets with one ion remains. Solvent evaporation will cause the ion to become gaseous. In the IEM model, a single ion droplet will be sent out from a larger droplet due to repulsive forces between the ions, and then become gaseous due to solvent evaporation. The MS inlet acts as the counter electrode to the capillary outlet, and the charged ions will be attracted towards it, thereby entering the MS.
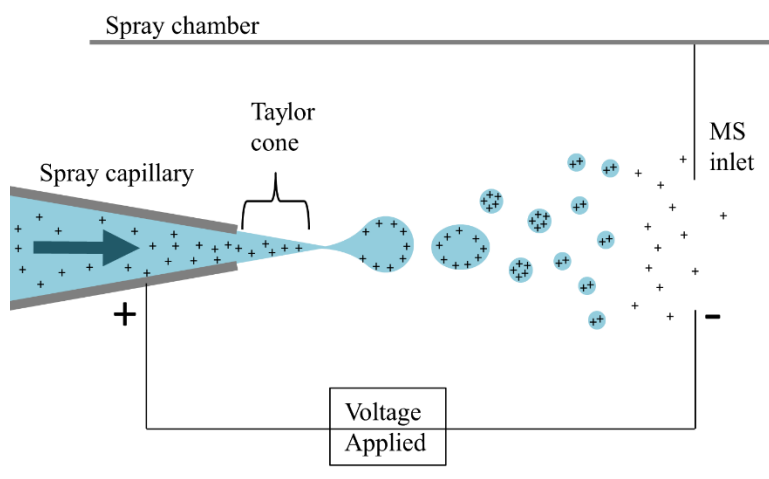
Figure 9: The electrospray ionization source in positive mode. A high voltage is applied to create an electric potential between the spray capillary and the MS inlet. The eluent containing the MP and protonated analytes forms a Taylor cone at the end of the capillary due to this potential. Adapted from [74].

An issue connected with ESI is ion suppression; a suppression of an analytes signal due to the sample matrix negatively affecting the efficiency of ionization. It arises when other species in a sample and the compound of interest compete for the ionization after exiting the spray capillary [75]. A way of minimizing ion suppression is using nano-ESI, which was introduced as a means of dealing with the often low analyte concentrations available in biosamples [69].

12

In this technique, a lower flow rate (nL min^{-1}) and smaller ID of the electrospray capillary (µm scale) are used compared to that of standard ESI. These two modifications reduce the dimensions of the Taylor cone and the droplets it produces. When the droplet size is reduced, the efficiency of desorption increases. Thereby increasing the ionization efficiency, giving less ion suppression. This means that more analyte can reach the entrance to the MS, increasing the sensitivity, which is beneficial when working with protein analytes in biological samples [76].

1.4.4 Mass spectrometry based proteomics

The MS is frequently used in proteomics as it is able to provide great selectivity and sensitivity, particularly due to the ability to perform MS/MS [77, 78]. There are two different methods for approaching analysis in MS-based proteomics; top-down and bottom-up. In top-down, intact proteins are brought into the MS where they are fragmented and analyzed. For the more common method, bottom-up, the proteins are broken down via proteolytic digestion into peptides prior to fragmentation in the MS and the peptide is the precursor ion in MS/MS [79].

Proteolytic digestion

Proteolysis is the digestion of a protein into smaller peptide chains through hydrolysis of its peptide bonds. This is a process catalysed by a proteolytic enzyme, a protease. Different proteases will have a different specificities, meaning they will cleave peptide bonds following specific amino acids [80]. The reasons for bottom-up (*Figure 10*) being the more common of the two methods is firstly, the obtainable signal intensity. A peptide will have fewer ionizable groups than a protein, limiting the number of charges (z) it can obtain compared to a protein. Each new z value from a given mass is detected as a separate signal in the MS. So, a higher number of possible z values (e.g. 20) can give an increased number of signals, which then will be of lower intensity than if a given mass only has a few possible z value (e.g. 2). Also, the many possible modifications of proteins creates more complex MS spectra. Lastly, the MS will obtain sequence information of a shorter peptide more efficiently than from a whole protein [70].

(○ amino acid residue)
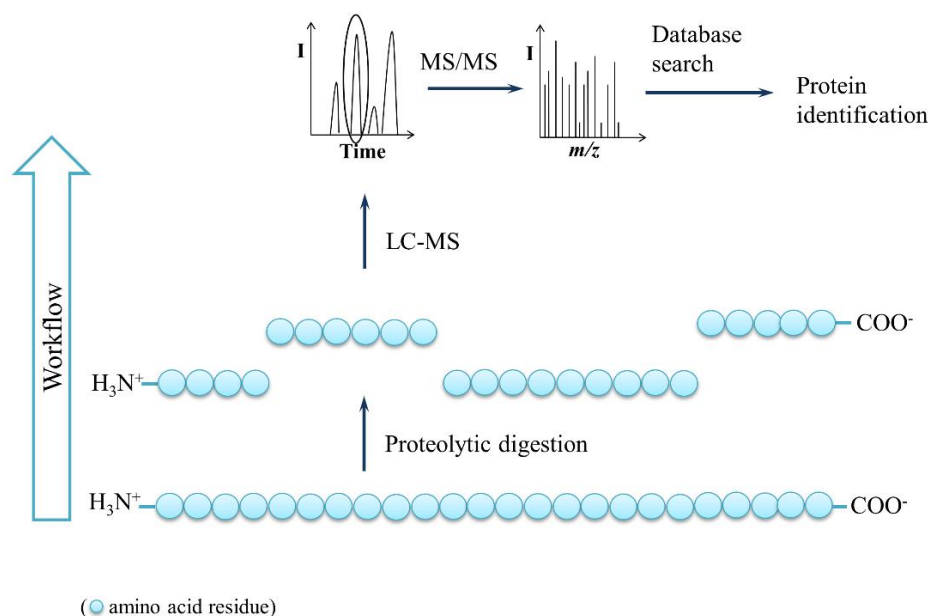
Figure 10: Bottom-up MS-based proteomics workflow. Through proteolytic digestion, a protein is broken down to its constituent peptides. These are introduced into an LC-MS system. Further fragmentation of the peptides and comparison of theoretical fragmentation spectra via computer programs of peptides can lead to protein identification. Adapted from [81]. See **Section 1.5** *for further explanation of LC.*

Digestion of proteins can be done in-gel, in-solution or in a reactor. The ideal digestion conditions will not be the same for different proteins. Hence, there is no optimal, universal digestion procedure [82] and it is also important that reagents used in the digestion step do not interfere with the subsequent MS analysis.

Extraction

Prior to proteolytic digestion proteins have to be extracted from the cells (including the PM and intracellular membranes), which is achieved by opening the cell membranes by disrupting the membrane molecules. This disruption can be done through sonification or, using enzymes or chemicals. Extraction (and digestion) of membrane proteins can be challenging because they often have large hydrophobic domains (the area found in the PM), and these will easily precipitate at the conditions used for tryptic digestion [83]. For this reason, detergents can be added. These are molecules with both hydrophilic and hydrophobic groups. One part of the detergent can bind to the hydrophobic chains of the proteins and extract them from the membrane, while still being soluble due to their hydrophilic domain. The detergent sodium dodecyl sulfate (SDS, *Figure 11A*) is an ionic detergent and is considered to be the most efficient at solubilizing membrane proteins. Because of how this detergents interact with proteins, it can sterically hinder proteolytic digestion [84]. Also, the ionic nature of such a detergent, makes them problematic for MS experiments, as the detergent can supress the analyte signal. Hence, non-ionic detergents (*Figure 11B*) are more applicable for MS-based

14

proteomics. In addition, they do not interact with the protein in a way that sterically hinder proteolytic enzymes [84, 85].
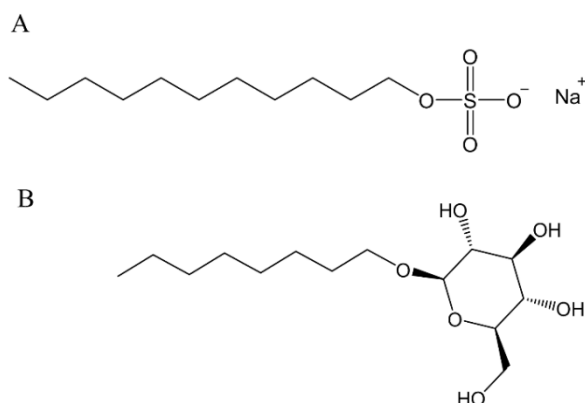
Figure 11: Two different detergents. *A: SDS, an ionic detergent. B: octyl β-D-glucopyranoside, a non-ionic detergent.*

Denaturation, reduction and alkylation

It is important that the protease has access to the cleavage site, so first, the protein is denatured i.e. unfolded. For in-gel digestion approaches the proteins are subjected to heat before a GE, whilst for in-solution digestion, a chaotropic agent is usually added. This chaotropic agent stabilize the unfolded protein by weakening the hydrophobic effect, an important factor in protein folding [86]. Another step performed to ensure that the protease can access the cleavage site, is a reduction to break disulfide bridges (a covalent bond between the thiol (-SH) group on two cysteine side-chains) that arise in a reducing environment. In the reducing process, the disufide bridge is reduced to form the free thiol groups of the cysteine side-chains [87].

Figure 12 illustrates the reduction process with dithiothreitol (DTT). In order to avoid re-oxidation of the reduced thiol groups, the SH-groups are alkylated using e.g. idoacetamide (IAM). This forms a thioether, which is less reactive than the thiol group [88]. ***Figure 13*** shows the reaction mechanism for the alkylation of the thiol group with IAM.
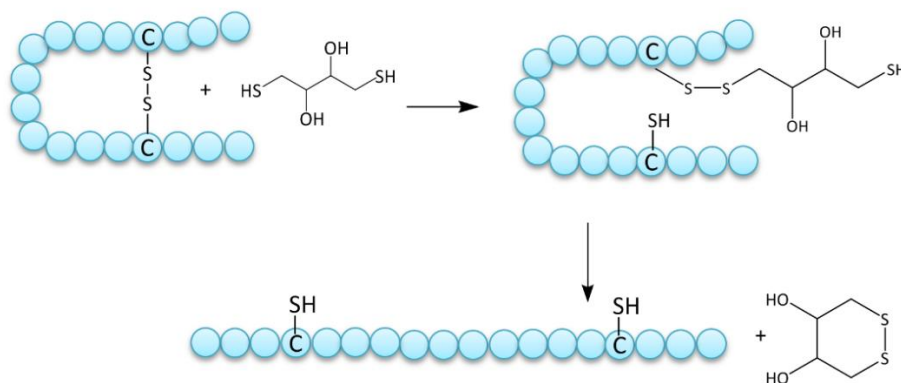
Figure 12: Reduction of a disulfide bridge. *The reaction takes place via DTT, a reducing agent and results in free thiol groups on the protein. Adapted from [89].*
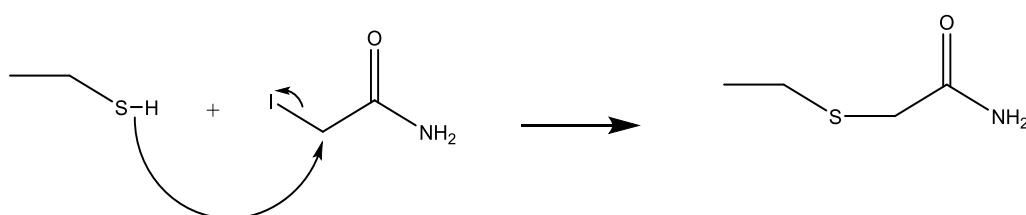
Figure 13: Alkylation of a thiol group with IAM. *This reaction ensures that the disulfide bridge reforms between cysteine residues. Adapted from [90].*

Digestion

Trypsin is usually the protease of choice in bottom-up proteomics. It cleaves a protein at the carboxyl-terminus (C-terminus) of arginine (Arg or R) and lysine (Lys or K), both basic residues. This is illustrated in *Figure 14*. However, miscleavages do occur and whilst some are predictable e.g. if R or K is followed by a proline [91], random miscleavages also do occur [92]. The activity of trypsin is greatest at a pH between 7 and 9 [93].
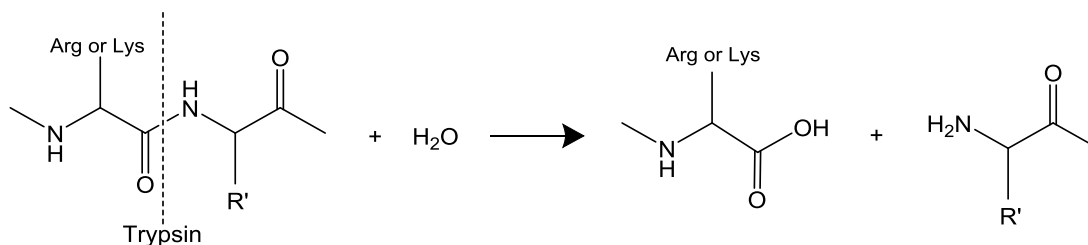
Figure 14: Hydrolysis of a peptide bond with trypsin. R' represents a random amino acid residue except for proline.

Trypsin is used in MS-based proteomics for several reasons. Its cleavage specificity usually gives peptides with no more than 20 amino acids. This puts the resulting peptides within the preferred mass range of the MS for efficient fragmentation in MS/MS. Its high efficiency

16

minimizes the potential complexity of peptide samples, giving few unexpected missed cleavages between the individual proteins, and the resulting peptides will have basic C-terminus residue. This basic residue ensures that the peptide is charged, and detectable with MS [91, 92]. In MS-based proteomics, the peptides are identified through database searches of the obtained MS/MS spectra.

1.4.5 Peptide identification

Two different modes of MS/MS are used in proteomics; data-dependent acquisition (DDA) mode and parallel reaction monitoring (PRM). In DDA mode, a full scan is performed first and a fixed number of the most abundant ions (giving the highest intensity) is "chosen" automatically as precursor ions and are fragmented and detected. This gives data-dependant MS/MS (dd/MS/MS) [61]. With PRM, the precursor ions are defined in the method and only these ions are fragmented and detected [94]. Hence, PRM is a targeted MS/MS method, whilst DDA creates an untargeted MS/MS mode.

When using the HCD-cell for fragmentation mainly the peptide bond in the backbone is broken. The peptide backbone can fragment at three different places, and the nomenclature for the possible resulting fragments can be seen in *Figure 15* [95-97]. HCD-fragmentation usually results in b-ions or y-ions, depending on if the charge is retained on the C-terminus or amino terminus (N-terminus) side [70, 98]. Through computer programs these fragments can be used to find the amino acid sequence of the precursor peptide, and from such information from multiple peptides, a protein can be identified.
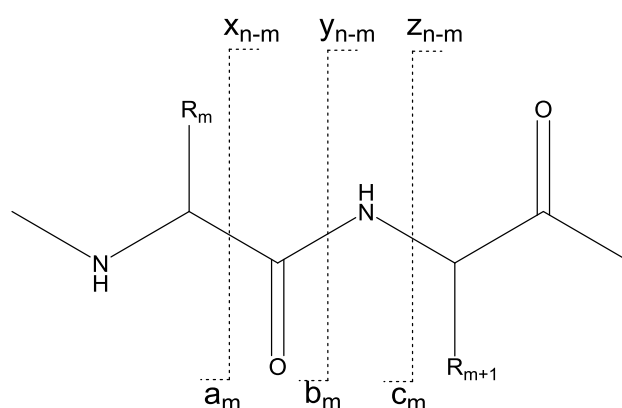
Figure 15: Fragmentation of a peptide. The fragments a_m, b_m, or c_m are named sequentially from the initial N-terminus, where "m" denote the number of amino acids side chains the fragment contain. Fragments x_{n-m}, y_{n-m}, or z_{n-m} are named sequentially from the initial C-terminus. "n" is the total number of residues in the protein so "n-m" gives the total of side chains in these fragments.

Bioinformatics

MS-based proteomic studies generate large amounts of data, and interpretation of mass spectra is done through various available data processing tools [99]. Different computer programs exist to interpret fragmentation spectra for protein identification. One of these are SEQUEST [100], and the process is illustrated in *Figure 16*. First, a list of peptides that would result from digestion of given proteins is created, using a given protease, *in silico*. Secondly, the SEQUEST algorithm then compares the theoretical MS/MS spectrum of a peptide to an experimentally obtained fragment spectrum. The program will then give a correlation score for each identified peptide. This correlation gives an indication of how well the experimental and theoretical fragmentation spectra for a peptide correlate, where 0 implies no correlation. A total score is also provided, reflecting how well all the MS/MS data of the peptides fits a given protein, where 0 is the lowest score [101, 102]. The program also gives a coverage factor which tells how much of the entire protein was identified.
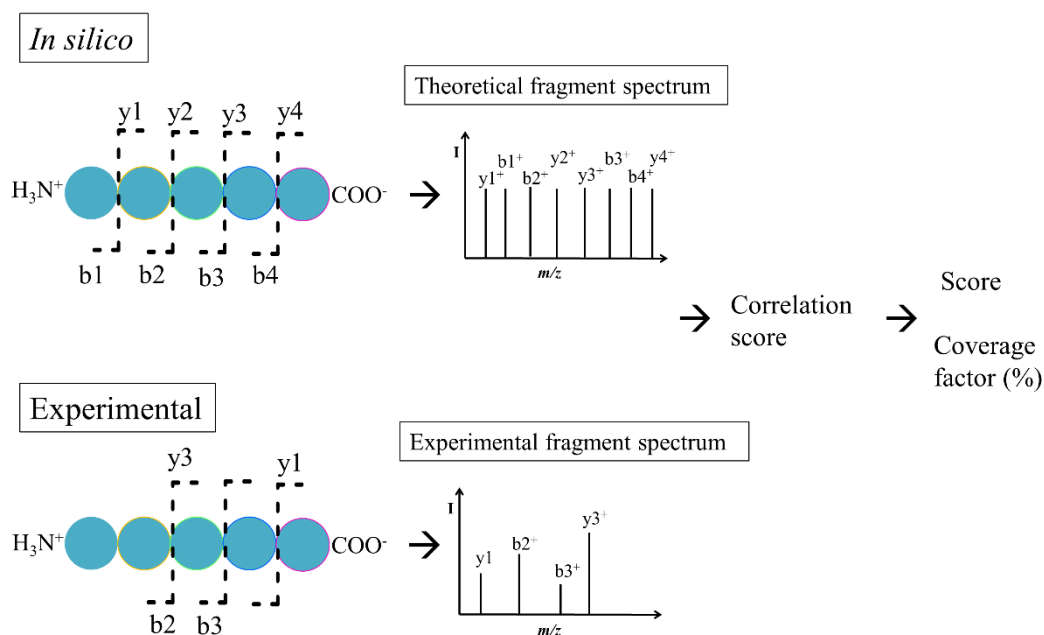
Figure 16: Proteomic data processing. After an in silico digestion and fragmentation of target proteins this can be used to identify experimentally analyzed peptides. Shown here is how the fragmentation spectrum of one experimentally acquired peptide and an in silico acquired peptide may compare. How well the two fragmentation spectra overlap give rise to a correlation score. By assessing the correlation scores for all the peptides the database search could find fragments from, a total score is given. A coverage factor that tells how much of the protein the search was able to "find" is also provided.

In comprehensive studies, the obtained spectra are searched against those of the proteins found in a certain organism from a database. For targeted, the specific proteins amino acids sequence can be given to the program through a given FASTA-file, a text based file format for

representing a peptide sequence. So for integrins, which is made up of two polypeptide chains, one FASTA-file will only represents either an α- or a β chain.

For a secure identification of a protein, a key aspect is to have identified a peptide unique to that particular protein, a signature peptide [103]. Whether or not a given amino acid sequence can only be found in one particular protein can be determined using the algorithm Basic Local Alignment Search Tool (BLAST), which can find similarities between biological sequences (e.g. amino acid sequences).

In order to detect as many peptides as possible, it is useful not to introduce all of them at once into the MS. There are different reasons for this being disadvantageous. It will give rise to excessive ion suppression, which the nano-ESI is able to reduce, but not completely remove. An MS will have a given scan rate to go through the set mass range. At one point in time only one mass is allowed through. Introducing all the masses at the same time can cause many of the compounds to be lost as the MS has these time constraints. For this purpose, MS-based proteomics is often coupled with liquid chromatography (LC), in which the sample components are separated before entering the MS [70, 104].

1.5 Chromatography

Chromatography is a method for separating different compounds in a mixture. The separation is based on compounds having varying affinity to a stationary phase (SP) situated within a column, causing them to travel through the column at different speeds. If a compound has high affinity to the SP, it will be more strongly retained, and elute from the column later than a compound with low affinity to the SP. A mobile phase (MP), that is either a liquid (LC) or a gas (gas chromatography), is used to introduce onto, and transport compounds through the column. The time passed from a compound is introduced onto a column until it elutes is defined as its retention time (t_R) [74]. Theoretical principles of chromatography is further explained in **Appendix 7.2**.

A chromatogram can be obtained from the MS by plotting the intensity of the ions detected as a function of time. A total ion current chromatogram (TICC) plots the signal from a complete mass spectrum, which is the sum of all the different ion currents from the ions of different *m/z* values, as a function of time. An extracted ion chromatogram (EIC) plots one or a set of chosen

m/z values as a function of time [61]. Chromatograms from MS-detection gives the relative abundance (%) of the peak in the y-axis, and a normalized level (NL) chromatogram gives the peak with the highest intensity, in a selected time window, at 100%.

1.5.1 Reversed phase liquid chromatography

There are several different separation principles used in LC. The most common is reversed phase (RP), which is a principle often used in proteomics. Here, the SP is nonpolar carbon chains bonded to particles, which is illustrated in *Figure 17*. The separation of peptides will be based on their hydrophobicity. More hydrophobic peptides will interact more strongly with the SP and elute later than less hydrophobic peptides. How hydrophobic a peptide is, depends on the properties of the side chains of its constituent amino acids.
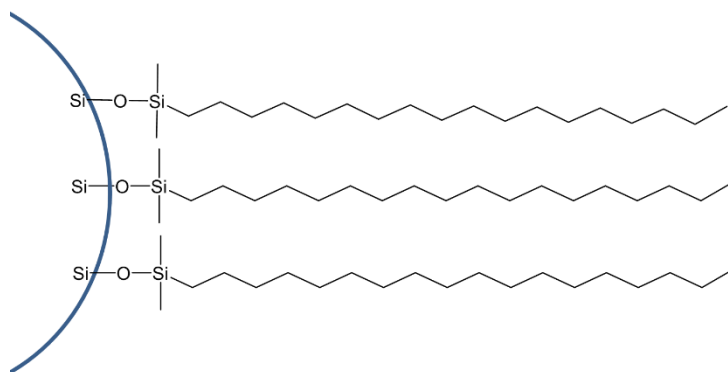
Figure 17: The structure of C18 SP bonded to a silica particle. Adapted from [74].

In RP LC the MP is a mixture of water with water miscible solvents and a pH control. In proteomics, a water/acetonitrile (ACN) mixture is often used as MP with 0.1% formic acid (FA) as pH control. The FA ensures that the peptides are positively charged when entering the ESI and MS, where charge is essential for producing ions in the gas phase and detection. Elution of peptides is done by increasing the amount of organic in the MP, called gradient elution. By comparison, isocratic elution is done by having a constant water/organic ratio, and is used when separating compounds with similar hydrophobicity.

1.5.2 Liquid chromatography columns

In RP LC, the column is typically 50 to 250 mm long and packed with porous particles (often silica based) covalently bonded with the SP. Particles used in LC usually have a diameter between 2 and 5µm. Decreasing particle size will give a more uniform flow through the column

and increases the rate at which a compound equilibrates between the MP and SP, enhancing the efficiency of separation. However, small particles will give rise to a resistance in solvent flow and pumps able to work against this high back pressure are necessary. LC at this pressure level is termed high performance- or high pressure (both giving the abbreviation HPLC). The particles can also be core-shell particles, having a solid core and a thin porous surface layer (0.2 − 0.7 µm) with the SP. These kind of particles provide a higher separation efficiency compared to porous particles under the same chromatographic conditions, and are often used for the separation of macromolecules, like peptides [105]. See **Appendix 7.2.1** for further explanation of increased efficiency from core-shell particles.

Considerations of inner diameter of column for biological samples

Protein samples are often extracted from cells (e.g. tumour cells) or bodily fluids like plasma or saliva. All of these make up complex sample matrices, containing a multitude of different biomolecules and have a high dynamic range of protein concentration [106, 107]. Culturing (growing) cancer cells from patient biopsies has shown to be a challenging and slow process [108-110]. These issues will often lead to smaller sample sizes being available, and the amount of protein available for analysis as well. Protein biomarkers can also be found in extracellular vesicles originating from e.g. cancerous cells [111, 112]. These vesicles can be obtained from a blood sample, which is a less invasive sampling technique compared to a biopsy. However, because of the low concentration of vesicles only a small amount of sample is available [113]. The expected sample size for both of these samples will require analysis techniques that are sensitive. This can be obtained by using columns with a narrow inner diameter (ID) together with a high resolution MS and nano-ESI.

The ID of packed analytical columns in LC ranges from 5 mm down to 0.01 mm. Columns with ID of 1-0.5 mm are called microbore columns and columns with ID of 0.5-0.1 mm capillary columns. LC using columns IDs from 0.1-0.01 mm is termed nano-LC, where the name is related to the nanoliter per minute flow rates typically used with these IDs [114, 115].

1.5.3 Nano-liquid chromatography

In LC ESI MS proteomic studies, nano-LC is often applied for obtaining sufficient sensitivity [116, 117], and nano-LC also gives the added benefits from nano-ESI. A decrease in column ID will be beneficial when using concentration sensitive detectors, as the sample will

experience less dilution (***Figure 18***). ESI makes the MS behave as a concentration sensitive detector. The relationship between column ID and dilution (D) of the analyte is described by Equation 2.

$$D = \frac{\varepsilon \pi r^2 (1+k)\sqrt{2\pi LH}}{V_{inj}} = \frac{c_0}{c_{max}} \qquad (2)$$

Here ε is the void fraction of the column particles, r is the column radius, c_0 is the concentration at injection and c_{max} is the concentration at detection [115].

It follows, that for concentration sensitive detectors, the signal intensity will increase with a decrease in column ID as it will lead to less radial dilution. When comparing two columns the signal increase factor (F) can be found with Equation 3.

$$F = \frac{ID_1^2}{ID_2^2} \qquad (3)$$

Here $ID_1 > ID_2$ [74].
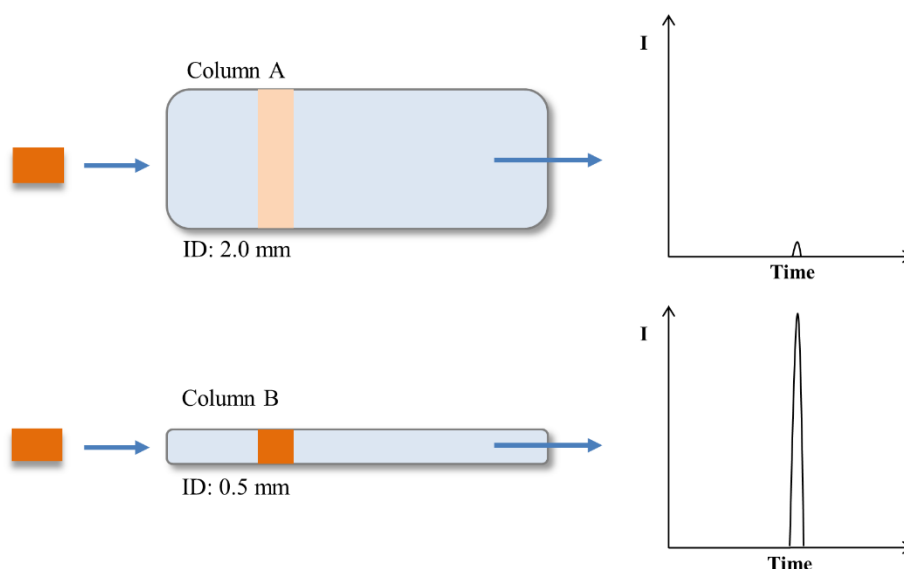
Figure 18: Increase in signal intensity from decrease in column ID. *A signal will be 16 times higher from a column with ID of 0.5 mm than a signal from a column with ID of 2.0 mm if the same sample volume is injected. Adapted from [117].*

A disadvantage with decreasing column ID is the decrease in injected sample volume before overloading the column, creating a broad starting band and compromising chromatographic

performance [118]. Hence, less sample can be injected giving the method a higher detection limit. For solving this, an online pre-column can be used, allowing injection of larger volumes and a focusing of the starting band to be injected onto the analytical column [114, 119].

1.5.4 Pre-columns

Having a pre-column onto which the sample is loaded, before being eluted to the analytical column can allow larger volumes to be injected without producing the aforementioned issues. Also, a pre-column is usually only 3-5 cm long, which produces less back pressure compared to the longer analytical column, allowing faster sample loading (μL min^{-1} vs. nL min^{-1}). The analytes are retained on the SP (as well as other compounds that interact with the SP) in the pre-column, also called solid phase extraction (SPE) column. The anlytes are retaind by being loaded onto the pre-column in non-eluting conditions. Elution of the retained compounds onto the analytical column is done by increasing the elution strength of the MP. Preparation of protein samples use buffered salt solutions, and salts entering the ESI-MS lead to increased ion suppression [120, 121] as well as precipitates and deposits on parts of the MS. When using an RP SPE, salts and other compounds not retained on the hydrophobic SP will elute to waste. Although many interferences can be removed using a pre-column, the sample clean up might not be a sufficient. The RP SP will retain hydrophobic compounds, hence, many compounds from a biological sample will be allowed to enter the analytical column, maintaining the complexity of the sample. And even with a selective high resolution MS/MS detection after a nano-LC separation, the complexity a more extensive and targeted sample preparation could be necessary to obtain the necessary sensitivity.

1.6   Targeted biological sample preparation

Especially in biological samples of small volumes can the complexity and the dynamic range of the protein concentration [106, 107] create issues when it comes to sensitivity and accuracy in analysis. These issues can arise from co-elution of compounds, causing ion suppression, and high noise levels and also prompt long analysis time for sufficient separation and detection [122]. Clean-up steps, as well as the preparation described in **Section 1.4.4**, and separation using chromatography are all necessary prior to MS analysis. For a comprehensive (untargeted) proteomic study of a cellular sample, a GE is common as a fractionation step of the sample, to limit the complexity [123]. When there is one or more known (target) analytes, a more selective

sample preparation is beneficial, removing as much as possible of matrix components. A targeted sample preparation then minimizes ion suppression and noise levels. A way of achieving a sensitive and targeted method can be by combining ABs specificity abilities of binding and the sensitivity of nano-LC-MS.

1.6.1 Immuno-based isolation

A popular form of biological sample clean up for targeted protein analysis is utilizing the high specificity and affinity between a protein and its "designated" AB to isolate and concentrate a specific analyte protein from complex sample matrices [124, 125]. A common method is immunoprecipation, where ABs specific for the analyte are attached to a solid support, usually magnetic beads or agarose (a polysaccharide). Then non-binding components can be washed or removed from the sample while the analyte is held by the AB [126]. ABs can also be immobilized onto a solid support inside a column, where they can "trap" analytes. Here, the ABs work as a SP for extraction of a target analyte, and the target analyte can be eluted off the AB after matrix components have been washed off. This can be called "immunoaffinity SPE", "immunosorbents" or "immunoaffinity chromatography" [127-129]. A solid support that is becoming increasingly popular are monolithic polymers [129].

1.6.2 Monoliths as carrier of antibodies

An alternative to particles as support for the SP is a monolithic structure, which creates a lower back-pressure compared to a column of the same length packed with particles [130, 131]. A monolith is a continuous piece of a porous structure that fills the entire column. *Figure 19* illustrates the inside of a packed column and a monolithic column. Monolithic columns can be used as both pre- and/or analytical column, where the constituent parts of the polymer functions as the SP.
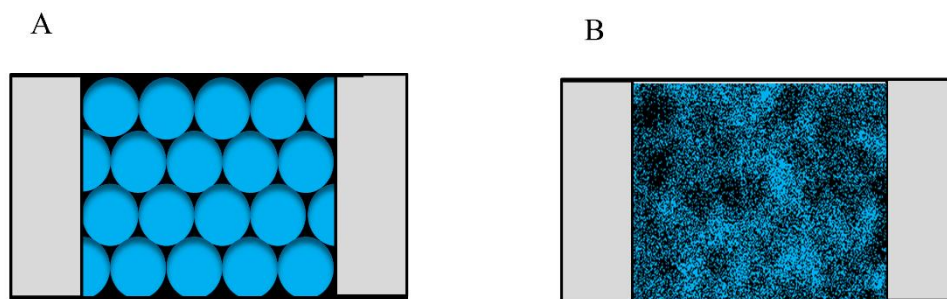
Figure 19: A packed vs monolithic column. A: illustration of how particles are packed within a column. B: illustration of how a monolithic structure may appear within column.

A monolithic column can be organic polymer-based or inorganic (silica)-based [132]. Both organic- and silica-based monoliths have macropores (> 50 nm). The MP flow through these large pores, causing the monolith to generate low back-pressure [133]. A silica-based monolith also has mesopores (2-50 nm) and micropores (> 2 nm) and these smaller pores make silica-based monoliths beneficial for separation of smaller molecules. However, organic polymer monoliths (which has few/no mesopores and micropores) has been found to be better when working with larger biomolecules (e.g proteins and peptides). Other benefits with organic polymer monoliths is an easier preparation process compared to preparation of silica-based and that an organic polymer can maintain its stability at higher pH values compared to silica based support. There is also a wide choice of monomers that can be polymerised and an organic polymer offers easy surface modifications [132]. Such modifications can be immobilization of proteases, making a reactor allowing for online protein digestion [134, 135] or ABs for targeted extraction [136].

An organic polymer-based monolithic column is made by an *in situ* polymerization of organic monomers in a mixture also containing an initiator, a cross-linker, and porogens. Porogens are solvents in which the monomers and cross-linker are soluble, but not the polymer. A good solvent will create large pores in the polymer, a poor solvent will make smaller ones. By a pre-treatment of the inside of capillary, the monolith can become chemically bound to the column wall. The initiator is a radical which triggers the polymerization of the monomers whilst the cross-linker links the polymers together [137]. In **Appendix 7.3**, pretreatment of the capillary and polymerization of an organic polymer monolith is shown.

Adequate mechanical strength of the monolith is important. For this reason, organic monoliths are often methylacrylate-based. To allow surface modification of the monolith these monomers are co-polymerised with other monomers [134, 136]. An example of a common monomer used

for immobilization of biomolecules onto organic monoliths is 2-vinyl-4,4-dimethyl azlactone (VDMA) [134, 138]. An amine (e.g. an N-terminus of an AB) can react with VDMA in a ring opening reaction, shown in ***Figure 20***, thereby covalently attaching the AB (see ***Figure 6***) to the monolith [139].
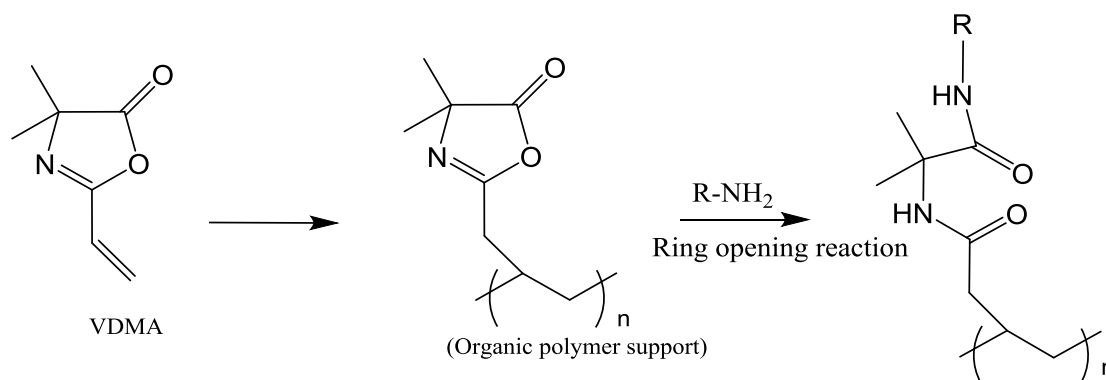
Figure 20: Attachment of amine group to VDMA. *The amine group on an ABs N-terminus can bond to the azlactone group on VDMA, which is covalently boned to an organic-based monolith, in a ring opening reaction. Adapted from [139].*

For trapping a specific protein or peptide with an AB, hydrophobic secondary interactions that can cause unspecific binding between the organic monolith and various compounds in a sample is unwanted. To minimize such interaction the acryl-monomer should be as hydrophilic as possible. A monomer often used for this purpose is ethylene dimethacrylate (EDMA) [135, 140]. See **Appendix 7.3.1** for the structure of EDMA.

Traditionally, immobilized ABs (on any support) are used to isolate intact protein in an offline preparative step prior to further sample preparation (e.g. digestion) and analysis [128, 129]. However, any sample preparation step that can be performed online reduces the possibility for contamination or loss of the sample, is less time consuming and can allow easier automation of the method [119].

1.6.3 Online entrapment of peptides

Procedures performed online with an LC-MS setup, has to use appropriate eluting conditions in regards to the performance of the rest of the system e.g. trapping on an RP pre-column and possible ion suppression. Elution of proteins is usually done by an acidic solution "deactivating" the AB, making the protein detach by disrupting hydrogen bonds and ionic bonds between the antigen and AB [124]. Using a digested protein, where only the epitope-containing peptide will attach, can be beneficial. The binding of only a peptide, and not the entire protein,

can create a lower affinity towards the AB. This will make elution of a peptide easier than elution of a protein. Which also means elution of a peptide can be done faster and with a smaller amount of acid. Less acid can also allow for a more complete regeneration of the ABs [129]. Hence, by trapping only the epitope-containing peptide it can be easier to implement an online immunoaffinity extraction in a bottom-up MS-based targeted proteomic study, without having to use potentially damaging eluting conditions.

When the AB only traps a peptide from a specific protein, it gives a major decrease in the complexity of the sample, as it not only give the opportunity to wash away all the other components in the sample, but also other peptides from the target protein. Such a decrease in complexity can be useful for possibly detecting proteins (e.g. integrins) and small changes in protein concentration from small sample volumes even with lower resolution, and cheaper, MS instruments or other detection instruments. In the last 15 years, the development of such methods has gained popularity [141-143]. Some methods have also removed the LC-step, and directly elute the trapped peptide into the MS [144, 145]. There are commercialized methods that offer antibodies produced for a target signature peptide, such as the stable isotope standards and capture by anti-peptide antibodies (SISCAPA) method [146]. Such antibodies are very expensive and time consuming to generate [147]. Also, ABs grown to target a peptide and not the intact protein, particularly if only a few amino acids in length, can often show a weaker affinity towards its antigen [141, 148].

2 Aim of study

Selective extraction of a target protein from a biological sample prior to LC-MS detection can eliminate issues arising from such a complex sample matrix. Performing this extraction online makes it less susceptible to handling errors and more time efficient. Elimination of the limitations that can arise when only low amounts of biological sample is available (e.g. tumour cells), can be a challenge, but is essential for ensuring that methods are sufficiently sensitive. The hypothesis was that a selective and sensitive system for detection of integrins could be achieved by combining online trapping of tryptic peptides using ABs immobilized in a monolithic column in combination with miniaturized LC and a high resolution MS.

The aim of this study was to develop a method for entrapment of integrin peptides originating from cancer cells in a miniaturized online system using already commercially available mABs. As a part of this, obtaining successful digestion of the target proteins also became a goal.

3 Experimental

3.1 Chemicals

3.1.1 Proteins and reagents

Recombinant human integrins α3β1 and α5βV were purchased from Merck Millipore (Darmstad, Germany) in octyl-β-D-glucopyranoside formulation with concentrations of 0.153 mg mL^{-1} and 0.157 mg mL^{-1}, respectively. Recombinant human integrin αVβ1 (25 µg) was from R&D Systems (Minneapolis, MN, USA). Human serum albumin (HSA), DTT (≥ 99.0%), IAM (≥ 99.0%), trypsin from bovine pancreas, urea (98%), ammonium bicarbonate (ABC) (≥ 99.9%), FA (reagent grade, 95%) and (LC-MS grade 98%), BioXtra sodium phosphate (≥ 99.0%), proteomics grade Peptide N-glycosidase F (PNGase F) and trypsin inhibitor from *glycine max* powder, BioReagent were all from Sigma Aldrich (St. Louis, MO, USA). HiPerSolv LC-MS grade water was from VWR international (Radnor, PA, US). 2,2-Diphenyl-1-picrylhydrazyl (DPPH), N,N-dimethylformamide (DMF) (99.8%) and 3-(trimethoxysilyl)propylmethacrylate (γ-MAPS) (98%), EDMA, α-α'-azoisobutyronitrile (AIBN) (≥ 98.0%), 1-propanol (99.7%) and Reagent Plus 1,4-butandiol (≥ 99%) were all from Sigma Aldrich. VDMA was purchased from Polyscience Inc. (Warrington, PA, USA). ACN (100%), acetone (100.0%) and technical methanol were all from VWR. Analytical grade NaOH pellets (99.0%) and Extra Pure ammonium acetate (≥ 96.0%) were obtained from Merck. Type 1 water was acquired from a Milli-Q® Integral water purification system with Q-POD dispenser (0.22 µm filter) from Merck Millipore. A "frit kit" with Kasil 1624 (potassium silicates/water (29/71(*w/w*)) (SiO$_2$/K$_2$O ratio of 1.65 (*w/w*))) and formamide were both purchased from Next Advance (Averill Park, NY, USA). Solid core silica particles, size 2.6 µm, pore size 80 Å, SP C18 (packed in conventional columns) were from Thermo Scientific (Waltham, MA, USA). N$_2$ gas for column preparation (≥ 99.9%) and in the MS (≥ 99.999%) was purchased from Praxair Norge (Oslo, Norway). Coomassie Brilliant Blue was from Bio-Rad (Hercules, CA, USA). Tris-HCl (pH 6.6), bromophenol blue, SDS, mercaptoethanol, glycerol Trizma® base (≥ 99%), ethylenediaminetetraacetic acid (EDTA) and glycine (≥ 99%, HPLC) were all from Sigma Aldrich. MOPS (3-morpholinopropane-1-sulfonic acid) SDS running buffer (20X) was acquired from Thermo Fischer, non-fat dry milk powder was from PanReac AppliChem ITW reagents (Darmstad, Germany) and Tris buffered saline (TBS) –Tween (TBS-T) tablets from

Medicago (Uppsala, Sweden). PageRuler™ Prestained protein ladder, gels (4-12% 2-bis (2-hydroxyethyl) amino-2-(hydroxymethyl)propane-1, 3-diol (Bis-Tris)) and nitrocellulose membrane were from Thermo Fischer. Acetic acid (99.7%) was from ACROS Organics, which is a Thermo Fischer scientific brand. Enhanced chemiluminescence (ECL)-prime was from GE Healthcare Life Science (Chicago, IL, USA). Primary rabbit monoclonal ABs for integrin chains αV, β1 and β5 were all purchased from Abcam (Cambridge, UK). A mouse anti-rabbit AB from Santa Cruz Biotechnology (Dallas, TX, USA) served as a secondary AB. Pierce™ BCA (bicinchonic acid) Protein Assay Kit was from Thermo Fischer. GBM cells were obtained from Langmoen Lab at Oslo University Hospital, Norway. See **Appendix 7.4.1** more information of the cell culturing. This step was performed at Langomen Lab.

3.1.2 Solutions

Integrin standard solutions

Integrin αVβ1 was dissolved in 160 µL type 1 water (if not stated otherwise, "water" will from now on indicate type 1 water) to give a concentration of 0.156 µg µL⁻¹. αVβ5 and α3β1 were purchased in solution (25 µg each), with concentrations of 0.157 and 0.0.153 µg µL⁻¹, respectively. αVβ5 was solved in a TBS solution with 100 mM octyl β-D-glucopyranoside and sodium azide. α3β1 was solved in Tris-HCl with 100 mM octyl β-D-glucopyranoside and some salts at mM concentrations. The integrin solutions were kept at -80 °C.

In-solution digestion solutions

A 100 mM ABC solution was prepared by dissolving 102.7 mg ABC in water with a final volume of 13 mL. The 10 mM solution was used to make a 50 mM ABC solution by diluting 5 mL 100 mM ABC with 5 mL water. These solutions were stored in 4 °C. A freshly made solution of 6 M urea/100 mM ABC was made by adding 1 mL of 100 mM ABC solution to 360 mg urea. Solutions of 0.5 M IAM, 0.5 M DTT and 10 mg mL⁻¹ trypsin solved in water were made by Henriette Engen Berg, and all kept at -80 °C. Prior to use the trypsin solution was diluted to an end concentration of 0.1 µg µL⁻¹ by diluting 10 µL with 990 µL water (also used for FASP digestion).

DTT, IAM and ABC solutions were also used in both FASP and in-gel digestion, some with further dilutions.

30

Filter-aided sample preparation solutions

An 8 M urea/100 mM ABC solution was made by solving 0.48 g of urea in 1 mL 100 mM ABC. A 0.5 M NaCl solution was prepared by solving 1.7 g in 40 mL water, and 40 mM NaCL was made by diluting 20 µL of 0.5 M NaCl with 230 µL water. A 10% ACN solution and a 20% ACN solution (v/v) was made by mixing 4 mL and 8 mL ACN, respectively, with water to give a total volume of 40 mL.

Gel electrophoresis solutions

A 4x loading buffer was pre made by Max Lycke at Rikshospitalet and was made up of 8 mL 1 M Tris-HCl (pH 6.8), 8 g bromophenol blue, 0.8 g SDS, 1.6 mL 14.7 β-mercaptoethanol, 16 mL glycerol and 1 mL 0.5 M EDTA. Aliquots of 6.4 µL (giving about 1 µg protein) of protein solution were diluted with 5.6 µL distilled water. To this solution, 4 µL loading buffer were added, giving a total of 16 µL protein-loading buffer solution, meaning the loading buffer was diluted to 1x. About 3 000 000 GBM cells were solved in 15 µL water, with 5 µL loading buffer. The standard- and the cell solutions were placed in a heating block for 2 min at 90° C for denaturing. The running buffer was prepared by 10 mL 3-morpholinopropane-1-sulfonic acid (MOPS) SDS (20x) diluted with 200 mL tap water to yield 1x running buffer.

In-gel digestion solutions

Fixation buffer was made by Frøydis Sved Skottvoll. It was made by adding 400 mL of water and 100 mL acetic acid to 500 mL technical methanol. A 10 mM DTT/100 mM ABC solution was made by mixing 15 µL of 0.5 M DTT with 735 µL 100 mM ABC. A solution with 10% ACN in 10 mM ABC (v/v) was prepared by first diluting 1 mM 100 ABC with 9 mL water, then adding 1 mL ACN to 9 mL of this solution. A trypsin solution of about 13 ng µL^{-1} trypsin was made by adding 1.3 µL of a 10 mg mL^{-1} trypsin solution to 9998 µL ABC/ACN (90/10, v/v) solution with 10% ACN. An extraction buffer made up of 5% FA in ACN (1/2, v/v) was prepared by first diluting 250 µL FA to 5 mL with water and then adding this to 10 mL ACN.

Solution for immobilization of antibodies

A 50 mM phosphate buffer was made by solving 0.234 g of NaH$_2$PO$_4$ in 40 mL of water. An ammonium acetate buffer was made by solving 0.771 g of ammonium acetate in 200 mL of

water. Both of these were pH adjusted with 1 M NaOH, the phosphate buffer to pH 7.2 and ammonium acetate to 8.75, using a pH-meter.

Antibody solutions

All ABs were received in 10 µL solutions, with concentrations of 0.921, 0.314 and 0.654 µg µL^{-1} for the αV, β1 and β5 ABs, respectively. Before immobilization onto the monolith, they were diluted in phosphate buffer with pH 7.2 to give an end volume of 1 mL.

Solutions for western blot

A 5% TBS-T was made by adding 10 TBS-Tween tablets to 5 L water in a glass flask. A 5% (w/v) milk solution in TBS-T was prepared by adding 25 g non-fat dry milk powder with 500 mL 5% TBS-T in a 1 L glass flask, which was stored at 4°C. All primary (integrin) ABs were diluted in 5 mL milk solution to their respective dilution factors given by the producer (given as AB/ milk solution (v/v)). For the β1 AB, 2 µL AB solution were added to the milk solution (dilution factor: 1/2000), whilst for the β5 AB (dilution factor: 1/1000) 5 µL AB solution were added to the 5 mL milk solution. The AB for αV had already been diluted 100 times in phosphate buffer and used for immobilization (**Section 3.3.1**). So even though its dilution factor of 1/5000 was used (100 µL AB solution in 5 mL 5% TBS-T milk solution), the concentration of αV AB in the solution was uncertain. A 10 x transfer buffer was pre made by Frøydis Sved Skottvoll at Rikshospitalet mixing 30.3 g Trizma® base and 144 g glycine with 1000 mL water. Before use 10 mL of this solution were mixed with 200 mL technical methanol and 700 mL water so the transfer buffer was diluted giving a 1x transfer buffer.

Solutions for preparing monolithic columns

A 1 M NaOH solution was made by dissolving 1.6 g NaOH pellets in water to a final volume of 40 mL. Both the silanization and the polymerization solutions were freshly made and sonicated before use. The silanization solution consisted of 67.5% DPPH, 0.5% DMF and 32% γ-MAPS (w/w/w), whilst the polymerization solution was made up of 1% AIBN, 23% VDM, 16% EDMA, 34% 1-propanol and 26% 1,4-butandiol (w/w/w/w).

3.2 Equipment and consumables

All protein solutions were prepared and all procedure steps with proteins were done in 1.5 mL "Protein LoBind" tubes from Eppendorf (Hamburg, Germany). The protein solutions were dried in an Eppendorf Concentrator Plus centrifugal evaporator also from Eppendorf, as was a bench top 5424 R centrifuge which was used for the FASP protocol (**Section 3.5.2**). A Grant-Bio Thermoshaker from Grant Instruments (Shepreth, Cambridge, UK) was used for incubation. For weighing a Delta Range or an AT200 analytical balance, both from Mettler-Toledo (Greifensee, Switzerland), were used. A Thermo Scientific Orion^{TM} 720Aplus pH-meter from Fischer Scientific (now a part of Thermo Fischer) was used for pH adjustments. For all volumes not related to the GE and WB automatic pipettes from Thermo Scientific were used except when ranging from $0.5 - 10\,\mu L$. Then a pipette from Eppendorf Research was operated. For these volumes pipette tips were from Thermo Fischer. For GE and WB the pipettes and pipette tips were from VWR. A heating block from Grant Instruments was used. GE was performed in a mini Cell electrophoresis chamber from Thermo Fishcer. The transfer chamber, Extra Thick Blot Filter Paper and a Chemidoc^{TM} touch imaging system was from Bio-Rad. The nitrocellulose membrane was acquired from Thermo Fischer. A roller from Stuart (Stone, Straffordshire, UK) was used. Nobo Transparency films were purchased from ACCO Brands (Lake Zurich, IL, US). For the FASP protocol Amicon® Ultra centrifugal 10 k filter units and collector tubes were acquired from Merck. A Nanodrop 2000 spectrophotometer, used for BSA assay, came from Thermo Fischer. Polyimide-coated fused silica capillaries was from Polymicro Technologies (Phoenix, AZ, US). Two Valcon polyimide 0.3 mm ID sizes of fused silica adapters (ferrules) from Vici Valco (Houston, TX, USA) were used (1/32" and 1/16"). These were drilled more open with a 0.38 mm drill by Inge Mikalsen. The fittings and screws used for couplings were then 1/32" or 1/16".

3.3 Column preparation

Fused silica capillaries were used as column bodies for both monolithic and in-house packed nano-LC columns. Monoliths were prepared inside capillaries with inner diameter (ID) of $180 \pm 6\,\mu m$ and outer diameter (OD) of $360\,\mu m$. The nano-LC columns were packed in capillaries with $50 \pm 6\,\mu m$ ID and $363\,\mu m$ OD. All columns were prepared using a pressure bomb system, shown in ***Figure 21***. Vials used in the system were 1.5 mL Chromatography Autosampler Vials from VWR. Stirring in the vial was done with a 3 x 3 magnet (VWR), with the pressure bomb

system placed on a Topolino magnetic stirrer from Ika (Staufen im Bresgau, Germany). A GC-17A from Shimadzu (Kyoto, Japan) was used as oven. Sonification was done using an ultrasonic bath (model 5510) from Branson (Danbury, CT, US). The pH was checked with MColorpHast indicator strips from Merck. A microscope from Motic (Xiamen, China) was used to observe packing and formation of monoliths.
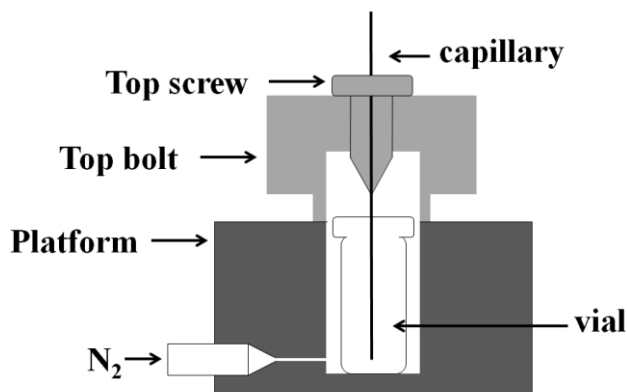
Figure 21: The pressure bomb set up. The vial was filled with the required solution/liquid and the capillary was pushed through the top bolt and fastened with a screw. The top bolt was then fastened to the platform and N$_2$ was turned on. Adapted from [89].

3.3.1 Preparation of monolithic columns

In this study, the monolithic support was prepared by an *in situ* copolymerisation of EDMA and VDMA. The capillary was flushed, dried and filled in all the steps using the pressure bomb system shown in *Figure 21*.

Pretreatment: A capillary of length between 1-2 m was filled with 1 M NaOH, sealed with a rubber septum and left overnight at room temperature. It was then flushed with water until pH ≤ 7. Then the capillary was flushed with 1.5 mL ACN and dried with N$_2$ gas for 20 min.

Silanization: The capillary was filled with the silanization solution (67.5% DPPH, 0.5% DMF and 32% γ-MAPS (w/w/w)), sealed and placed in an oven at 110 °C for ≥ 1 h. The capillary was cooled at room temperature for ~3 min, flushed with 1.5 mL ACN and dried with N$_2$ gas for 20 min.

Polymerization: The capillary was cut into desired lengths of the monolith columns (about 15 cm). They were then filled with the polymerisation solution (of 1% AIBN, 23% VDM, 16% EDMA, 34% 1-propanol and 26% 1,4-butandiol (w/w/w/w)), sealed and placed in an oven at 70 °C for 24 h. After 3 min of cooling the capillaries were flushed with 1.5 mL acetone, in order

34

to remove unreacted monomers, porogens and other soluble compounds from the pores, and then dried with N_2 gas for 20 min. Finally, they were sealed and stored dry before the attachment of ABs.

Immobilization of antibodies: The monolith was first flushed with phosphate buffer. Then, an AB-phosphate buffer solution was slowly flushed through for about 3.5 h. The monolithic column was then filled with ammonium acetate buffer and stored in a refrigerator until use.

The pretreatment and silanization were based on [149], whilst the polymerization and immobilization were based on [135].

3.3.2 Preparation of pre- and analytical packed columns

Packed nano-LC columns were made following a standard operating procedure by Henriette Engen Berg [89]. The pressure bomb system shown in *Figure 21* was used for washing, drying and filling the capillary.

Frit preparation

Prior to packing, polymerized frits were made by dipping the ends of the capillaries (~ 40 cm) into a Kasil 1624/formamide (3/1, v/v) for 5 s, and leaving them in an oven at 100 °C overnight. The capillary was cut so the remaining frit was about 1 mm, before washing the capillary with ACN and drying.

Column packing

Commercial, conventional (4.6 mm ID x 150 mm) columns were emptied by Henriette Engen Berg to acquire the Accucore particles. The particles were then air-dried. A slurry of 30 mg particles in 1 mL of 20% water/80% ACN (v/v) was prepared in a vial and a 3 x 3 mm magnet was added. The vial was placed in an ultrasonic bath for 10 min. After ultrasonic treatment, the slurry was used to pack the capillary using the pressure bomb platform in *Figure 21*. A magnetic stirrer was placed underneath the pressure bomb platform to keep the particles suspended during the packing process. When the capillary was to be used as an analytical column, it was packed at least 2 cm longer than the desired column length and cut to the desired length prior to use. If the capillary was to be used as a pre-column it was not packed beyond 5

cm and 10 cm were left empty. The packing process was controlled by monitoring the capillary in a microscope.

3.4 Gel electrophoresis and western blot

All steps in these procedures were performed at the unit for Cell Signaling at Rikshospitalet in Oslo. GBM cells were also included for GE together with integrin standards.

3.4.1 Gel electrophoresis

Two gels were placed in a mini Cell electrophoresis chamber. The chamber was filled with the running buffer. Either 16 µL integrin standard-loading buffer solution, 20 µL GBM cell-loading buffer solution or 10 µL protein ladder were loaded to a well in the gel using microcapillary pipette tips (loading of GBM cells was performed by Frøydis Sved Skottvoll). For each protein to be used for western blot, two replicates and one protein ladder where used, whilst one replicate of the protein standard and cells to be subjected to in-gel digestion. A voltage of 75 V was applied for the first hour, before it was increased to 90 V and kept there for 30 min, before lastly increased to 95 V which was kept for 20 min, all at 150 mA. The gels were cut with a scalpel; integrin standards meant for in-gel digestion made up one piece and the GBM cells another. Standards for WB were cut to give one piece for each of the three integrin standards. See *Figure 22* for an illustrative explanation. The pieces for in-gel digestion were kept in the fixation buffer overnight at 4° C. See **Section 3.5.3** for further procedure of the in-gel-digestion.
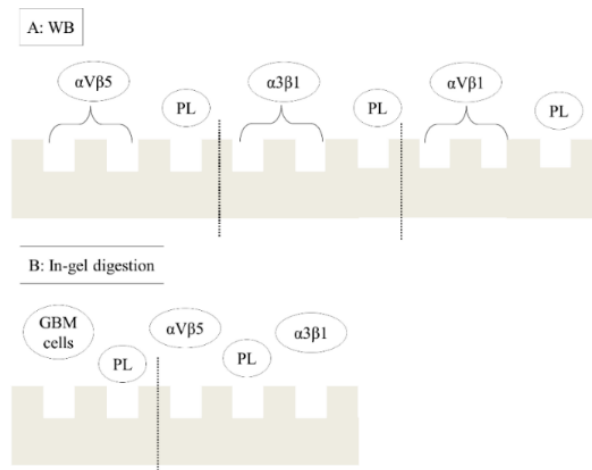
Figure 22: Loading of integrin standards*, GBM cells and protein ladders (PL) onto gels. The dotted lines indicates where the gel was cut after GE to make up the various pieces that underwent either A: WB or B: in-gel digestion.*

3.4.2 Western blot

Protein transfer

A piece of nitrocellulose membrane was cut to fit the three gel pieces, and the membrane and gels were incubated in 1x transfer buffer for 15 min. Two Extra Thick Blot Filter Papers were soaked with 1x transfer buffer. The membrane was placed onto one of the filter papers, and then the gels onto the membrane, with the other filter paper on top, inside a transfer chamber. For every layer 1x transfer buffer was added to maintain moisture. In order to remove air bubbles from the "sandwich", a 10 mL glass pipette was rolled over it. The transfer chamber was kept at 1 W at 4° C overnight.

Immunolabeling

The membrane was cut to give three pieces, one for each protein standard (the gels were discarded). Each of the membrane pieces were placed in separate plastic containers and blocked by soaking them in the 5% TBS-T milk solution for 1 h on a mixing plate. The milk solution was then removed and the membranes were placed in 50 mL tubes containing 5 mL of the corresponding primary AB solution. The ABs had been diluted with a 5% TBS-T milk solution. These tubes were kept on a roller at 4° C overnight. The AB for αV had already been diluted 100 times in phosphate buffer and used for immobilization (**Section 3.3.1**). Therefore, even though its dilution factor of 1/5000 was used, the concentration of ABs in the phosphate buffer was uncertain.

Visualizing

After immunolabeling the membranes were placed in a plastic container and rinsed with 5% TBS-T for 1.5 h on a mixing plate. After rinsing, the membranes were again transferred to 50 mL tubes, this time containing 5 mL of secondary AB solutions (all mouse anti-rabbit, 1/5000). The tubes were kept on a roller for 2 h at 4 °C and then rinsed in a plastic container with 5% TBS-T for 30 min on a mixing plate. Next, the TBS-T was removed and the membranes were rinsed with 1 mL of ECL-prime for about 2 min, using a pipette. Two sheets of transparency film were cut and all three membranes placed in between the two sheets. Air bubbles and excess fluid were removed by pressing filter paper across it. A Chemidoc™ touch imaging system, set to chemiluminescence, was used for imaging of the bands. For β5 and β1 an exposure time of 600 s was sufficient for visualization, whilst for αV 5000 s was required to obtain a satisfactory image. The image files were handled using the Image Lab™ Software (version 6.0) from Bio-Rad.

3.5   Protein digestion

After in-solution-, in-gel-, and FASP digestion, the peptide solutions were evaporated to dryness in a concentrator at 30 °C and resolved in the appropriate solution based on what was investigated. Peptides were resolved in 50 mM ammonium acetate buffer pH 8.75 when they were to be injected onto an AB monolith. For analysis without an AB monolith, they were resolved in 0.1% FA/LC-MS water.

3.5.1 In-solution digestion

This method was used for all three integrins.

Prior to digestion, the protein solution was evaporated to dryness in a centrifugal evaporator. An aliquot of 1 µg of protein was solved with 50 µL of 6 M urea/100 mM ABC solution to a protein concentration of 0.02 µg µL^{-1}, and 2.5 µL of DTT were added. This solution was left to incubate at 30 °C for 30 min. Next, 3.75 µL IAM were added to the solution and left to incubate at 25 °C for 1 h in the dark. The enzymatic digestion was done by adding 160 µL 50 mM ABC to dilute the urea, and trypsin was added to a trypsin/protein ratio of 1/20 (w/w). A subsequent incubation was performed at 37° C for at lest 18 h and for no more than 22 h. The digestion was ended by inactivating the protease through adding 5 µL 50 % FA (v/v).

Deglycosylation step

When deglycosylation was implemented, PNGase F was added to give a ratio of 0.25/1, (enzyme unit/µg protein) and left at 37 °C overnight (~19 h). This step was then before the trypsin solution was added and was based on [150]

Heating

When a heating step was applied, the resolved peptide solution was kept for 10 min in a thermoshaker at 100° C, before being cooled for 5 min on ice. This step was based on [151].

Trypsin inhibitor

When trypsin inhibitor was added, it was with a 1/1 (w/w) relation to the amount of trypsin in the solution. After addition, the vials were shaken for about 30 s.

3.5.2 Filter-aided sample preperation

The method was based on [152] and all centrifugations were done at 14 000 x g. Only αVβ1 was subjected to this method.

One µg of the αVβ1 standard was first solved in 50 µL 8 M urea/100 mM ABC and reduced by adding 1.25 µL 0.1M DTT. This solution was incubated at 30 °C for 30 min, before it was transferred to a 10 k filter unit together with another 200 µL of 8 M urea/100 mM ABC. This solution was centrifuged for 40 min. The flow through in the collection tube was discarded and 100 µL of 50 mM IAM/8 M urea solution were added to the filter unit and mixed at 600 rounds per minute (rpm) for 1 min in a thermoshaker. The filter unit was then incubated at 25 °C, in the dark, for 20 min. The filter unit was centrifuged at for 30 min. After this, 100 µL of 8 M urea were added and the filter unit was centrifuged for 15 min. Next, 100 µL 50 mM ABC were added to the filter unit and centrifuged for 10 min, and this step was done twice. Afterward 0.5 µL of 0.1 µg µL^{-1} trypsin (in 50 mM ABC) were added and this solution was left to incubate at 37° C overnight, without mixing. The filter was then moved to a new collection tube and centrifuged for 10 min, before 30 µL of extraction solution was added and the filter unit was centrifuged for 10 min. This extraction step was also performed twice. Lastly, 2 µL 50% FA was added.

3.5.3 In-gel digestion of integrin standards

For staining, the gels (**Section 3.4.1**) were covered with Coomassie Brilliant Blue for 4 h at room temperature and destained by covering them with water overnight at 4 °C. By using the images from WB and the protein ladders, 4 pieces were cut, 2 from each gel, one where the β-unit was expected to be, the other one for the α-unit. See **Appendix 7.5** for illustration. The pieces were further cut into smaller parts, and placed in Protein LoBind Eppendorf tubes. For the cutting of the gel piece containing GBM cells, see **Appendix 7.4.2**. Further destaining was done by adding 500 µL ACN and incubating at 37° C for 10 min at 1000 rpm in a thermoshaker. The ACN was subsequently removed, 100 µL 10 mM DTT/100 mM ABC were added (to entirely cover the pieces) and the tubes were incubated at 56 °C for 30 min. The samples were cooled to room temperature and 500 µL ACN were added and removed after incubation at 37 °C for 10 min at 1000 rpm. Then 55 mM IAM was added to cover the pieces and they were left to incubate in the dark for 20 min at 25 °C. Once again 500 µL of ACN were added, and the tubes were now incubated for 1 h for a final destaining step. ACN was removed, and next the pieces were covered with 13 ng µL^{-1} trypsin solution (about 100 µL). This was left to saturate for 30 min on ice, and then another 50 µL of trypsin solution were added. After a 90 min saturation on ice, 20 µL 10 mM ABC were added and the tubes were left in an oven at 37 °C overnight. Extraction of the peptides was done by adding 100 µL extraction buffer to each tube and incubation for 15 min. Then, the supernatant was transferred to a new tube using a pipette and centrifuged for dryness. The in-gel digestion was based on [153]. This procedure was also used for digestion of GBM cells, which was performed by Henriette Engen Berg.

3.6 Glioblastoma cells

Culturing of GBM cells is described in **Appendix 7.4.1**, and was performed at Oslo University Hospital. The GBM cells had been lysed with NP-40 buffer from Thermo Fischer Scientific and added phosphatase- and protease inhibitor (done by Henriette Engen Berg). The lysates had undergone separation via gel electrophoresis and in-gel tryptic digestion (10 aliquots), and had been evaporated to dryness. The digestion was performed by Henriette Engen Berg, using the same procedure as given in **Section 3.5.3**. The protein content of each aliquot was solved in 20 µL 0.1% FA and 10 µL from each aliquot were transferred to one Eppendorf tube, making the protein sample. See **Appendix 7.4.2** for illustrative explanation.

Protein concentration of the GBM cells was measured with a BCA assay (see **Appendix 7.4.3** for further explanation of BCA assays). Reagent A and B were mixed with a 50/1 ratio (v/v) and 100 µL of this solution were added to 9 wells (6 calibration solutions + 3 sample replicates) in a 96-microwell plate. Bovine serum albumin (BSA) calibration standard was added to 5 of the wells and diluted to 10 µL with 0.1%, to give a total volume of 110 µL. BSA was added to give standards with 0, 2, 5, 10, 15 and 20 $\mu g \, \mu L^{-1}$ BSA concentration. In the 6th well, only 0.1% FA was added to give a blank standard. The wells for the sample replicates were added 5µL protein sample and 5 µL 0.1% FA and the plate was shaken and put in an oven at 37 °C for 30 min. The protein concentration was measured using a spectrophotometer. After obtaining the concentration, the remaining sample was dried and resolved in ammonium acetate buffer pH 8.75 to a total protein concentration of about 1 µg μL^{-1}. Calibration curve and sample measurements are given in the **Appendix 7.4.3**.

3.7   Liquid chromatography mass spectrometry

3.7.1 Instrumentation

A Q-Exactive MS with a Nanospray Flex ion source was used for analysis in combination with an Easy-nLC1000 pump with autosampler, all from Thermo Scientific. The autosampler had a 20 µL NanoViper polyetheretherketone (PEEK) sample loop, also from Thermo Fischer. Two different setups were used. For examination of the different digestion methods, and no AB monolith was included, the LC-MS setup shown in *Figure 23* (referred to as Setup I) was used. In *Figure 24* the second setup (Setup II) is shown. Here, an AB monolith was incorporated online via an external 6-port two-position valve from Vici Valco.

The external 6-port was coupled to an Agilent 1200 Series Capillary Pump from Agilent Technologies (Santa Clara, CA, US) as a flushing pump. For injection onto the monolith in Setup II, a 1/16" syringe port (Vici Valco) and a 25 µL syringe from Hamilton Company (Rena, NV, US) was used. When stated, the analytical column in Setup II was replaced with a 10 µm ID x 100 mm fused silica tubing.
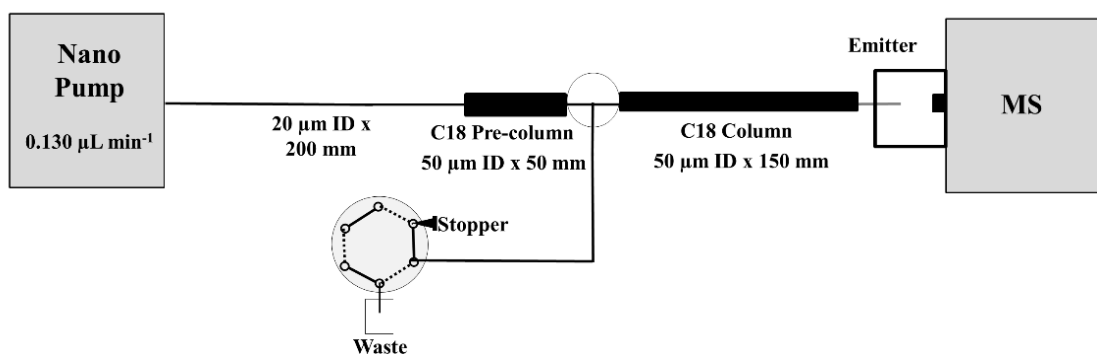
Figure 23: Setup I*: The nanopump was connected to a C18 pre-column (50 µm ID x 50 mm) through a 200 mm tubing (20 µm ID). This pre-column was coupled to a T-piece, which was also coupled to the waste outlet and a C18 analytical column (50 µm ID x 150 mm). The analytical column was coupled to an emitter at the end.*
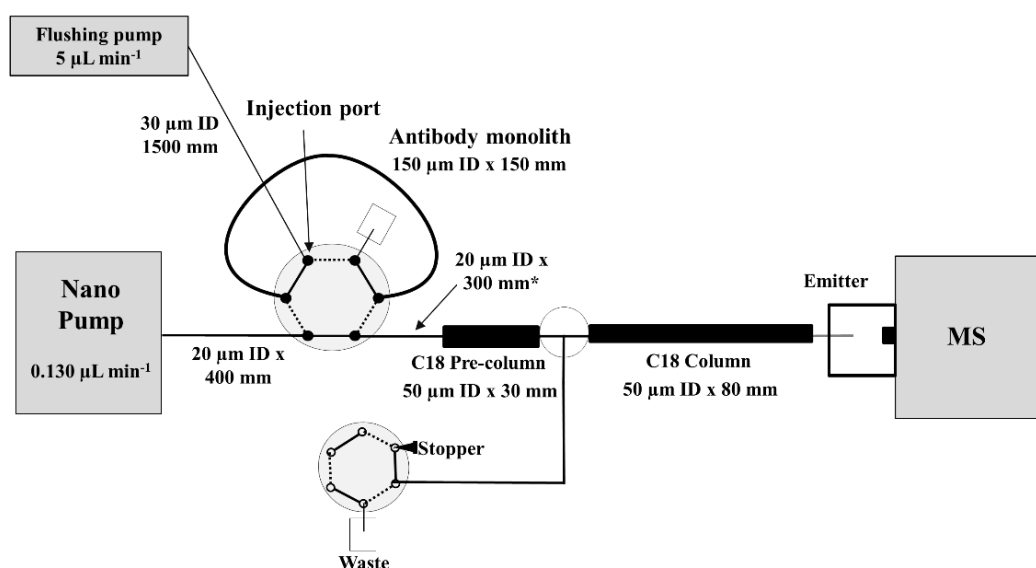
Figure 24: Setup II*: The nanopump was coupled to an external 6-port two-position valve through a 400 mm tubing (20 µm ID). An AB monolith was coupled onto the external valve, where a syringe port or a flushing pump was connected. Through a 450 mm long tubing (20 µm ID) the external port was coupled to a C18 pre-column (50 µm ID x 50 mm). Via a T-piece this pre-column was coupled to a waste outlet and a C18 analytical column (50 µm ID x 150 mm). The analytical column was coupled to an emitter at the end. When denoted, the analytical column was replaced with a 10 µm ID silica tubing. *A longer tubing between the external port and the pre-column was also used (it is stated when in the text).*

Couplings

The connecting tubing used was either fused silica capillary (Polymicro Technologies) with ID of 20 and OD of 360 µm or Nanoviper PEEK tubing (ID 20 µm) from Thermo Fischer. All tubings shown in ***Figure 23*** and ***Figure 24*** were fused silica capillary. For the couplings between capillaries, and capillary and columns, stainless steel unions, nuts, ferrules and T-piece from Vici Valco were used. The couplings were all 1/16", except for the three in the T-piece,

which was 1/32". A stainless steel nanobore emitter (20 µm ID x 40 mm) from Thermo Scientific was connected at the end of the analytical column (or fused silica tubing when no analytical column was used) using an Upchurch PEEK Microtight® union with MicroFingertight fittings and 360 µm Upchurch Microtight tubing sleeve with ID 360 µm from Sigma Aldrich.

3.7.2 Mobile phases and gradients

For both setups, the channels of the nanopump contained LC-MS grade water/0.1% FA (v/v) and ACN/0.1% FA (v/v), termed MP A and MP B, respectively. ***Table 2*** gives the gradients used with Setup I and Setup II. The MP of the flushing pump in Setup II was a 50 mM ammonium acetate buffer with pH 8.75. Prior to each run the columns were equilibrated with MP A, with a maximum pressure limit of 500 bar limiting the flow rate. In Setup I and II, the pre-column was equilibrated with 3 µL and the analytical column with 4 µL. For Setup II without the analytical column, the pre-column was equilibrated with 5 µL. Loading the peptides onto the pre-column was done with 100% MP A, where the flow rate was restricted by a maximum pressure limit of 500 bar.

Table 2: The gradient used for Setup I and Setup II, with the time (min) of the gradient and percentage of MP B at the given times. Gradient 1 was used for Setup I. Gradient 2 was used for Setup II, as was Gradient 3 when the analytical column was replaced with empty silica capillary.

Gradient 1 (130 nL min^{-1})		Gradient 2 (130 nL min^{-1})		Gradient 3 (200 nL min^{-1})	
Time (min)	% MP B	Time (min)	% MP B	Time (min)	% MP B
0	3	0	3	0	3
30	15	15	15	8	50
33	50	20	50	13	95
35	95	25	95	18	95
50	95	30	95		

3.7.3 Trapping on the monolith and elution onto the pre-column

Standard/samples were manually injected onto the AB monolith with varying injection volumes (***Figure 25A***). Directly after, the flushing pump was coupled to the AB monolith via the

injection port (**Figure 25B**). While the flushing was ongoing, the nanopump was started, and the auto sampler was set to pickup 5 µL of the acidic solution meant for eluting the peptides from the monolith (this was for most injections 2% FA in LC-MS grade water). When the nanopump started loading the acidic solution onto the system, the external valve was switched (**Figure 25C**), so the AB was online with the nanopump, and the epitope-containing peptide would elute onto the pre-column. The loading volume was 25 µL. The time it took for the nanopump to be ready to load the sample was 5 min (±0.5 min) when the silica capillary replaced the analytical column, and 10 min (±0.5 min) with the analytical column. At the time the loading onto the pre-column was done, the external valve was switched back, to allow for reactivation of the ABs while the peptides were eluted to the analytical column and analyzed in the MS.

(A)

(B)   (C)
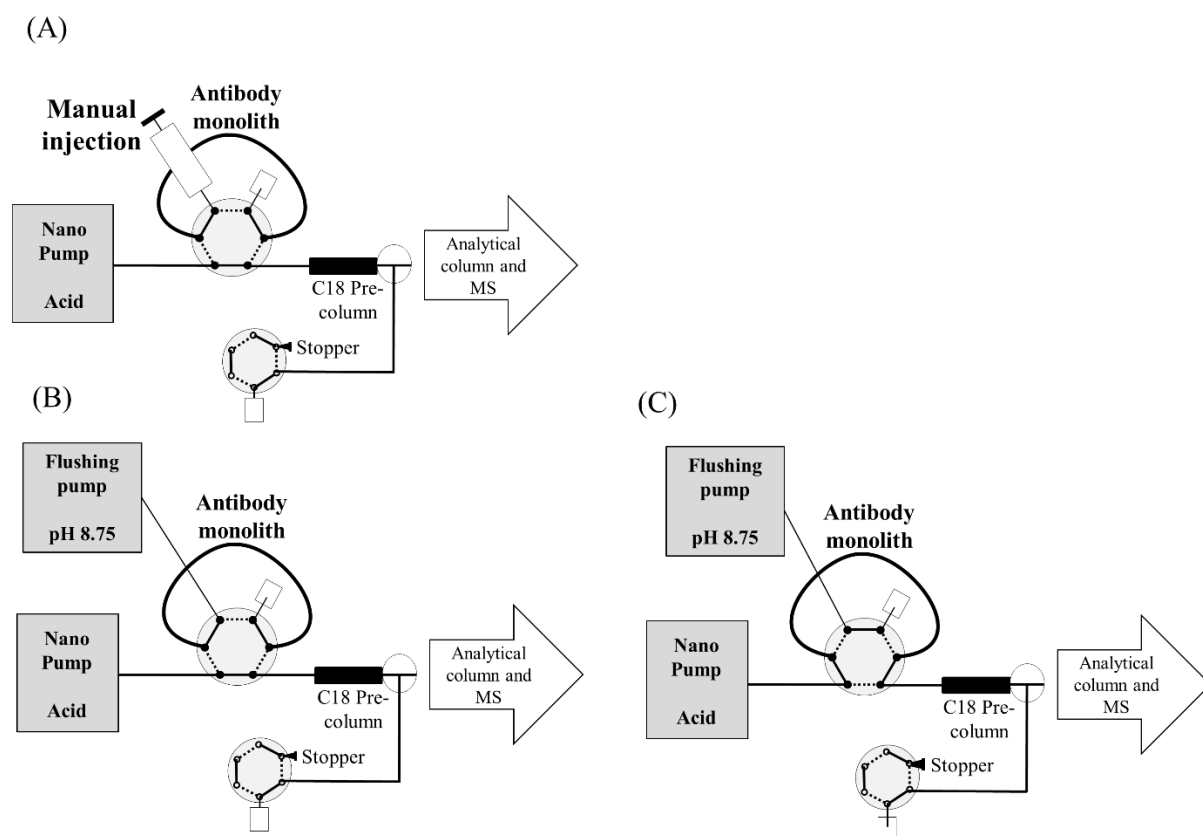
Figure 25: Injection onto the AB monolith. *A: The integrin standard or protein sample is manually injected onto the AB monolith coupled to an external 6-port injection valve coupled to a nano-LC-MS system. B: A flushing pump is coupled to the external 6-port and flushes the AB monolith. C: The external 6 port is switched and the AB monolith is online with the nanopump, which injects an acidic plug (5 µL 2% FA injected via the autosampler) onto the AB monolith, deactivating the ABs and the captured peptide is eluted onto a C18 pre-column. It is stated when the analytical column was replaced with silica tubing.*

3.7.4 Mass spectrometry settings

The MS was operated with positive polarity. A capillary voltage of 1.80 kV was employed and the ion source temperature was 275 °C. For the full scan MS spectra the mass filter was scanned from *m/z* 450 to 1850. The resolution was set at 70 000, the automatic gain control (AGC) at $1x10^6$ and the maximum injection time to 120 ms. In dd/MS/MS the resolution was set to 17 500, AGC to $1x10^5$ and maximum injection time to 60 ms. Charges of 1, 7 and ≥ 8 were excluded, and dynamic exclusion was 50 s. The method permitted sequential isolation of up to twelve of the most intense ions, with an intensity threshold of $2.0x10^4$ and isolation window of 1.8 *m/z*. Normalized collision energy in the HCD cell was set to 35.

In PRM mode the resolution of the MS/MS was set to 17 500, the AGC target to $2x10^5$ maximum injection time to 100 ms and isolation window of 4 *m/z*. The values set for the precursor ions are given in ***Table 3***.

Table 3: *The m/z values for the given peptides in the PRM method, their charge and if the peptide had missed cleavages.*

m/z	charge (+)	Peptide	Missed cleavages
683.07	3	CQPIEFDATGNRDYAKDDPLEFK	2
587.79	2	SHQWFGASVR	0
700.36	2	ILACAPLYHWR	0
513.30	2	RALFYSR	1

3.7.5 Data Processing

Mass spectra and chromatograms were obtained by Xcalibur™ software. The identification of peptides was done via Proteome Discoverer™ 1.4 software. Both of these are from Thermo Scientific. For identification of integrins their respective FASTA-file, was downloaded from UniProt websites and searched against mass spectra using the SEQUEST algorithm. For searches of the entire human proteome, a database downloaded from SwissProt was used.

For protein searches, the mass tolerance was set to 10 ppm and 0.6 Da for the precursor ion and fragment ions, respectively. Acetylation of N-terminus was allowed as a dynamic peptide modification. Oxidation of methionine and tryptophan were allowed as dynamic side chain

modifications. Carbamidomethylation of cysteine was set as a static side chain modification. A maximum of 3 missed cleavages was allowed. The uniqueness of amino acid sequences was established using the Basic Local Alignment Search Tool (BLAST) program by the US National Library of Medicine, restricted to *Homo sapiens* (taxonomy ID:9606) as organism. The PyMOL Molecular Graphics System, Version 2.0 Scrödinger, LLC was used to make images of protein structures with the structures being acquired from the PDB website.

Evaluation of data

When evaluating the results after online AB trapping of a peptide, it was a combination of the obtained correlation score and the fragment spectra of the peptide that was considered together with t_R. The total score will be considerably lower when only one peptide of a protein, compared to many, is detected, as will the coverage factor. A correlation score of 1 or more was considered acceptable. A correlation score ≥ 2 was deemed good [154]. It was desired to detect as many fragments as possible, and if 4 or less fragments were detected, this was not considered to be a successful identification. Three or more sequential fragments were considered a good indication of a successful identification. Correlation score and fragment patterns are related, so a high similarity (i.e. many fragments) between an experimental and theoretical spectrum would give a higher correlation score, compared to few similarities. The presence of proteins that should not be present (e.g. non-integrin peptides/proteins when an integrin standard had been injected) was examined by searching the obtained spectra against the SwissProt database.

Blanks were injected between injections of standard/cells, to ensure no carryover would affect the results of a subsequent injection. If a no carryover could be found in blanks after three injections of the same amount of substance, the remaining injections of this amount was performed without blanks in between injections.

4 Results and discussion

The goal of this study was to develop an online trapping method for integrin derived peptides prior to LC-MS analysis. The prospects for such a method could be as a diagnostic tool for cancer and metastasis, with the high sensitivity of nano-LC-MS and the high specificity of the AB monolith allowing for the detection of integrins when only low sample amounts are available.

For this, a selection of relevant integrin targets, monolith for immobilization and ABs were chosen. Secondly, the digestion method of the integrins were examined to ensure the best starting point for the trapping of peptides. As two of the three chosen integrins standards were more troublesome to digest, a closer investigation of digesting methods of these two was performed. Means of deactivation or removing trypsin prior to injecting protein standards and samples onto the AB monolith were examined. Following this, investigations of entrapment of epitope-containing peptides on an AB monolith was done, from both standards and cellular samples. In *Figure 26* is a flowchart of the workflow in this study, and the results will be presented in this order.
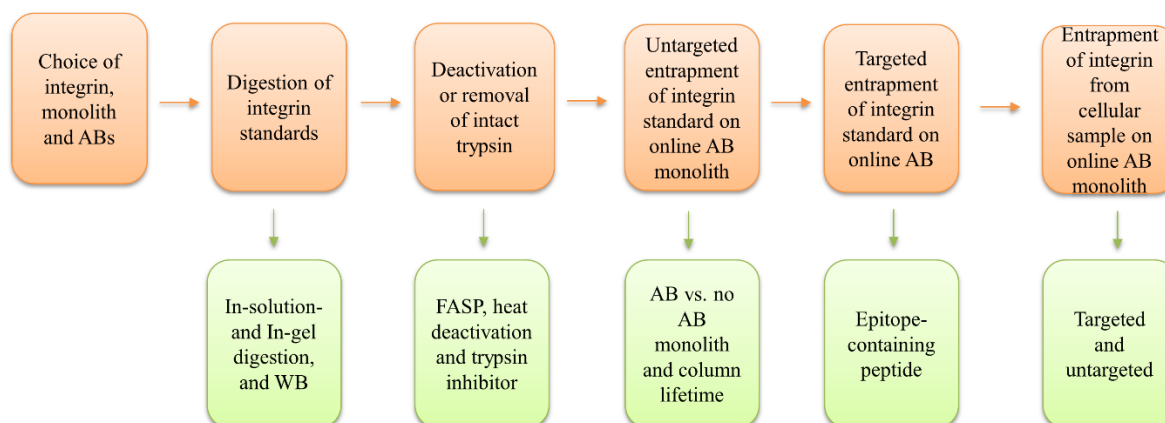
Figure 26: Chart showing how the results are presented.

4.1 Choice of integrins, monolith and antibodies

4.1.1 Integrins

Three integrins, αVβ1, α3β1 and αVβ5, were chosen as a starting point for the investigation in this study. They were selected on the basis that they had been found in extracellular vesicles from breast cancer cells analyzed in-house, by Frøydis Sved Skottvoll [81]. High expression of integrin α3β1 is linked to most cancers [33]. αVβ5 is linked to different cancers such as GBM [40] and metastasis [34]. αVβ1 was selected to work as a sort of negative control. The αV and β1 chain are found in different integrins (*Figure 4*), including the two others chosen in this study. With this integrin, the ability to distinguish between αVβ1, αVβ5 and α3β1 could be investigated. It was also ensured that the integrins were solved in an detergent that was applicable for MS experiments, which was octyl β-D-glucopyranoside for this study.

4.1.2 Organic polymer-based monolith

In this study, the ABs were immobilized on an organic polymer-based monolith. More specifically, an EDMA-*co*-VDMA monolith (see **Appendix 7.3.2** for an image of a monolith produced in this study). VDMA was included for the ability to covalently bond to an N-terminus in biomolecules. EDMA was used as a monomer to obtain a rigid monolith and minimize possible secondary, hydrophobic interactions between the peptides and the monolith. An EDMA-co-VDMA polymer was used in [135] for the immobilization of pepsin.

4.1.3 Antibodies

Regarding ABs to be immobilized on the monolithic structure for trapping integrin peptides, a few considerations had to be taken. In [147] it was shown that commercially available ABs could be used for offline enrichment of peptides prior to LC-MS/MS identification.

As the AB was to trap a peptide, and not the intact protein, an AB that recognizes a linear epitope was required. Therefore, ABs that could be used in WB was obtained. Since proteins are unfolded for WB and the ABs will then most likely recognize a linear epitope. As the purpose was to trap the same peptide from multiple injections, a mAB were used. With a

polyclonal AB multiple peptides could be trapped. It cannot be certain that polyclonal AB from two different batches will recognize the same epitopes [155]. This variation is disadvantageous, as an established method could no longer work due to a new batch of ABs being used. A mAB is specific to one amino acid sequence and this sequence will be the same between batches as well. mAbs has also been used in other studies of integrins, many of them exploring their cellular functions [156, 157], however mABs has not been used for online trapping of integrin peptides before. Trapping of intact integrins has been done previously, but offline, and most often through ligand affinity chromatography [158, 159]. The exact amino acid sequence of an epitope is usually proprietary, and producers will only provide a range of the protein sequence in which the epitope is located (hereby called the epitope range). Three ABs that satisfied the aforementioned considerations and were specific for αV, β1 and β5, respectively, were obtained (no α3 AB was found at the time that suited all the requirements). In **Table 4,** the epitope range for the three ABs are given, whilst **Table 5** gives the peptides from the epitope range for αV after a tryptic digest. Such tables for β1 and β5 can be found in **Table 14** and **Table 15** in **Appendix 7.6**, respectively.

Table 4: *The integrin chains that the ABs are specific for and the given epitope range.*

AB specific for	Epitope range given by producer
αV	32-236
β1	21-220
β5	440-661

Table 5: The resulting peptides from the epitope range after a tryptic digest, with no missed cleavages. The number (No) indicates the number of the amino acid in the integrin polypeptide chain.

Sequence	No	Sequence	No
NLDVDSPAEYSGPEGSYFGFAVDFFVPSASSR	32-64	ILACAPLYHWR	136-146
MFLLVGAPK	65-73	TEMKQER	147-153
ANTTQPGIVEGGQVLK	74-89	EPVGTCFLQDGTK	154-166
CDWSSTR	90-96	TVEYAPCR	167-174
CQPIEFDATGNR	97-109	SQDIDADGQGFCQGGFSIDFTK	175-194
DYAK*	110-113	ADR*	195-197
DDPLEFK	114-120	VLLGGPGSFYWQGQLISDQVAEIVSK	198-223
SHQWFGASVR	121-130	YDPNVYSI	224-232
SK*	131-132	KYNN*	233-236
QDK*	133-135		

* Sequences also found in other proteins (see **Section 4.4.4** for further discussion on signature peptides)

In this study, the integrins αVβ1, α3β1 and αVβ5 were selected. ABs for integrin chains αV, β1 and β5 were selected to be immobilized on an EDMA-co-VDMA monolith.

4.2 Digestion of integrin standards

α3β1 and αVβ5 were delivered in solution from Merck Millipore, both with octyl β-D-glucopyranoside and salts. These two integrins proved more challenging to digest successfully using in-solution digestion than αVβ1, which was acquired dried, from R&D systems.

4.2.1 Digestion of α3β1 and αVβ5

Digestion of αVβ5 and α3β1 using the in-solution method stated in **Section 3.5.1** did not produce any successful detection of either of these integrins using LC-MS/MS. Various changes were made to the in-solution method, to see if any of them could give a tryptic digestion. Addition of 20% ACN in the denaturing buffer was investigated, as well as a higher concentration of urea in the denaturing buffer. A deglycosylation step was also implemented

into the method, to see if sugar groups on the integrin were sterically hindering the digestion. Whenever a digestion of an integrin was done, an in-solution digestion of the protein HSA was performed in parallel as a control, to ensure that unsuccessful identification of integrins was not due to the materials used or a mistake in a step of the digestion method.

None of these measures resulted in a successful digestion of these two integrins, even though HSA was successfully digested. Comparative chromatograms and numbers from Proteome Discoverer from one analysis of HSA and integrin standards are given in **Appendix 7.7**.

Western blot

A WB was done in order to ensure that the integrins αVβ5 and α3β1 actually were present in the purchased vial. Only ABs specific for the β chain was applied. Since integrins always appear together in the PM, the presence of one of the chains in the standard would imply that the other chain also is present. The WB gave successful detection of the β chains of the integrins, and these are shown in *Figure 27*. Hence, the WB verified the presence of integrins in the standards.
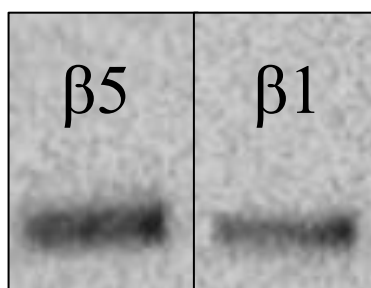
Figure 27: WB of integrin standards β5 and β1 after a GE. For both standards 1 μg protein was loaded on the gel. Exposure time was 10 min, anti-itgb5 had dilution factor 1/1000 and anti-itgb1 1/1000. Two replicates were performed for each integrin.

WB was also performed on the αVβ1 standard, to ensure the αV AB was active towards its target protein. The AB did bind and WB of the αV chain can be seen in *Figure 51* in **Appendix 7.5**.

In-gel digestion

An in-gel digestion of 1 μg of each of the two integrins was performed (**Section 3.5.3**). To investigate whether separation of the integrins from the other components present in the purchased solution would enable the proteins to be digested. After an in-gel digestion both integrins were identified, with injections of 5 μL with concentrations of 10 ng μL^{-1} with Setup I, given in *Figure 23*. In *Table 6* the scores and coverages obtained are stated.

Table 6: *The score and coverage of the respective α- and β chains from integrin αVβ5 and α3β1 after an in-gel digestion.*

Integrin chain	Score	Coverage (%)
α3	6.2	32
β1	15	44
αv	91	60
β5	67	53

For both integrins, two pieces were cut out from the gel and underwent in-gel digestion. One where the β chain was expected to be (β piece), based on the WB results, and one for the α chain (α piece). See **Appendix 7.5** for more information. However, the α chains, as well as the β chains, were identified from the β piece.

Detection of integrins αVβ5 and α3β1 after in-gel digestion indicated that some components of the solution the integrins were solved in were hindering digestion. This hindering could be due to one or some of them either hindering the protease from R and K sites, or deactivating trypsin. The producer was not aware if any of the components would hinder digestion, but could not rule it out [160]. Compared to the in-solution digestion of 1 µg αVβ1 (see next section), which was detected with Setup I with a lower concentration (1 ng µL^{-1}) and only 5 µL injection volume, the scores of α3β1 and αVβ5 are comparably low. This could be due to inadequate extraction of the integrins from the gel.

4.2.2 In-solution digestion of αVβ1

Integrin αVβ1 was successfully digested following the method detailed in **Section 3.5.1**. The highest score obtained using this method was 755 with a coverage factor of 62% for αV and 493 and 63% for β1. Several peptides from the epitope range were also detected. ***Figure 28*** shows chromatograms for αV and ***Figure 29*** shows chromatograms for β1. In both figures the TICC and EIC for the peptides from the epitope range are shown.
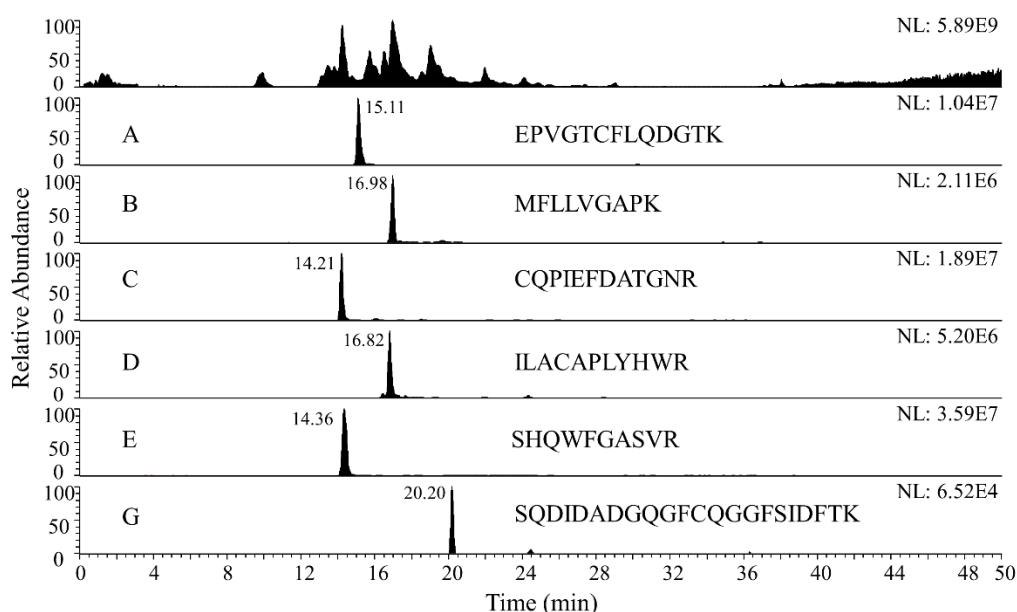
Figure 28: TICC (top) and EIC (A-G) of peptides found in the range of the epitope for αV. Protein concentration was 10 ng μL⁻¹ with 1 μL injection volume. Pre-column was 5.1 cm and the analytical column was 15 cm. The gradient is given in **Table 2** (Gradient 1). Flow rate was 130 nL min⁻¹. Gaussian smoothing of 15 was applied. A is peptide EPVGTCFLQDGTK (m/z 726.34), B is MFLLVGAPK (m/z 496.29), C is CQPIEFDATGNR (m/z 704.32), D is ILACAPLYHWR (m/z 700.37), E is SHQWFGASVR (m/z 587.79) and lastly, E is SQDIDADGQGFCQGGFSIDFTK (m/z 798.33).
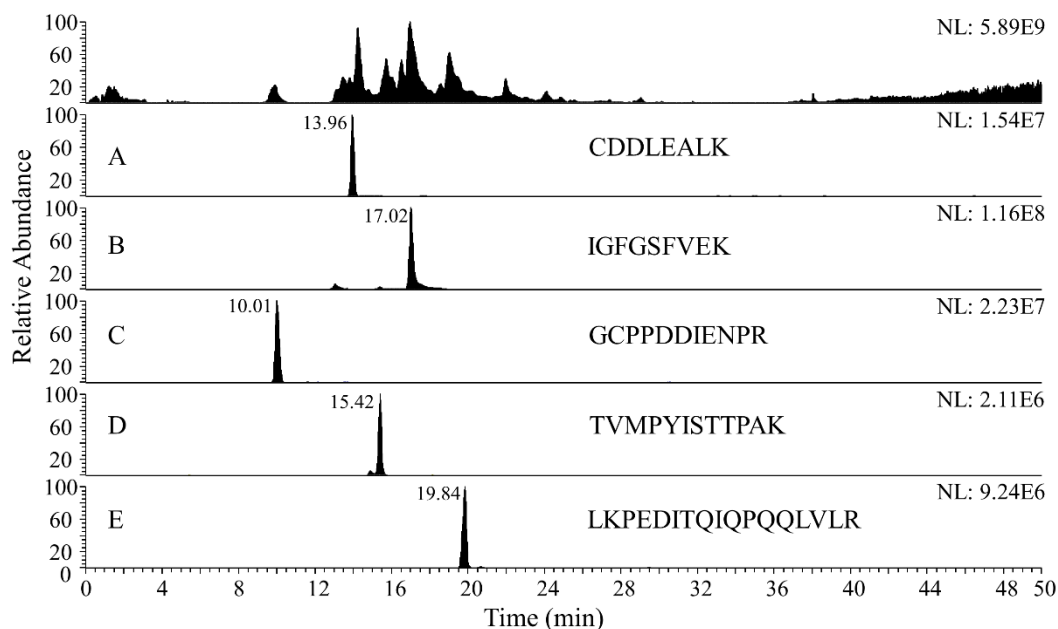
Figure 29: TICC (top) and EIC (A-E) of peptides found in the range of the epitope for β1. An identification was considered successful when the peptide had an individual score higher than one and at least three fragments. Protein concentration was 10 ng μL⁻¹ with 1 μL injection volume. Pre-column was 5.1 cm and the analytical column was 15 cm. The gradient is given in **Table 2** (Gradient 1). Flow rate was 130 nL min⁻¹ Gaussian smoothing of 15 was applied. A is peptide CDDLEALK (m/z 482.23), B is IGFGSFVEK (m/z 492.26), C is GCPPDDIENPR (m/z 635.27), D is TVMPYISTTPAK (m/z 654.85), and E is LKPEDITQIQPQQLVLR (m/z 673.72).

To summarize 4.2, integrins αVβ5 and α3β1 could not be digested using an in-solution method, and had to be separated from other components in their solution through gel electrophoresis to be digested. Integrins αVβ5 and α3β1 were not investigated further with an AB monolith column. Integrin αVβ1 was successfully digested using an in-solution method, and the scores and coverage factors obtained in Proteome Discoverer were considered satisfactory for continue using αVβ1 for trapping with an AB monolith column. Despite being intended as a negative control, it was thought sufficient to use αVβ1 to obtain proof-of-concept of online AB trapping of integrin peptide.

4.3 Removal or deactivation of trypsin

In order to keep the ABs active, the integrins were solved in a solution with pH 8.75 for injection onto the AB monolith column. The alkaline pH of the sample presents a problem, as any intact trypsin protein that remains in the solution will be active. The active trypsin can digest the immobilized ABs, and make AB activity challenging to maintain. Loss of AB activity in the monolith will lead to poor trapping of peptides. Therefore, trypsin either had to be removed or deactivated.

Three different methods for inactivation/removal of trypsin were investigated. One alternative method for removal of trypsin would be through the use of an offline SPE (common desalting technique prior to LC-MS), but including such a step can also result in a loss of sample as recovery is not expected to be 100% [161]. Therefore, FASP, heating and trypsin inhibitor were examined for the ability to remove/deactivate trypsin.

An alternative approach to this challenge, is presented in [162] and [163]. Here, the intact protein is captured on an online AB monolith with subsequent elution onto an online trypsin monolith that digests the protein before elution. As the goal in this study is to capture and elute only the epitope-containing peptide onto the LC-MS system, online digestion after trapping was not studied. Trapping only the peptide can be beneficial for successful elution and reuse of the AB monolith column. As the binding between an AB and its antigen is often very strong, it is often necessary to use quite harsh elution conditions, e.g. strong acid, chaotropic agents, denaturants or high temperatures. Such conditions can damage the AB and the analyte protein and/or be troublesome for detection in an online method, and can make reuse of the ABs challenging [127, 129]. In this study, the immobilizing the AB to the polymer was done under physiological conditions (pH around 7), which is the optimal pH for AB binding. However, when the target analyte is to be introduced the pH was kept somewhat higher (pH 8.75). This

is what is usually done to avoid the analyte to bind to the AB so strongly that elution becomes problematic [129].

Further development of the method presented in this study could be implementing an online digestion step prior to online peptide trapping.

4.3.1 Filter-aided sample preparation to remove trypsin

FASP (**Section 3.5.2**) was investigated in order to remove trypsin from the peptide solution, with the tryptic digestion being performed on the filter. As trypsin is 23.3 kDa, a filter with a 10 k cut-off would hold any intact trypsin. The protocol [164] calls for 0.5 M NaCl to be used for extraction, and an offline SPE desalting step is used. Extraction with 10% and 20% ACN in water was tested, as well as with 0.5 M and 40 mM NaCl, as done in [165]. Offline SPE was not used in this study. ACN was examined to see if it could aid extraction through hydrophobic interactions with peptides. Lower salt concentration was tested as injection of 0.5 M NaCl onto the LC-MS system was thought to be high and could shorten the lifetime of the online RP pre-column. The ACN extraction solutions did not give any protein hits in the database. Decreasing the salt concentration to 40 mM did not give noticeably different scores compared to 0.5 M. *Table 7* gives the scores and coverage factor of the investigated protocol and the different extraction solution used in this study.

Table 7: The score and coverage factor when extracting with 0.5 M and 40 mM NaCl and ACN using the FASP method for digestion of protein αVβ1.

	Score (coverage (%))	
Integrin chain	αV	β1
0.5 M NaCl	18 (27%)	30 (29%)
40 mM NaCl	15(25%)	28 (30%)
10% and 20% ACN	0 (0%)	0 (0%)

The obtained scores and coverages are lower than that obtained from a "normal" in-solution digestion (**Section 4.2.2**). The loss of peptides when performing FASP when working with small amounts of protein has also been seen in other groups [164]. The FASP method might be better suited for untargeted and exploratory proteomics studies and lager amounts of protein.

For attachment to an AB monolith the presence of the epitope-containing peptide is critical. This could make FASP method unsuitable for this study because of unspecific loss of peptides which could contain the epitope. With these low coverage factors, compared to the "standard" in-solution protocol (**Section 3.5.1**), the FASP digested integrin standards were not studied together with the AB monolith.

4.3.2 Deactivation of trypsin using heat

Only intact and folded trypsin enzymes would be a problem when injected together with the integrin peptide. As proteins denature when subjected to high temperatures, the digested and resolved integrin standards were heated to see if this could give an irreversible denaturing of trypsin. The deactivation of trypsin after heating had been found to be maintained at room temperature by others [151], but had not been examined at alkaline pH.

Initial studies of integrin peptide trapping on an AB column were done with Setup II (**Figure 24**), with no analytical column and a shorter gradient (**Table 2**, gradient 3) was used to speed up analysis time. The effect of heating to deactivate trypsin was investigated by evaluation of the fragmentation spectra and correlation score of identified peptides from injecting digested integrin standards onto an AB monolith after the heating step. Before the standards were injected onto an AB monolith, the effect of heating regarding score and/or coverage factor was investigated using the chromatographic Setup I (**Figure 23**). No noticeable differences in the scores or coverage factors were observed between standards subjected to heating and those not.

Analysis of αV after heating step

The given epitope range in the αV chain was between amino acid 32 and 236. In a tryptic digest, assuming no missed cleavages, this range will result in twelve peptides. The peptide SHQWFGASVR (amino acid 89-98) was identified successfully on three separate αV AB monoliths, with injection of 100 ng digested αVβ1, whilst no other peptide was identified. No other peptide from αVβ1 was identified from the same injection. Three different loading volumes of the nanopump were tested; 15, 20 and 25 µL. Only when 25 µL were loaded was SHQWFGASVR successfully identified, this equals about 12.5 AB column volumes (assuming the monolith takes up 50% of the column volume). This is similar to that found in [166], where peptides (from the protein type II collagen in rat urine) were eluted from an online AB column onto a pre-column with 15 column volumes.

Figure 30 shows the fragment mass spectrum of this peptide from one of the injections onto αV monoliths. In *Figure 31* the fragmentation of SHQWFGASVR that gives rise to the spectrum in *Figure 30* is shown. For all three injections, the same fragments were found. The average correlation score of the three identifications of SHQWFGASVR was 1.6. The correlation scores from all three injections are given in **Appendix 7.8.1**. In **Appendix 7.8.2**, an outline of all the possible fragments that could arise from fragmentation of the peptide SHQWFGASVR is presented. No chromatogram is shown in this section, as no analytical column was used for the elution.
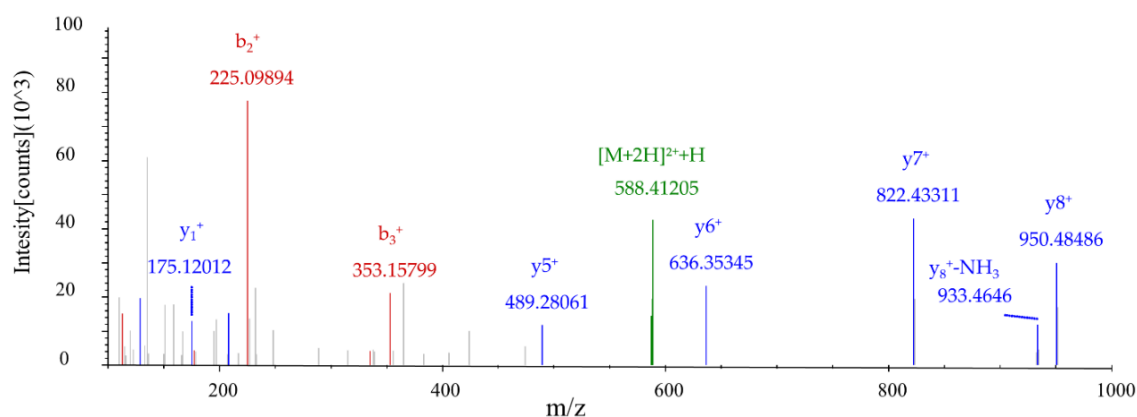
*Figure 30: The fragment spectrum of peptide SHQWFGASVR. From injection of 100 ng digested αVβ1 on an αV AB monolith. This spectrum was found using Setup II, but with a fused silica tubing replacing the analytical column. Gradient 3 from **Table 2** was used. The y-fragments are shown in blue, the b-fragment in red, and the peptide (precursor ion) is in green.*
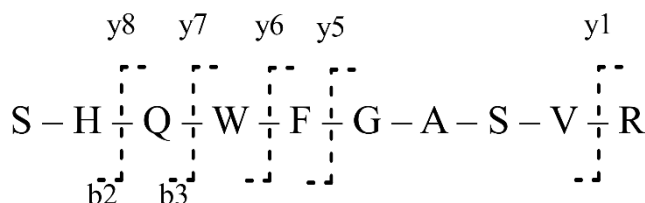
Figure 31: Fragmentation pattern of SHQWFGASVR from Figure 30.

SHQWFGASVR could not be identified with the requirements for a successful identification (**Section 3.7.5**) from successive injections on the same AB monolith. Indicating that trypsin could still be active in a basic environment at room temperature after being subjected to heat.

Analysis of β1 after heating step

For the β1 chain the epitope range was between amino acid 21 and 220. A tryptic digest will theoretically result in twelve peptides from this range (with no missed cleavages). No peptides

were identified from injection of 100 ng digested αVβ1 on a β1 AB monoliths. To elute a potentially trapped peptides from the AB, three different elution methods (on three different β1 AB monoliths) were examined; 5 µL of either 2% FA, 5% FA and a 5% FA/5% ACN (v/v). An increase in FA content was believed to promote elution if the AB-peptide interaction was particularly strong. Hydrophobic side chains on the peptides could experience secondary interactions to the organic monolithic support. The addition of ACN could aid elution if the peptide was particularly hydrophobic. However further increasing of ACN percentage could prevent subsequent trapping on the RP pre-column and was not investigated. A reason no peptide were identified, could be that the epitope was broken apart during the tryptic digestion. A way of examining if the epitope was broken could be by using a different protease that does not cut at R and K, but at other amino acids. Due to time limitations, this was not examined further. Alternatively, if the epitope was still intact the β1 AB could have low affinity to only a peptide and only bind the intact protein, causing any epitope-containing peptide to be washed away. The binding between the epitope and the AB could also be too strong to break, and even higher concentrations of acid would be necessary although this could make reactivation of the ABs difficult.

Only the αV chain was further investigated using a trypsin inhibitor.

4.3.3 Deactivation by addition of trypsin inhibitor

Addition of trypsin inhibitor in the digested integrin standard prior to loading onto the AB monolith, gave successful identification of SHQWFGASVR. The peptide could also be identified from successive injections on the same monolithic column, which was not possible using heat as a deactivation method. This indicates that the trypsin was successfully inactivated using trypsin inhibitor. In addition to the peptide SHQWFGASVR, three other peptides were identified multiple times, and two peptides ("others") were identified once each, from several injection on two different monolithic AB columns (*Figure 32*). The different monolithic AB columns are referred to as "AB X", where X represents a number, throughout the text. In *Table 8*, the average correlation scores from these identifications are given, with the correlation scores for all peptides on all AB monoliths shown in **Appendix 7.9.1**. SHQWFGASVR was the peptide that could be identified most times from the 11 injections, but the peptide RALFLYSR had a higher average correlation score. The identified peptides did not have repeatable t_R between the different injections, very likely due to the absence of an analytical column.

58
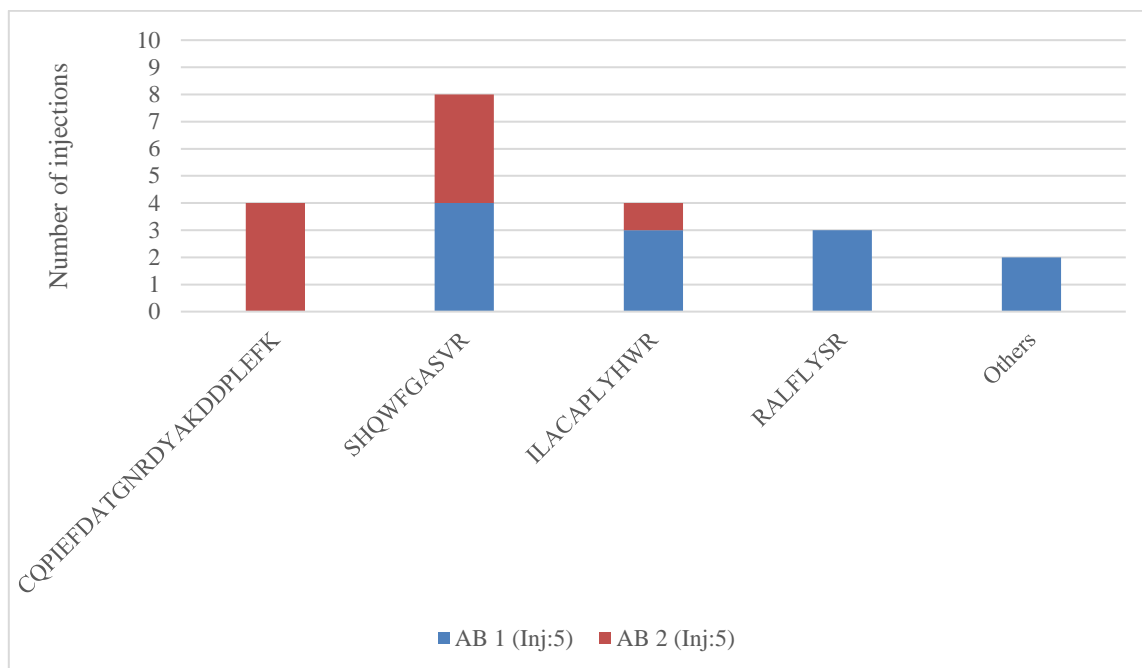
Figure 32: Number of times peptides were identified after online trapping on an αV AB monolith. *The peptides were identified using Setup II, but with a 10 cm long fused silica capillary replacing the analytical column. 10 µL of digested integrin αVβ1 standard with a concentration of 10 ng µL^{-1} was injected. The peptides were found using an untargeted MS method, with gradient 3 from **Table 2**. The two different peptides identified and grouped in the "others" column were both peptides from the αV chain.*

Table 8*: The average correlation score, with standard- and relative standard deviations, from the identification of four peptides and the two other αV peptides that were only identified one time each ("others").*

Peptide	Number of identification (from a total of 10)	Average correlation score	Standard deviation	Relative standard deviation (%)
CQPIEFDATGNRDYAKDDPLEFK	4	1.1	0.2	18
SHQWFGASVR	8	1.6	0.5	31
ILACAPLYHWR	4	2.0	0.5	25
RALFLYSR	3	2.5	0.6	24
Others	2	1.7	0.3*	18*

* As there were only two peptides, the numbers stated are based on the difference found between the two correlation scores, not the standard deviation.

To summarize 4.3, of the three different approaches for deactivating/removing trypsin, the addition of trypsin inhibitor was found to be best and used for further study of trapping αV on an AB monolith. Four peptides from the αV chain were successfully identified from trapping on αV AB monoliths. No peptide from β1 could be identified when using a β1 AB monolith, hence this integrin chain was not subjected to further studies.

4.4 Further untargeted investigation of αV trapping

For further investigation of trapping of the αV epitope, experiments were performed with an 8 cm long analytical column (Setup II, shown in *Figure 24*). Injections of 100 ng digested αVβ1 standard (10 µL with concentration of 10 ng µL^{-1}) onto a αV AB monolithic column and elution off the monolith using 5 µL of 2% FA were carried out. The use of an analytical column was believed to provide a higher repeatability of the identifications, as well as including the retention time as an a additional parameter for secure identification.

4.4.1 Untargeted detection after trapping of αV

As for experiments in **Section 4.3.3**, untargeted analyses was done using dd/MS/MS, and the same four peptides that are given in *Figure 32* were also identified with this setup. *Figure 33* shows how many identifications that could be made from a total of 8 injections on 4 different AB monoliths. It should also be noted that for the injections in **Section 4.3.3** and here, no peptides originating from β1 could be identified by Proteome Discoverer from any of the injections.
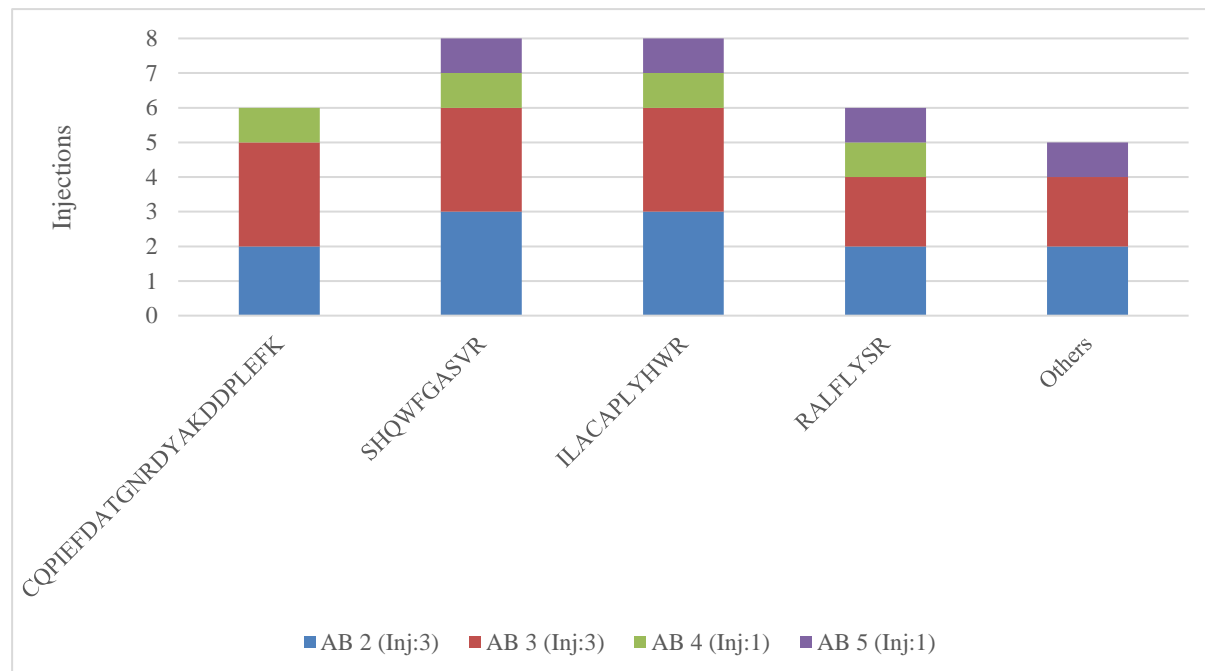
Figure 33: Number of times peptides were identified from an LC-MS analysis after online trapping on an αV AB monolith. *The peptides were identified using Setup II. 10 µL of digested integrin αVβ1 standard with a concentration of 10 ng µL^{-1} was injected onto the αV Aβ monolith. The peptides were found using an untargeted MS method, with gradient 2 from **Table 2**. The five different peptides identified and grouped in the "others" column were all peptides found in the αV chain.*

In *Table 9* the average correlation score for all the four peptides identified and the sum of the score of the peptides only identified once ("others") are given. The peptides that only were identified once could be experiencing unspecific binding to the AB or secondary interactions with the organic polymer monolith. Many of the values are similar between the peptides, except for the relative standard deviation for SHQWFGASVR, which is only 4%. This is low compared to that for the other peptides, which were between 24% and 44%. These numbers show that trapping of SHQWFGASVR with Setup II has a better repeatability compared to the other peptides. These values are calculated from data given in **Appendix 7.9.2**.

Table 9: *The average correlation score, with standard- and relative standard deviations, from the identification of four peptides and from the five other αV peptides that were only identified one time each.*

Peptide	Number of identification (from a total of 8)	Average correlation score	Standard deviation	Relative standard deviation (%)
CQPIEFDATGNRDYAKDDPLEFK	6	1.5	0.4	27
SHQWFGASVR	8	2.3	0.1	4
ILACAPLYHWR	8	2.1	0.8	38
RALFLYSR	6	2.0	0.9	45
Others	5	1.5	0.4	29

A chromatogram from one injection is given in *Figure 34*, with EICs of the four identified peptides. Note, chromatograms shown from trapping of peptides on an AB monolith only shows the first 20 min of the gradient. The last 10 min was only a washing step and no peptides were identified from this part of the gradient.
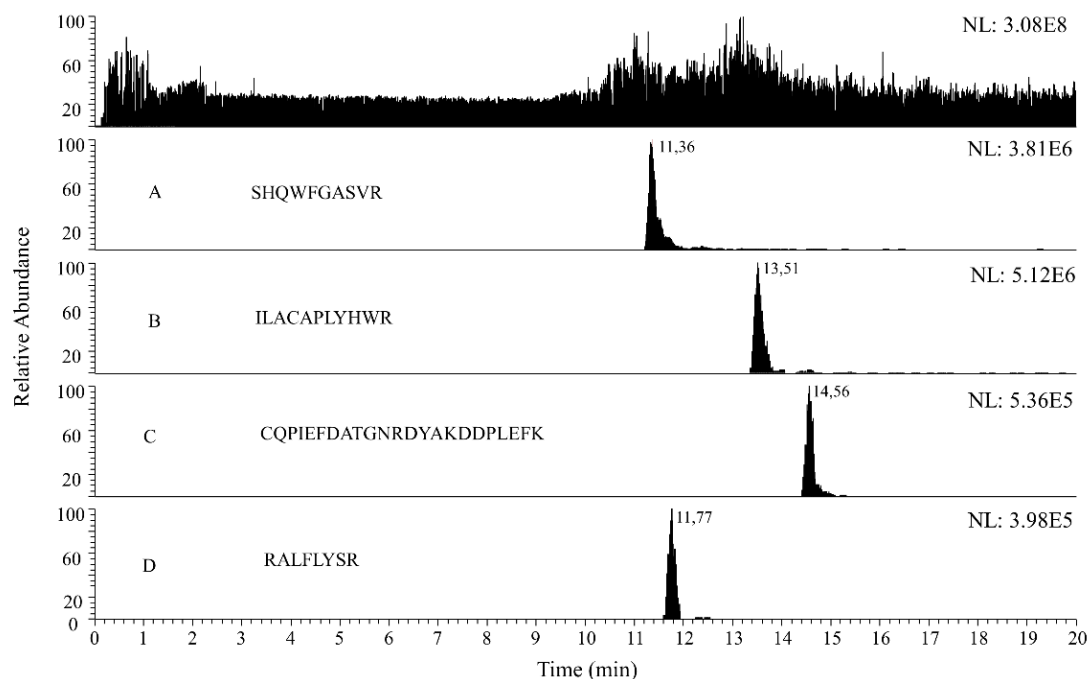
Figure 34 : TICC (top) and EIC (A-D) of peptides identified using setup II. *All four peptides come from the integrin αV chain. Standard concentration was 10 ng µL⁻¹ with 10 µL injection onto the online AB monolith, with 10 min flusing and a dd/MS/MS method. The pre-column was 3 cm and the analytical column was 8 cm. The gradient is given in **Table 2** (Gradient 2). The flow rate was 130 nL min⁻¹. Gaussian smoothing of 15 was applied. A is peptide SHQWFGASVR (m/z 587.79), B is ILACAPLYHWR (m/z 700.37), C is CQPIEFDATGNRDYAKDDPLEFK (m/z 683.07), and D is RALFLYSR (m/z 513.30). Note, the tubing denoted * in **Figure 24** was 450 mm for this injection.*

4.4.2 Missed cleavages and peptide not from the epitope range

Three of the four identified peptides originate from the given epitope range. Two of these are consecutive peptides, CQPIEFDATGNRDYAKDDPLEFK (97-120) and SHQWFGASVR (121-130). It should be noted that CQPIEFDATGNRDYAKDDPLEFK has two missed cleavages. The correctly digested peptides (***Table 5***) were not observed after injection onto the αV AB monolith, but could be observed with Setup I (***Figure 28***). The reason that only the longer peptide chain was observed with the AB monolith could be that it will experience a higher affinity to the AB than the three peptides that comes from a complete digestion.

The fourth identified peptide, RALFLYSR (which also has a missed cleavage), is amino acids 540-547 and then outside the epitope range. Some other peptides were identified outside the given range as well, but unlike RALFLYSR, never more than once. RALFLYSR was identified with noticeably high correlation from several injections. Even in physiological conditions, this amino acid sequence is noticeably distant from the given epitope range. This is illustrated in ***Figure 35***. Why exactly this peptide is also trapped on the αV AB monolith is unknown.

62
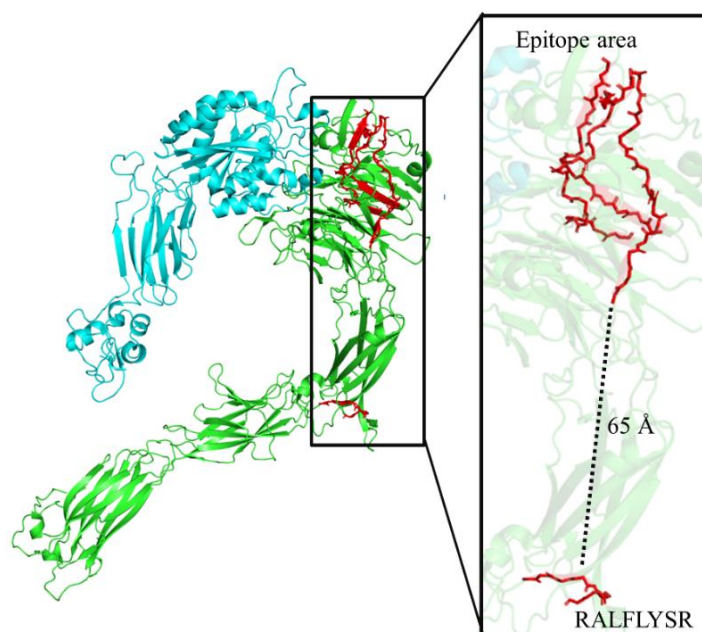
Figure 35: Structure of the extracellular part of αVβ3. The extracellular part of αVβ3 is in active conformation, with the αV chain in green and β3 in blue. The four peptides identified are marked in red. Image made from PDB ID 6AVU [167] using Pymol software. The crystal structure of integrin αVβ1 has not been published to the author's knowledge, but as the chain of interest is the same, the distance could be visualized.

4.4.3 Comparing αV detection with and without an AB monolith

By comparing the obtained coverage from injections of digested integrin standard with and without an αV AB monolithic column, the effect of the AB monolith as a targeted sample-preparation method can be visualized. In *Figure 36*, two ranges both representing the entire integrin αV is shown (amino acid 1 to 1048). Here, the peptides from αV identified by Proteome Discoverer from untargeted detection is marked in green. The top range shows the peptides detected from an injection when an αV AB was used (Setup II). This was the four peptides CQPIEFDATGNRDYAKDDPLEFK, SHQWFGASVR, ILACAPLYHWR and RALFLYSR (as found in **Section 4.4.1**). The bottom range shows the peptides that was detected without using an AB monolith. From one injection without the αV AB monolith, 53 peptides was successfully identified from the αV chain. For comparison, the total score obtained without the αV AB monolith was 424 and a coverage of 50% and with the αV AB monolith the total score was 39 and coverage was 7%.
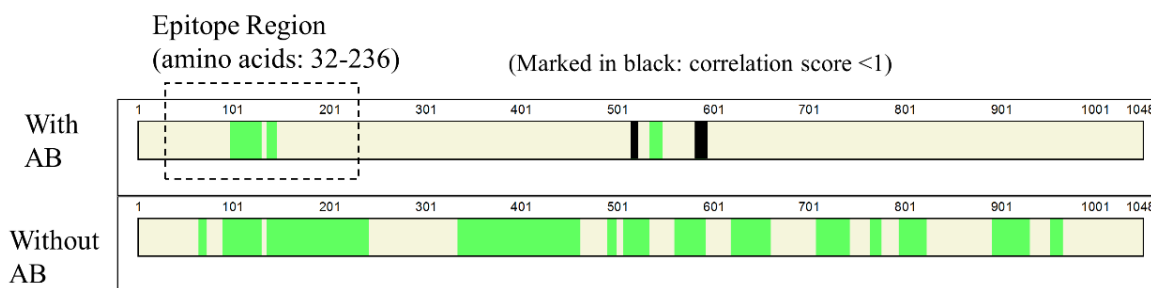
αV-chain

Figure 36: Comparison of detected αV peptides from two injections, one with and one without an αV AB monolith. The range shown is the entire αV chain (amino acid 1-1048). Peptides that are detected by Proteome Discoverer employing the untargeted MS method are shown in green. On the top shows an injection of 100 ng digested αVβ1 standard onto an online αV AB monolith (Setup II) with untargeted MS detection. Here, the epitope range is marked with a dotted line. Peptides marked in black did not fulfil the requirements. The bottom shows an injection of 50 ng digested αVβ1 standard on Setup I (no AB monolith), and the peptides detected from this injection.

The two peptides that do not satisfy the requirement set in this study (score < 1), but is still considered detected by Proteome Discoverer, could be peptides experiencing secondary interactions with the monolith or unspecific binding to the AB.

Figure 36 show that with an online αV AB monolith, much of the peptides from an integrin standard will be washed away whilst peptides from the epitope range will remain and can be detected. This indicates that an online AB monolith has the potential of being used as a selective sample-preparation step.

See **Appendix 7.9.3** for comparison of peptides detected from β1 of the same two injection as shown in *Figure 36*.

4.4.4 Uniqueness of identified peptides

All four identified peptides were examined using the BLAST algorithm. The three peptides identified that are within the given epitope range are all also in an "unnamed protein product". This protein product was found in an unpublished DNA sequencing study from 2008 [168]. The protein product is denoted as "highly similar to Integrin alpha-V precursor". This protein is made up of 481 amino acids, where amino acids 1-473 is identical to amino acids 1-473 in the integrin αV chain. Therefore, the ability for any peptides within this range to work as a signature peptide in a diagnostic method would require further investigation of this "unnamed protein product", but is beyond the scope of this study. This predicament was discovered after the

chosen AB had been obtained. However, the AB was still used in this study as a means of demonstrating the method. By using a different AB a technology transfer could be achieved.

The peptide RALFLYSR is outside the range of the unnamed protein product, and is found to be specific for only the αV integrin chain.

4.4.5 Antibody monolith column lifetime

A monolith was discarded after about 10 injections (including both injections of standard and blanks). This was because of a general decrease in score was observed between subsequent injections, and after a given number of injection no peptides could be identified. The decrease could be a result of the acidic elution conditions used, so that for each new injection, the reconstitution of the ABs was less efficient. As this was not intended as a quantitative study, this decrease was not considered a problem. A more thorough investigation of the lifetime of an AB monolith would be necessary for development of a diagnostic method.

Additionally, the monolith was held within 150 mm of fused silica capillary. At this length and with the coupling to the 6-port valve, the capillary was vulnerable to breaking (this fragility is also present in the nano-LC columns, which are packed in the same type of capillary). As a result, some AB monoliths in this study were used only once or a few times.

To sum up 4.4, by using an untargeted MS method using Setup II, four peptides were successfully identified multiple times, from several αV AB monoliths. Much of the αV peptides were washed off the αV AB monolith. One of the peptides, RALFLYSR is not from the epitope range. The potential of the three other identified peptides, which are within the epitope range, as signature peptides is uncertain. AB monoliths were not used for more than 10 injections due to lifetime issues.

4.5 Targeted detection after trapping of αV

A PRM method was made (**Section 3.7.4,** *Table 3*) where the four peptides identified from the untargeted method were set as the precursor ions. Addition of the peptide sequence SKQDK (mass: 604 Da and expected charge 2 or 3) in the method was examined. SKQDK is the peptide chain between SHQWFGASVR and ILACAPLYHWR. It is quite small, and theoretical digestion will give the peptides SK and QDK. With a missed cleavage, which is allowed in

Proteome Discoverer, it might attach to the AB and be possible to identify. This peptide could not be identified, possibly because it could be it does not experience missed cleavage. Or, because SKQDK has hydrophilic groups on every side chain the intact peptide is washed off the RP pre-column. From 6 injections of 100 ng digested αVβ1 standard with targeted detection, SHQWFGASVR was identified from all injections, ILACAPLYHWR was identified 3 times and RALFLYSR only 2 times. CQPIEFDATGNRDYAKDDPLEFK was not identified from any of these 6 injections. See **Appendix 7.10.1** for the correlation scores from these injections.

4.5.1 The epitope-containing peptide

Injections of decreasing amounts of digested αVβ1 standard onto a αV AB monolith were done to see if all the peptides identified would still be trapped and/or identified. All previous data presented were from injections of 100 ng digested integrin αVβ1 standard. From three injections of 50 ng, only SHQWFGASVR was identified and none of the other peptides. The average correlation score of this peptides from the 3 injections was 1.5 with a relative standard deviation of 18%. See **Appendix 7.10.2** for the data these values are calculated from. Injections of 10 and 1 ng digested integrin αVβ1 standard did also only allow identification of SHQWFGASVR. The correlation scores from the injection of 10 ng and 1 ng digested integrin standard was 1.9 and 1.5, respectively. *Figure 37* show the EIC of the peak for SHQWFGASVR from injections of 100, 10 and 1 ng.

These identifications, and the high repeatability from untargeted identification (*Table 9*, **Section 4.4.1**), can be an indication that the epitope is located within the peptide SHQWFGASVR. This shows that it may be possible to find the epitope-containing peptide experimentally using an online setup. In other studies, the epitope has been known as they used Abs against a known peptide, such as in [169-171]. The method presented in this study is then also an alternative method of investigating the application of commercially available ABs for peptide enrichment of a target protein, compared to [147] and [172], which uses an offline method trapping epitope-containing peptides with mABs attached to beads.
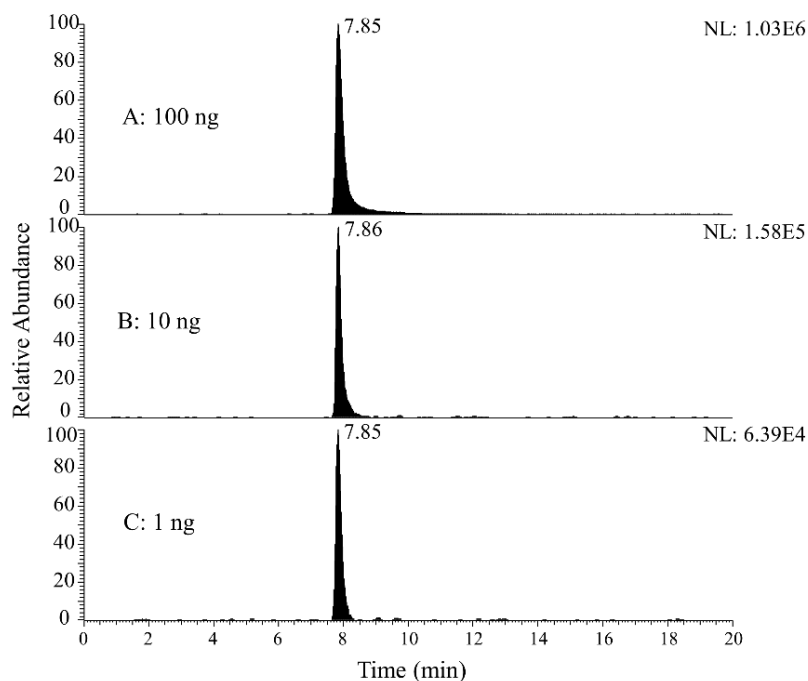
Figure 37: *EIC (A-C) of peptide SHQWFGASVR from injections of 100, 10 and 1 ng identified using setup II. All the EICs are of the fragment b_2^+ (m/z 225.10), which was the most intense for all injections. For A and B, the concentration of the injected standard was 10 ng μL^{-1}, with injection volumes of 10 and 1 μL, respectively. For C the concentration was 1 ng μL^{-1}, with an injection volumes of 1 μL. They were found using the PRM method given in **Table 3** with 10 min flushing. The pre-column was 3 cm and the analytical column was 8 cm. The gradient is given in **Table 2** (Gradient 2). The flow rate was 130 nL min^{-1}. Gaussian smoothing of 15 was applied.*

In *Figure 38* and *Figure 39* TICCs and EICs of all the identified fragments from injections of 100 ng and 1 ng are shown, respectively. TICC and EIC from injection of 10 ng can be found in **Appendix 7.10.3**. Injections of 10 and 1 ng were only performed one time each due to time constraints. From the injection of 100, 50 and 10 ng digested integrin standard, all the 6 fragments that are shown in *Figure 38* were identified, with decreasing NL values with decreasing amount. When 1 ng standard was injected, only 5 of the 6 fragments were identified (y_8^+ was not identified).

Figure 38: TICC (top) and EIC (A-F) of fragments from peptide SHQWFGASVR (m/z 587.79) identified using setup II with 100 ng standard injected. *Standard concentration was 10 ng µL⁻¹ with 10 µL injection onto the online AB monolith, with 10 min flushing and a PRM method. The pre-column was 3 cm and the analytical column was 8 cm. The gradient is given in* **Table 2** *(Gradient 2). The flow rate was 130 nL min⁻¹. Gaussian smoothing of 15 was applied. A is fragment b_2^+(m/z 225.10), B is fragment b_3^+(m/z 353.15), C is fragment y_5^+(m/z 489.27), D is fragment y_6^+(m/z 635.84), E is fragment y_7^+(m/z 821.92), and F is fragment y_8^+(m/z 949.98).*

Figure 39: TICC (top) and EIC (A-E) of fragments from peptide SHQWFGASVR (m/z 587.79) identified using setup II with 1 ng standard injected. The chromatographic setup is the same as in **Figure 38**.

Together with the issues mentioned in **Section 4.4.4**, the presence of W in a SHQWFGASVR can be problematic for the use of this peptide as a signature peptide. This is because this amino

68

acid can experience oxidation, giving a change in its mass and structure [173]. The oxidation of W was included as a possible modification for searches in Proteome Discoverer. However, if the AB is unable to bind if this modification is present, the peptide would be lost during flushing of the monolith. It is shown that tryptophan will appear in its non-oxidized form as SHQWFGASVR is identified. A possible oxidation will then be most problematic in regards to quantification.

To sum up 4.5, a PRM method for four peptides were made. Using Setup II, only peptide SHQWFGASVR could be found at concentrations below 100 ng. This could indicate that the epitope is located within this peptide.

4.6   Application of methods to cellular sample

A digested sample of GBM cells was injected onto an αV AB monolith to examine whether the peptides in the PRM method (***Table 3****)* could be identified. GBM is a very aggressive form of brain tumour [174], and this project is part of a larger project investigating the use of biomarkers to diagnose this form of brain cancer. The presences of the αV integrin chain in cellular samples from this tumour had already been verified through a comprehensive proteomics analysis by Henriette Engen Berg.

4.6.1 Detection of epitope-containing peptide in targeted mode

Three injections of digested GBM cells were performed. Each with a volume of 10 µL at a concentration of 1 µg µL^{-1} of total protein. The peptide SHQWFGASVR was successfully identified from the cell sample from all three injections, with an average correlation score of 1.6 with a relative standard deviation of 6% (n=3). (See **Appendix 7.11.1** for values). ***Figure 40*** shows the TICC and EICs of the identified fragments from one of the injections. Blanks were injected between all injections to ensure that no carryover was present.
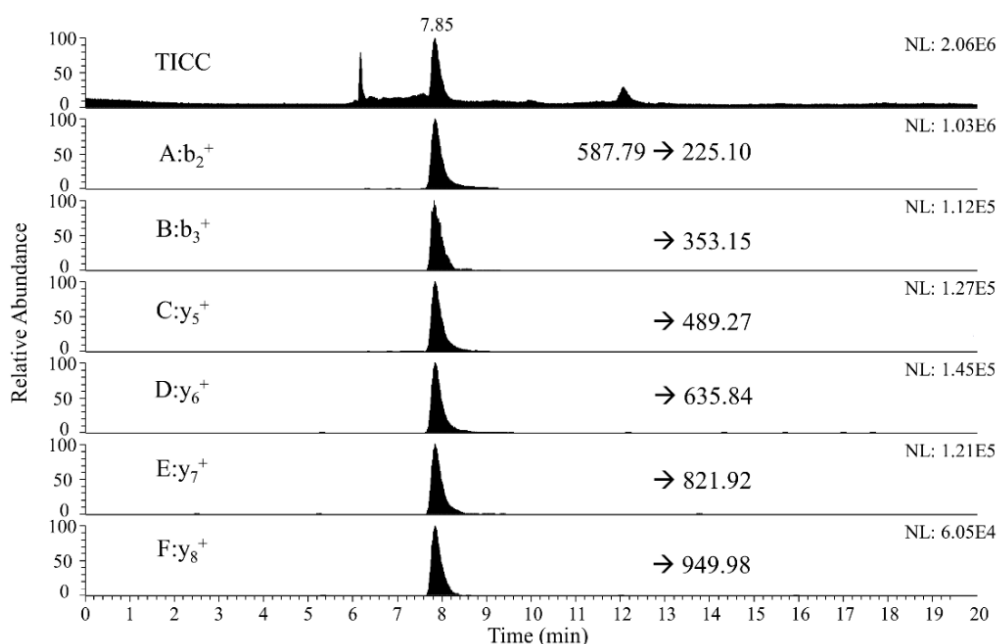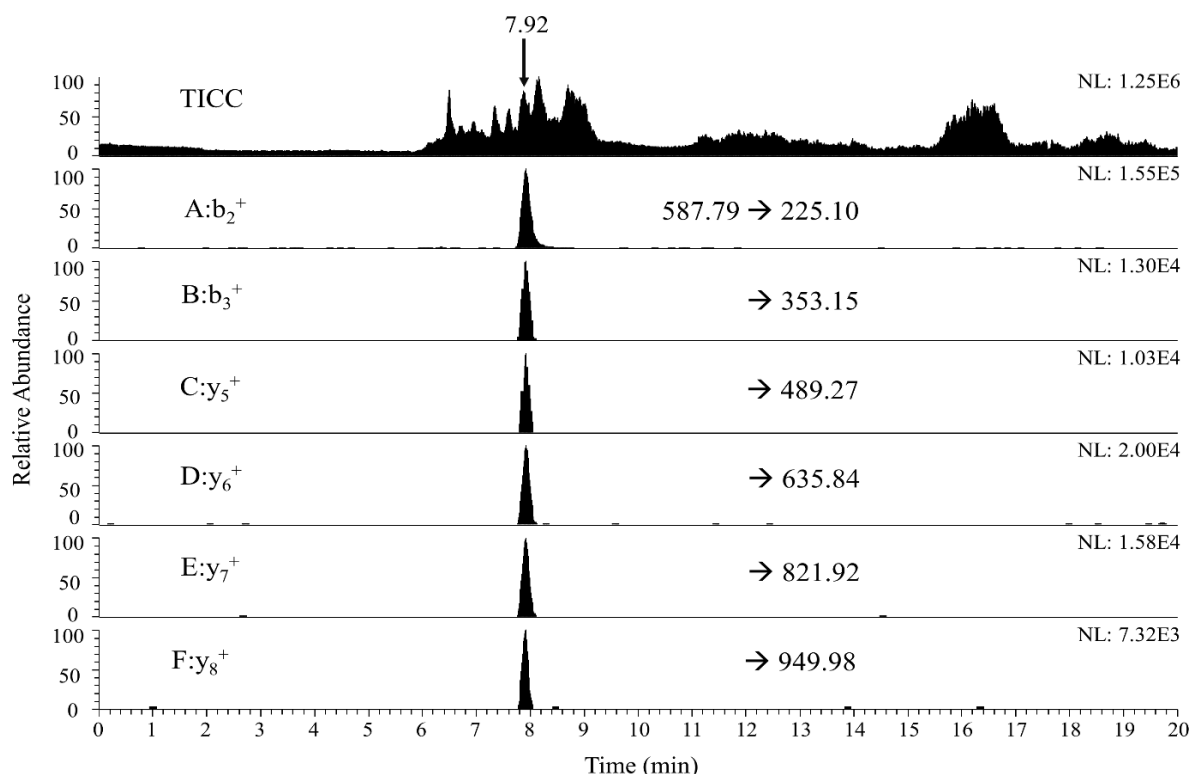
Figure 40: TICC (top) and EIC (A-F) of fragments from peptide SHQWFGASVR (m/z 587.79) identified using setup II from injection of a GBM cellular sample. *Total protein concentration was 1 µg µL^{-1} with 10 µL injection onto the online αV AB monolith, with 10 min flusing. The pre-column was 3 cm and the analytical column was 8 cm. The gradient is given in **Table 2** (Gradient 2). The flow rate was 130 nL min^{-1}. Gaussian smoothing of 15 was applied. A is fragment b$_2$$^+$(m/z 225.10), B is fragment b$_3$$^+$(m/z 353.15), C is fragment y$_5$$^+$(m/z 489.27), D is fragment y$_6$$^+$(m/z 635.84), E is fragment y$_7$$^+$(m/z 821.92), and F is fragment y$_8$$^+$(m/z 949.98).*

No other peptide in the PRM method from the PRM method was identified from the cell sample.

It should be noted that there are five different integrins in the human body that contains the integrin αV chain; aVβ1, αVβ3, αVβ5, αVβ6 and αVβ8 (see ***Figure 4***). Hence, the αV detected could be from any of these.

4.6.2 Evaluation of flushing efficiency with untargeted mode

Two injections of digested GBM onto an αV AB monolith were analysed with untargeted MS detection. This was done to see if any other proteins would be remaining on the AB monolith after a flushing period of 1 min and 10 min, respectively. Flushing for 1 min with 5 µL min^{-1} is close to 2.5 column volumes. A 10 min flushing (which was used throughout this study) with 5 µL min^{-1} is close to 25 column volumes (estimating that the monolith takes up 50% of the volume). If large amounts of proteins, not from αV, remained after flushing and entered the MS, the AB monolith could not be considered a sufficiently selective sample preparation method. In ***Table 10*** the numbers of the proteins identified from these two injections are given.

70

Table 10: *The protein numbers from the two different injections of GBM cells onto the αV AB monolith, with an untargeted MS-detection method.*

	Volume injected (µL) (protein concentration: 1 µg µL^{-1})	Number of proteins identified (score≠0)	Highest coverage (%)	Highest score
1 min flushing	10	207	52	227
10 min flushing	5	4	12	13

In *Figure 41* the TICCs from the two different injections are given. In *Figure 42* and *Figure 43* comparison of the scores and coverage factors, respectively, from the two injections are given.
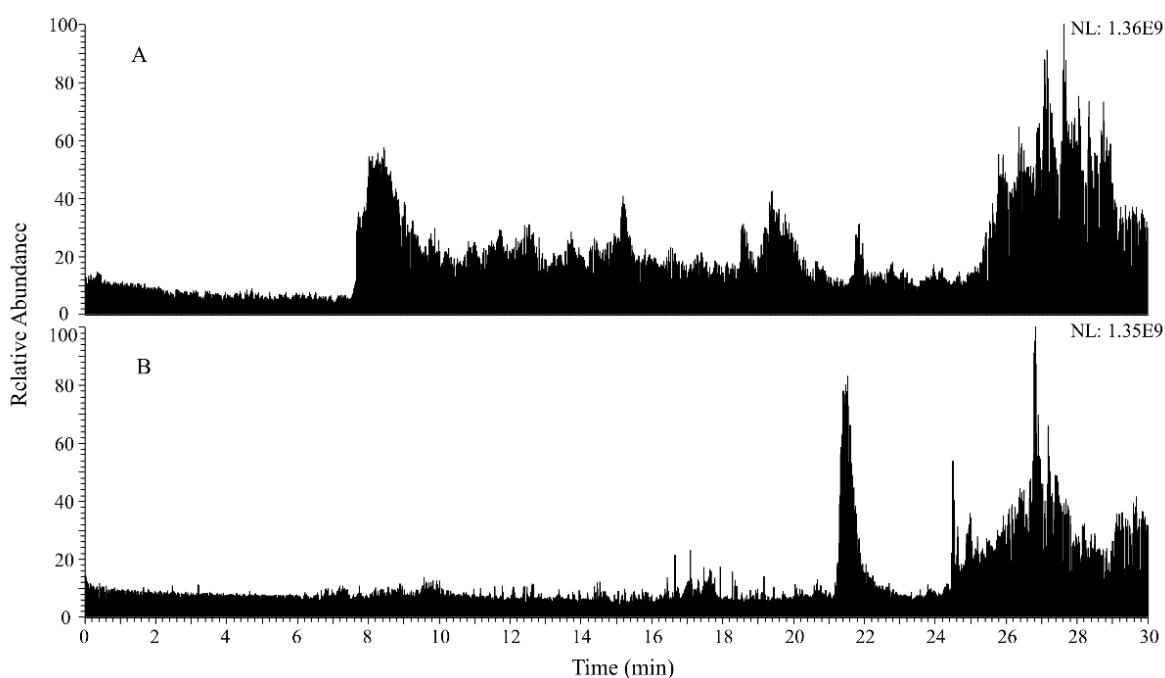
Figure 41: TICC of untargeted GBM cellular sample. *Both were found using Setup II with untargeted detection and gradient 2 in **Table 2**. A shows the TICC from injection of 10 µL sample that was flushed for 1 min. B shows the TICC from 5 µL injection, which was flushed for 10 min. The entire 30 min of the gradient is shown in the TICC, as peptides were also detected in the 10 min washing step.*
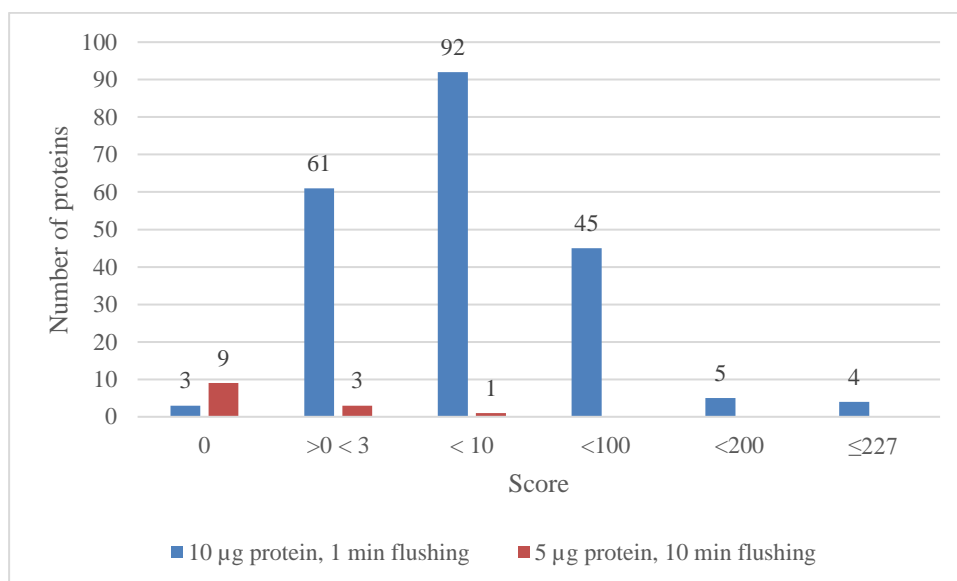
Figure 42: The scores of the proteins detected in cell samples with untargeted detection. The scores are grouped, showing the number of proteins found with a score of 0, lower than 3, 10, 100, 200 and 227.
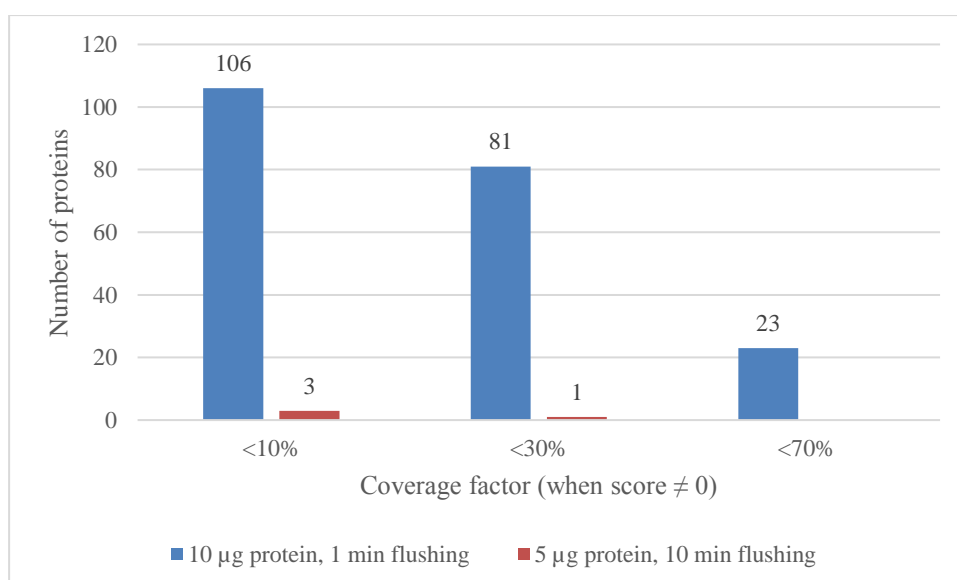
Figure 43: The coverage factors of the proteins detected in cell samples with untargeted detection. Values were only included when the score was not zero. The scores are grouped in three different values, does with scores below 10%, 30% and 70%, respectively.

Two different injection volumes were used, 10 µL and 5µL, due to small sample amount being available. Both had a total protein concentration of 1 µg µL^{-1}. This means that the results found from these experiments are not fully comparable, but they can be evaluated together.

For 10 µL injection with only 1 min flushing (2.5 column volumes), the total number of proteins identified was 201. Many of them with scores over 14 and coverage over 20%. These are comparatively higher numbers than the 13 proteins that was identified in Proteome Discoverer

from injection of 5 µL, with none of them having scores over 14 or coverage over 12%. A full list of the proteins identified, with score and coverage can be found in **Appendix 7.11.2**.

When the sample only was flushed for 1 min, the list of proteins may not be complete. The method used in this study had an 8 cm analytical column and a 30 min gradient. Comprehensive cellular proteomics studies usually have 15 cm analytical columns, with gradients up to 120 min to ensure efficient separation. An inefficient separation can mean more co-elution causing ion suppression and meaning the scan rate of the MS might not be sufficient.

Particularly the number of proteins identified can be an indication that flushing over a given amount of time can remove much of the proteins in a cellular sample. However, no αV peptide was identified from either of these two injection. But, together with the positive identification of the αV peptide SHQWFGASVR from GBM cells in a targeted method (**Section 4.6.1**), it shows the potential that for targeted, online sample clean-up an AB monolith could be a possible solution. The reason no αV peptide could be detected from injections of the untargeted method could be due to the AB monolith being "past its lifetime" (monolith lifetime had only been examined using integrin standards). Also, the proteins that were detected (score $\neq 0$) are all in the top 5% of the most abundant proteins in humans, (integrin αV is usually in the top 25% or lower) [107]. Therefore, even if SHQWFGASVR entered the MS it could be that the sensitivity obtained with the MS in untargeted mode is insufficient.

In a targeted PRM method, the peptide SHQWFGASVR was successfully identified from a GBM cellular sample. In an untargeted method, this peptide could not be identified from a cellular sample, but a noticeable decrease in protein content was obtained when the monolith was flushed for 10 min.

5 Conclusion

To the question "did this work give support for the hypothesis given in **Section 2**?" the answer is both yes and no. The developed system could detect an integrin peptide, but only from one of the two chains investigated for AB trapping.

Three integrins were chosen for this study; αVβ1, α3β1 and αVβ5, and ABs for the β1, β5 and αV chains were used. Peptides from α3β1 and αVβ5 could not be detected after an in-solution digestion using a "standard" nano-LC-MS setup (without an AB monolith). No modification of the in-solution digestion method resulted in successful detection of α3β1 or αVβ5. WB with β1 and β5 ABs verified the presence of the integrins in the purchased solution. α3β1- and αVβ5 peptides were identified using the "standard" nano-LC-MS setup after an in-gel digestion.

Integrin αVβ1 was successfully identified after an in-solution digestion. This integrin was intended as a negative control, but considered adequate to use to show proof of concept. Neither FASP nor heat was found suitable for removal/deactivation of trypsin, hence trypsin inhibitor was added to avoid AB degradation by trypsin. Injection of 100 ng digested αVβ1 onto an β1 AB monolith, with subsequent nano-LC-MS analysis, failed to give successful identification of a peptide. Injection of 100 ng digested αVβ1 onto online an αV AB monolith, with subsequent nano-LC-MS analysis, gave successful identification of four peptides; CQPIEFDATGNRDYAKDDPLEFK, SHQWFGASVR, ILACAPLYHWR and RALFLYSR. The first three are from the given epitope range. When injecting 10 ng and 1 ng of digested αVβ1 onto an αV AB monolith only SHQWFGASVR was detected. The results αV AB monolith results shows that trapping of integrin peptides using an AB monolith is possible. However, the results from β1 AB monolith shows that different integrin chains will not necessarily be trapped using the same sample preparations and setup.

When 10 µg of total protein from GBM cells were injected, SHQWFGASVR was detected with a targeted method. Showing that an integrin peptide can be trapped and detected from a cancerous sample, using the technique developed in this study. From analysis of a cellular sample with untargeted MS mode, flushing the monolith for 1 min and 10 min, gave successful detection of 207 proteins (10 µg protein injected) and 4 proteins (5 µg protein injected), respectively. SHQWFGASVR was not identified from the injections of cellular samples with untargeted MS mode.

5.1 Future work

The method developed here could be further automated, with more focus on the lifetime of the AB monolith. Investigations should also be made as to how much AB binds to the monolith, to investigate how many monoliths could be produced from a given amount of purchased AB. As mentioned earlier, an online digestion column preceding the AB monolith could be implemented.

This method of trapping peptides on an AB monolith should be possible to make for various integrins, and also other protein groups. Investigation of digestion methods might be necessary to ensure that the epitope remains intact. For integrins AB monoliths could be coupled in series, each for a different α or β chain, allowing detection of several integrins from one injection.

6 References

1. B. Alberts, *Essential Cell Biology*. 3rd ed. 2010, New York: Garland Science:121-127, 696-723.
2. M. Uhlen, C. Zhang, S. Lee, E. Sjöstedt, L. Fagerberg, G. Bidkhori, R. Benfeitas, M. Arif, Z. Liu, F. Edfors, K. Sanli, K. Von Feilitzen, P. Oksvold, E. Lundberg, S. Hober, P. Nilsson, J. Mattsson, J.M. Schwenk, H. Brunnström, B. Glimelius, T. Sjöblom, P.-H. Edqvist, D. Djureinovic, P. Micke, C. Lindskog, A. Mardinoglu, and F. Ponten, *A pathology atlas of the human cancer transcriptome*. Science. 357 (**2017**):eaan2507, DOI: 10.1126/science.aan2507.
3. R.J. Deberardinis, J.J. Lum, G. Hatzivassiliou, and C.B. Thompson, *The Biology of Cancer: Metabolic Reprogramming Fuels Cell Growth and Proliferation*. Cell Metabolism. 7 (**2008**):11-20.
4. S. Paget, *The distribution of secondary growths in cancer of the breast*. The Lancet. 133 (**1889**):571-573.
5. I.J. Fidler, *The pathogenesis of cancer metastasis: the 'seed and soil' hypothesis revisited*. Nature Reviews Cancer. 3 (**2003**):453-458.
6. M. Patrick and P. Alain, *Metastasis: a question of life or death*. Nature Reviews Cancer. 6 (**2006**):449-458.
7. C. Chaffer and R. Weinberg, *A Perspective on Cancer Cell Metastasis*. Science. 331 (**2011**):1559-1564.
8. L. Cheng, H. Zincke, M.L. Blute, E.J. Bergstralh, B. Scherer, and D.G. Bostwick, *Risk of prostate carcinoma death in patients with lymph node metastasis*. Cancer. 91 (**2001**):66-73.
9. M.S. Pepe, R. Etzioni, Z. Feng, J.D. Potter, M.L. Thompson, M. Thornquist, M. Winget, and Y. Yasui, *Phases of Biomarker Development for Early Detection of Cancer*. Journal of the National Cancer Institute. 93 (**2001**):1054-1061.
10. R.L. Siegel, K.D. Miller, and A. Jemal, *Cancer statistics, 2018*. CA: A Cancer Journal for Clinicians. 68 (**2018**):7-30.
11. R. Etzioni, N. Urban, S. Ramsey, M. Mcintosh, S. Schwartz, B. Reid, J. Radich, G. Anderson, and L. Hartwell, *The case for early detection*. Nature Reviews Cancer. 3 (**2003**):243-252.
12. A.J. Atkinson Jr, W.A. Colburn, V.G. DeGruttola, D.L. DeMets, G.J. Downing, D.F. Hoth, J.A. Oates, C.C. Peck, R.T. Schooley, B.A. Spilker, J. Woodcock, and S.L. Zeger, *Biomarkers and surrogate endpoints: Preferred definitions and conceptual framework*. Clinical Pharmacology & Therapeutics. 69 (**2001**):89-95.
13. L.T. Brinton, T.A. Brentnall, J.A. Smith, and K.A. Kelly, *Metastatic Biomarker Discovery Through Proteomics*. Cancer Genomics & Proteomics. 9 (**2012**):345-355.
14. C. Kan, G. Vargas, F. Le Pape, and P. Clezardin, *Cancer Cell Colonisation in the Bone Microenvironment*. International Journal of Molecular Science. 17 (**2016**):1674-1689.
15. S. D' Oronzo, J. Brown, and R. Coleman, *The value of biomarkers in bone metastasis*. European Journal of Cancer Care. 26 (**2017**):e12725-e12734.
16. J. Rusling, C. Kumar, J. Gutkind, and V. Patel, *Measurement of biomarker proteins for point-of-care early detection and monitoring of cancer*. Analyst. 135 (**2010**):2496-2511.

17. Z. Li, H. Lv, T. Li, G. Si, Q. Wang, J. Lv, and X. Hu, *Reagent-free simultaneous determination of glucose and cholesterol in whole blood by FTIR-ATR.* Spectrochimica Acta Part A: Molecular and Biomolecular Spectroscopy. 178 (**2017**):192-197.

18. C.E. Thomas, W. Sexton, K. Benson, R. Sutphen, and J. Koomen, *Urine Collection and Processing for Protein Biomarker Discovery and Quantification.* Cancer Epidemiology, Biomarkers & Prevention. 19 (**2010**):953-959.

19. L. Chung, S. Shibli, K. Moore, E.E. Elder, F.M. Boyle, D.J. Marsh, and R.C. Baxter, *Tissue biomarkers of breast cancer and their association with conventional pathologic features.* British Journal of Cancer. 108 (**2013**):351-360.

20. S.S. Salami, D. Hovelson, R. Mathieu, J. Kaplan, M. Susani, N. Rioux-Leclercq, S. Shariat, S.A. Tomlins, and G. Palapattu, *Comprehensive molecular profiling of multi-focal prostate cancer and concomitant lymph node metastasis: Implications for tissue-based prognostic biomarkers.* Journal of Clinical Oncology. 35 (**2017**):5061-5061.

21. A.W. Roddam, M.J. Duffy, F.C. Hamdy, A.M. Ward, J. Patnick, C.P. Price, J. Rimmer, C. Sturgeon, P. White, and N.E. Allen, *Use of Prostate-Specific Antigen (PSA) Isoforms for the Detection of Prostate Cancer in Men with a PSA Level of 2–10 ng/ml: Systematic Review and Meta-Analysis.* European Urology. 48 (**2005**):386-399.

22. S. Schuler-Toprak, O. Treeck, and O. Ortmann, *Human Chorionic Gonadotropin and Breast Cancer.* International Journal of Molecular Sciences. 18 (**2017**):1587-1599.

23. *IUPAC-IUB Joint Commission on Biochemical Nomenclature (JCBN) - Nomenclature and symbolism for amino acids and peptides. Recommendations 1983.* Biochemical Journal. 219 (**1984**):345-373.

24. D. Voet, J.G. Voet, and C. Pratt, *Principles of Biochemistry*. 4th ed. 2013, Hoboken: Wiley:210-263.

25. S. Iwata, J.W. Lee, K. Okada, J.K. Lee, M. Iwata, B. Rasmussen, T.A. Link, S. Ramaswamy, and B.K. Jap, *Complete Structure of the 11-Subunit Bovine Mitochondrial Cytochrome bc1 Complex.* Science. 281 (**1998**):64-71.

26. G.A. Petsko and D. Ringe, *Protein Structure and Function*. Primers in Biology. 2004, London: New Science Press:24-25.

27. R.O. Hynes, *Integrins: A family of cell surface receptors.* Cell. 48 (**1987**):549-554.

28. R.O. Hynes, *Integrins: Bidirectional, Allosteric Signaling Machines.* Cell. 110 (**2002**):673-687.

29. UniProt, *P05556 (ITB1_HUMAN).* [Accessed 09.03. 2018]; Available from: http://www.uniprot.org/uniprot/P05556

30. UniProt, *P06756 (ITAV_HUMAN).* [Accessed 09.03. 2018]; Available from: http://www.uniprot.org/uniprot/P06756

31. J.S. Desgrosellier and D.A. Cheresh, *Integrins in cancer: biological implications and therapeutic opportunities.* Nature Reviews Cancer. 10 (**2010**):9-22.

32. G. Wenjun and G.G. Filippo, *Integrin signalling during tumour progression.* Nature Reviews Molecular Cell Biology. 5 (**2004**):816-826.

33. G.J. Mizejewski, *Role of Integrins in Cancer: Survey of Expression Patterns.* Proceedings of the Society for Experimental Biology and Medicine. 222 (**1999**):124-138.

34. A. Hoshino, B. Costa-Silva, T.-L. Shen, G. Rodrigues, A. Hashimoto, M. Tesic Mark, H. Molina, S. Kohsaka, A. Di Giannatale, S. Ceder, S. Singh, C. Williams, N. Soplop, K. Uryu, L. Pharmer, T. King, L. Bojmar, A.E. Davies, Y. Ararso, T. Zhang, H. Zhang, J. Hernandez, J.M. Weiss, V.D. Dumont-Cole, K. Kramer, L.H. Wexler, A. Narendran, G.K. Schwartz, J.H. Healey, P. Sandstrom, K. Jørgen Labori, E.H. Kure, P.M. Grandgenett, M.A. Hollingsworth, M. de Sousa, S. Kaur, M. Jain, K. Mallya, S.K. Batra, W.R. Jarnagin, M.S. Brady, O. Fodstad, V. Muller, K. Pantel, A.J. Minn, M.J.

Bissell, B.A. Garcia, Y. Kang, V.K. Rajasekhar, C.M. Ghajar, I. Matei, H. Peinado, J. Bromberg, and D. Lyden, *Tumour exosome integrins determine organotropic metastasis.* Nature. 527 (**2015**):329-335.

35. M.-Y. Hsu, D.-T. Shih, F.E. Meier, P. Van Belle, J.-Y. Hsu, D.E. Elder, C.A. Buck, and M. Herlyn, *Adenoviral Gene Transfer of β3 Integrin Subunit Induces Conversion from Radial to Vertical Growth Phase in Primary Human Melanoma.* The American Journal of Pathology. 153 (**1998**):1435-1442.

36. E. Sloan, N. Pouliot, K. Stanley, J. Chia, J. Moseley, D. Hards, and R. Anderson, *Tumor-specific expression of alphavbeta3 integrin promotes spontaneous metastasis of breast cancer to bone.* Breast Cancer Research. 8 (**2006**):R20-R50.

37. V. Sung, J.T. Stubbs, L. Fisher, A.D. Aaron, and E.W. Thompson, *Bone sialoprotein supports breast cancer cell adhesion proliferation and migration through differential usage of the alpha(v)beta3 and alpha(v)beta5 integrins.* Journal of Cellular Physiology. 176 (**1998**):482-494.

38. N.P. McCabe, S. De, A. Vasanji, J. Brainard, and T.V. Byzova, *Prostate cancer specific integrin αvβ3 modulates bone metastatic growth and tissue remodeling.* Oncogene. 26 (**2007**):6238-6243.

39. R. Hosotani, M. Kawaguchi, T. Masui, T. Koshiba, J. Ida, K. Fujimoto, M. Wada, R. Doi, and M. Imamura, *Expression of integrin alphaVbeta3 in pancreatic carcinoma: relation to MMP-2 activation and lymph node metastasis.* Pancreas. 25 (**2002**):e30-35.

40. L. Bello, J. Zhang, R.S. Carroll, D.C. Nikas, J.F. Strasser, R. Villani, P.M. Black, M. Francolini, P. Marthyn, and D.A. Cheresh, *αvβ3 and αvβ5 integrin expression in glioma periphery.* Neurosurgery. 49 (**2001**):380-390.

41. T. Meyer, J.F. Marshall, and I.R. Hart, *Expression of alphav integrins and vitronectin receptor identity in breast cancer cells.* British Journal of Cancer. 77 (**1998**):530-536.

42. S.Y. Bai, N. Xu, C. Chen, Y.L. Song, J. Hu, and C.X. Bai, *Integrin αvβ5 as a biomarker for the assessment of non‐small cell lung cancer metastasis and overall survival.* Clinical Respiratory Journal. 9 (**2015**):457-467.

43. S. Hazelbag, G. Kenter, A. Gorter, E. Dreef, L. Koopman, S. Violette, P. Weinreb, and G. Fleuren, *Overexpression of the αvβ6 integrin in cervical squamous cell carcinoma is a prognostic factor for decreased survival.* Journal of Pathology. 212 (**2007**):316-324.

44. R. Bates, D. Bellovin, C. Brown, E. Maynard, B. Wu, H. Kawakatsu, D. Sheppard, P. Oettgen, and A.M. Mercurio, *Transcriptional activation of integrin beta6 during the epithelial-mesenchymal transition defines a novel prognostic indicator of aggressive colon carcinoma.* Journal of Clinical Investigation. 115 (**2005**):339-347.

45. C. Fedele, A. Singh, B.J. Zerlanko, R.V. Iozzo, and L.R. Languino, *The αvβ6 integrin is transferred intercellularly via exosomes.* The Journal of Biological Chemistry. 290 (**2015**):4545-4551.

46. L. Klaus, R.-N. Jesus, J.S. William, and S. Sanford, *Integrin-based therapeutics: biological basis, clinical use and new drugs.* Nature Reviews Drug Discovery. 15 (**2016**):173-183.

47. W.S. Carbonell, M. Delay, A. Jahangiri, C.C. Park, and M.K. Aghi, *β1 integrin targeting potentiates antiangiogenic therapy and inhibits the growth of bevacizumab-resistant glioblastoma.* Cancer Research. 73 (**2013**):3145-3154.

48. M.R. Wilkins, J.C. Sanchez, A.A. Gooley, R.D. Appel, I. Humphery-Smith, D.F. Hochstrasser, and K.L. Williams, *Progress with proteome projects: why all proteins expressed by a genome should be identified and how to do it.* Biotechnology & Genetic Engineering Reviews. 13 (**1996**):19-50.

49.   *Method of the year 2012: new method and tool developments are helping to bring targeted proteome analysis technologies to a broader array of biologists.(Editorial).* Nature Methods. 10 (**2013**):1.

50.   R.C. King, P.K. Mulligan, and W.D. Stansfield, *"Immunoglobulin"*, A Dictionary of Genetics 2013, Oxford University Press.

51.   H.W. Schroeder and L. Cavacini, *Structure and function of immunoglobulins.* The Journal of Allergy and Clinical Immunology. 125 (**2010**):348-348.

52.   M. Torres and A. Casadevall, *The immunoglobulin constant region contributes to affinity and specificity.* Trends in Immunology. 29 (**2008**):91-97.

53.   G. Kohler and C. Milstein, *Continuous cultures of fused cells secreting antibody of predefined specificity.* Nature. 256 (**1975**):495-497.

54.   W.N. Burnette, *"Western Blotting": Electrophoretic transfer of proteins from sodium dodecyl sulfate-polyacrylamide gels to unmodified nitrocellulose and radiographic detection with antibody and radioiodinated protein A.* Analytical Biochemistry. 112 (**1981**):195-203.

55.   T. Mahmood and P. Yang, *Western blot: Technique, theory, and trouble shooting.* North American Journal of Medical Sciences. 4 (**2012**):429-434.

56.   M. Baker, *Reproducibility crisis: Blame it on the antibodies.* Nature. 521 (**2015**):274-276.

57.   J. Nissen-Meyer, E. Boye, B. Osterud, and T. Skotland, *WADA-accredited doping analyses cannot always be trusted.* Lab Times. 5 (**2015**):18-23.

58.   E. Papadopulos-Eleopulos, V.F. Turner, and J.M. Papadimitriou, *Is a Positive Western Blot Proof of HIV Infection?* Nature Biotechnology. 11 (**1993**):696-707.

59.   A.N. Hoofnagle and M.H. Wener, *The fundamental flaws of immunoassays and potential solutions using tandem mass spectrometry.* Journal of Immunological Methods. 347 (**2009**):3-11.

60.   D.C. Harris, *Quantitative chemical analysis.* 8th ed. 2010, New York: Freeman:512-519.

61.   K.K. Murray, R.K. Boyd, M.N. Eberlin, G.J. Langley, L. Li, and Y. Naito, *Definitions of terms relating to mass spectrometry (IUPAC Recommendations 2013).* Pure and Applied Chemistry. 85 (**2013**):1515-1609.

62.   A. Michalski, E. Damoc, J.-P. Hauschild, O. Lange, A. Wieghaus, A. Makarov, N. Nagaraj, J. Cox, M. Mann, and S. Horning, *Mass Spectrometry-based Proteomics Using Q Exactive, a High-performance Benchtop Quadrupole Orbitrap Mass Spectrometer* Molecular & Cellular Proteomics. 10 (**2011**):DOI 10.1074/mcp.M111.011015.

63.   A. Makarov, E. Denisov, A. Kholomeev, W. Balschun, O. Lange, K. Strupat, and H. Stevan, *Performance evaluation of a hybrid linear ion trap/orbitrap mass spectrometer.* Analytical Chemistry. 78 (**2006**):2113-2120.

64.   W. Paul, *Electromagnetic traps for charged and neutral particles.* Reviews of Modern Physics. 62 (**1990**):531-540.

65.   A. Makarov, *Electrostatic axially harmonic orbital trapping: A high-performance technique of mass analysis.* Analytical Chemistry. 72 (**2000**):1156-1162.

66.   F.W. McLafferty, *Tandem mass spectrometry.* Science. 214 (**1981**):280-287.

67.   J.V. Olsen, B. Macek, O. Lange, A. Makarov, S. Horning, and M. Mann, *Higher-energy C-trap dissociation for peptide modification analysis.* Nature Methods. 4 (**2007**):709.

68.   R. Bakhtiar, S.A. Hofstadler, and R.D. Smith, *Electrospray ionization mass spectrometry Part II: Applications in characterization of peptides and proteins.* Journal of Chemical Education. 73 (**1996**):A118-A123.

69. M.S. Wilm and M. Mann, *Electrospray and Taylor-Cone theory, Dole's beam of macromolecules at last?* International Journal of Mass Spectrometry and Ion Processes. 136 (**1994**):167-180.

70. H. Steen and M. Mann, *The abc's (and xyz's) of peptide sequencing.* Nature Reviews Molecular Cell Biology. 5 (**2004**):699-711.

71. A.P. Bruins, *Mechanistic aspects of electrospray ionization.* Journal of Chromatography A. 794 (**1998**):345-357.

72. M. Dole, L.L. Mack, R.L. Hines, R.C. Mobley, L.D. Ferguson, and M.B. Alice, *Molecular Beams of Macroions.* The Journal of Chemical Physics. 49 (**1968**):2240-2249.

73. J.V. Iribarne and B.A. Thomson, *On the evaporation of small ions from charged droplets.* The Journal of Chemical Physics. 64 (**1976**):2287-2294.

74. E. Lundanes, L. Reubsaet, and T. Greibrokk, *Chromatography : Basic Principles, Sample Preparations and Related Methods*. 1st ed. Chromatography. 2013, Hoboken: Wiley:3-87.

75. T.M. Annesley, *Ion suppression in mass spectrometry.* Clinical Chemistry. 49 (**2003**):1041-1044.

76. A. Schmidt, M. Karas, and T. Dülcks, *Effect of different solution flow rates on analyte ion signals in nano-ESI MS, or: when does ESI turn into nano-ESI?* Journal of the American Society for Mass Spectrometry. 14 (**2003**):492-500.

77. R. Aebersold and M. Mann, *Mass-spectrometric exploration of proteome structure and function.* Nature. 537 (**2016**):347-355.

78. B. Domon and R. Aebersold, *Mass spectrometry and protein analysis.* Science. 312 (**2006**):212-217.

79. B.T. Chait, *Mass Spectrometry: Bottom-Up or Top-Down?* Science. 314 (**2006**):65-66.

80. F.L. Garcia-Carreon and M.A. Navarrete del Toro, *Classification of Proteases without tears.* Biochemical Education. 25 (**1997**):161-167.

81. F.S. Skottvoll, *Critical evaluation of isolation and characterization techniques of breast cancer exosomes*. 2017, Master Thesis, Department of Chemistry, University of Oslo

82. J.L. Proc, M.A. Kuzyk, D.B. Hardie, J. Yang, D.S. Smith, A.M. Jackson, C.E. Parker, and C.H. Borchers, *A quantitative study of the effects of chaotropic agents, surfactants, and solvents on the digestion efficiency of human plasma proteins by trypsin.* Journal of Proteome Research. 9 (**2010**):5422-5437.

83. U.K. Kar, M. Simonian, and J.P. Whitelegge, *Integral membrane proteins: bottom-up, top-down and structural proteomics.* Expert Review of Proteomics. 14 (**2017**):715-723.

84. N. Zhang and L. Li, *Effects of common surfactants on protein digestion and matrix‐assisted laser desorption/ionization mass spectrometric analysis of the digested peptides using two‐layer sample preparation.* Rapid Communications in Mass Spectrometry. 18 (**2004**):889-896.

85. A.E. Speers and C. Wu, *Proteomics of integral membrane proteins-theory and application.* Chemical Reviews. 107 (**2007**):3687-3714.

86. G. Salvi, P. De Los Rios, and M. Vendruscolo, *Effective interactions between chaotropic agents and proteins.* Proteins: Structure, Function, and Bioinformatics. 61 (**2005**):492-499.

87. W. Wedemeyer, E. Welker, M. Narayan, and H. Scheraga, *Disulfide bonds and protein folding.* Biochemistry. 39 (**2000**):4207-4216.

88. J. Paulech, N. Solis, and S.J. Cordwell, *Characterization of reaction conditions providing rapid and specific cysteine alkylation for peptide-based mass spectrometry.* Biochemica et Biophysica Acta - Proteins and Proteomics. 1834 (**2013**):372-379.

89. H.S. Berg, *Optimization of in-house packing of nano liquid chromatography columns - How to pack low-cost nano liquid chromatography columns?* 2016, Master Thesis, Department of Chemistry, University of Oslo

90. I. Rombouts, B. Lagrain, M. Brunnbauer, J. Delcour, and P. Koehler, *Improved identification of wheat gluten proteins through alkylation of cysteine residues and peptide-based mass spectrometry.* Scientific Reports. 3 (**2013**):2279-2299.

91. J.V. Olsen, S.-E. Ong, and M. Mann, *Trypsin cleaves exclusively C-terminal to arginine and lysine residues.* Molecular & Cellular Proteomics. 3 (**2004**):608-614.

92. E. Vandermarliere, M. Mueller, and L. Martens, *Getting intimate with trypsin, the leading protease in proteomics.* Mass Spectrometry Reviews. 32 (**2013**):453-465.

93. M.M. Vorob'ev, M. Dalgalarrondo, J.M. Chobert, and T. Haertlé, *Kinetics of beta-casein hydrolysis by wild-type and engineered trypsin.* Biopolymers. 54 (**2000**):355-364.

94. A.C. Peterson, J.D. Russell, D.J. Bailey, M.S. Westphall, and J.J. Coon, *Parallel reaction monitoring for high resolution and high mass accuracy quantitative, targeted proteomics.* Molecular & Cellular Proteomics. 11 (**2012**):1475-1488.

95. B. Paizs and S. Suhai, *Fragmentation pathways of protonated peptides.* Mass Spectrometry Reviews. 24 (**2005**):508-548.

96. A. Michalski, N. Neuhauser, J. Cox, and M. Mann, *A systematic investigation into the nature of tryptic HCD spectra.* Journal of Proteome Research. 11 (**2012**):5479-5491.

97. R. Boyd and Á. Somogyi, *The mobile proton hypothesis in fragmentation of protonated peptides: A perspective.* Journal of the American Society for Mass Spectrometry. 21 (**2010**):1275-1278.

98. P. Roepstorff and J. Fohlman, *Proposal for a Common Nomenclature for Sequence Ions in Mass Spectra of Peptides.* Biomedical Mass Spectrometry. 11 (**1984**):601.

99. R. Smith, A.D. Mathis, D. Ventura, and J.T. Prince, *Proteomics, lipidomics, metabolomics: A mass spectrometry tutorial from a computer scientist's point of view.* BMC Bioinformatics. 15 (**2014**):DOI 10.1186/1471-2105-15-S7-S9.

100. J. Eng, A. McCormack, and J. Yates, *An approach to correlate tandem mass spectral data of peptides with amino acid sequences in a protein database.* Journal of the American Society for Mass Spectrometry. 5 (**1994**):976-989.

101. Thermo Fisher Scientific. *Proteome Discoverer, Version 1.4 User Guide*. Version 1.4 User Guide 2012 [Accessed 18.11. 2017]; Available from: https://tools.thermofisher.com/content/sfs/manuals/Man-XCALI-97506-Proteome-Discoverer-14-User-ManXCALI97506-A-EN.pdf

102. R. Sadygov, *Using SEQUEST with Theoretically Complete Sequence Databases.* Journal of The American Society for Mass Spectrometry. 26 (**2015**):1858-1864.

103. M. Geng, J. Ji, and F.E. Regnier, *Signature-peptide approach to detecting proteins in complex mixtures.* Journal of Chromatography A. 870 (**2000**):295-313.

104. P. Feist and A.B. Hummon, *Proteomic Challenges: Sample Preparation Techniques for Microgram-Quantity Protein Analysis from Biological Samples.* International Journal of Molecular Science. 16 (**2015**):3537-3563.

105. J.J. Kirkland, F.A. Truszkowski, C.H. Dilks, and G.S. Engel, *Superficially porous silica microspheres for fast high-performance liquid chromatography of macromolecules.* Journal of Chromatography A. 890 (**2000**):3-13.

106. R.A. Zubarev, *The challenge of the proteome dynamic range and its implications for in-depth proteomics.* Proteomics. 13 (**2013**):723-726.

107. M. Wang, M. Weiss, M. Simonovic, G. Haertinger, S.P. Schrimpf, M.O. Hengartner, C. Von Mering, C. Wang, C. Weiss, C. Simonovic, and C. Haertinger, *PaxDb, a database*

of protein abundance averages across all three domains of life. Molecular & Cellular Proteomics. 11 (**2012**):492-500.

108. D.P. Kodack, A.F. Farago, A. Dastur, M.A. Held, L. Dardaei, L. Friboulet, F. Von Flotow, L.J. Damon, D. Lee, M. Parks, R. Dicecca, M. Greenberg, K.E. Kattermann, A.K. Riley, F.J. Fintelmann, C. Rizzo, Z. Piotrowska, A.T. Shaw, J.F. Gainor, L.V. Sequist, M.J. Niederst, J.A. Engelman, and C.H. Benes, *Primary Patient-Derived Cancer Cells and Their Potential for Personalized Cancer Patient Care.* Cell Reports. 21 (**2017**):3298-3309.

109. X. Liu, E. Krawczyk, F.A. Suprynowicz, N. Palechor-Ceron, H. Yuan, A. Dakic, V. Simic, Y.-L. Zheng, P. Sripadhan, C. Chen, J. Lu, T.-W. Hou, S. Choudhury, B. Kallakury, D. Tang, T. Darling, R. Thangapazham, O. Timofeeva, A. Dritschilo, S.H. Randell, C. Albanese, S. Agarwal, and R. Schlegel, *Conditional reprogramming and long-term expansion of normal and tumor cells from human biospecimens.* Nature Protocols. 12 (**2017**):439-451.

110. I. Assanga, Gil-Salido, L. Luján, Rosas-Durazo, Acosta-Silva, Rivera-Castañeda, and J.L. Rubio-Pino, *Cell growth curves for different cell lines and their relationship with biological activities.* International Journal of Biotechnology and Molecular Biology Research. 4 (**2013**):60-70.

111. K. Sandvig and A. Llorente, *Proteomic analysis of microvesicles released by the human prostate cancer cell line PC-3.* Molecular & Cellular Proteomics. 11 (**2012**):DOI 10.1074/mcp.M111.012914.

112. M. Logozzi, A. De Milito, L. Lugini, M. Borghi, L. Calabrò, M. Spada, M. Perdicchio, M.L. Marino, C. Federici, E. Iessi, D. Brambilla, G. Venturi, F. Lozupone, M. Santinami, V. Huber, M. Maio, L. Rivoltini, and S. Fais, *High Levels of Exosomes Expressing CD63 and Caveolin-1 in Plasma of Melanoma Patients* PLoS ONE. 4 (**2009**):e5219, DOI: 10.1371/journal.pone.0005219

113. L. Muller, C.-S. Hong, D.B. Stolz, S.C. Watkins, and T.L. Whiteside, *Isolation of biologically-active exosomes from human plasma.* Journal of Immunological Methods. 411 (**2014**):55-65.

114. Y. Saito, K. Jinno, and T. Greibrokk, *Capillary columns in liquid chromatography: between conventional columns and microchips.* Journal of Separation Science. 27 (**2004**):1379-1390.

115. J.P.C. Vissers, H.A. Claessens, and C.A. Cramers, *Microcolumn liquid chromatography: instrumentation, detection and applications.* Journal of Chromatography A. 779 (**1997**):1-28.

116. J.P. Chervet, M. Ursem, and J.P. Salzmann, *Instrumental requirements for nanoscale liquid chromatography.* Analytical Chemistry. 68 (**1996**):1507-1512.

117. S.R. Wilson, T. Vehus, H.S. Berg, and E. Lundanes, *Nano-LC in proteomics: recent advances and approaches.* Bioanalysis. 7 (**2015**):1799-1815.

118. J.P.C. Vissers, A.H. de Ru, M. Ursem, and J.-P. Chervet, *Optimised injection techniques for micro and capillary liquid chromatography.* Journal of Chromatography A. 746 (**1996**):1-7.

119. M. Rogeberg, H. Malerod, H. Roberg-Larsen, C. Aass, and S.R. Wilson, *On-line solid phase extraction–liquid chromatography, with emphasis on modern bioanalysis and miniaturized systems.* Journal of Pharmaceutical and Biomedical Analysis. 87 (**2014**):120-129.

120. T. Constantopoulos, G. Jackson, and C. Enke, *Effects of salt concentration on analyte response using electrospray ionization mass spectrometry.* Journal of the American Society for Mass Spectrometry. 10 (**1999**):625-634.

121. H. Metwally, R.G. McAllister, and L. Konermann, *Exploring the mechanism of salt-induced signal suppression in protein electrospray mass spectrometry using experiments and molecular dynamics simulations.* Analytical Chemistry. 87 (**2015**):2434-2442.

122. S.R. Wilson, T. Vehus, H.S. Berg, and E. Lundanes, *Nano-LC in proteomics: recent advances and approaches.* Bioanalysis. 7 (**2015**):1799.

123. R. Aebersold and M. Mann, *Mass spectrometry-based proteomics.* Nature. 422 (**2003**):198-207.

124. M.-C. Hennion and V. Pichon, *Immuno-based sample preparation for trace analysis.* Journal of Chromatography A. 1000 (**2003**):29-52.

125. T. Boström, J.O. Takanen, and S. Hober, *Antibodies as means for selective mass spectrometry.* Journal of Chromatography B. (**2016**):3-13.

126. B. Kaboord and M. Perr, *Isolation of proteins and protein complexes by immunoprecipitation.* Methods in Molecular Biology. 424 (**2008**):349-364.

127. V. Pichon, F. Chapuis-Hugon, and M.C. Hennion, *2.19 Bioaffinity sorbents*, in *Comprehensive Sampling and Sample Preparation*. 2012, Academic Press: Oxford:359-388.

128. N. Delaunay, V. Pichon, and M.-C. Hennion, *Immunoaffinity solid-phase extraction for the trace-analysis of low-molecular-mass analytes in complex sample matrices.* Journal of Chromatography B: Biomedical Sciences and Applications. 745 (**2000**):15-37.

129. A.C. Moser and D.S. Hage, *Immunoaffinity chromatography: an introduction to applications and recent developments.* Bioanalysis. 2 (**2010**):769-790.

130. S. Hjerten, J. Liao, and R. Zhang, *High-performance liquid-chromatography on continuous polymer beds.* Journal Of Chromatography A. 473 (**1989**):273-275.

131. F. Svec and J.M.J. Frechet, *Continuous rods of macroporous polymer as high-performance liquid chromatography separation media.* Analytical Chemistry. 64 (**1992**):820-822.

132. J.C. Masini and F. Svec, *Porous monoliths for on-line sample preparation: A review.* Analytica Chimica Acta. 964 (**2017**):24-44.

133. M. Petro, F. Svec, and J.M.J. Fréchet, *Molded continuous poly(styrene-co-divinylbenzene) rod as a separation medium for the very fast separation of polymers Comparison of the chromatographic properties of the monolithic rod with columns packed with porous and non-porous beads in high-performance liquid chromatography of polystyrenes.* Journal of Chromatography A. 752 (**1996**):59-66.

134. S. Xie, F. Svec, and J.M.J. Fréchet, *Design of reactive porous polymer supports for high throughput bioreactors: Poly(2-vinyl-4;4 dimethylazlactone-co-acrylamide-co-ethylene dimethacrylate) monoliths.* Biotechnology and Bioengineering. 62 (**1999**):30-35.

135. L. Geiser, S. Eeltink, F. Svec, and J.M.J. Fréchet, *In-line system containing porous polymer monoliths for protein digestion with immobilized pepsin, peptide preconcentration and nano-liquid chromatography separation coupled to electrospray ionization mass spectroscopy.* Journal of Chromatography A. 1188 (**2008**):88-96.

136. J. Krenkova and F. Svec, *Less common applications of monoliths: IV. Recent developments in immobilized enzyme reactors for proteomics and biotechnology.* Journal of Separation Science. 32 (**2009**):706-718.

137. F. Svec, *Porous polymer monoliths: Amazingly wide variety of techniques enabling their preparation.* Journal of Chromatography A. 1217 (**2010**):902-924.

138. T.C. Logan, D.S. Clark, T.B. Stachowiak, F. Svec, and J.M.J. Fréchet, *Photopatterning Enzymes on Polymer Monoliths in Microfluidic Devices for Steady-State Kinetic*

Analysis and Spatially Separated Multi-Enzyme Reactions. Analytical Chemistry. 79 (**2007**):6592-6598.

139. M.E. Buck and D.M. Lynn, *Azlactone-functionalized polymers as reactive platforms for the design of advanced materials: Progress in the last ten years.* Polymer Chemistry. 3 (**2011**):66-80.

140. S. Xie, F. Svec, and J.M.J. Fréchet, *Preparation of porous hydrophilic monoliths: Effect of the polymerization conditions on the porous properties of poly (acrylamide‑co‑N,N′-methylenebisacrylamide) monolithic rods.* Journal of Polymer Science Part A: Polymer Chemistry. 35 (**1997**):1013-1021.

141. J.O. Becker and A.N. Hoofnagle, *Replacing immunoassays with tryptic digestion-peptide immunoaffinity enrichment and LC–MS/MS.* Bioanalysis. 4 (**2012**):281-290.

142. A. Thomas, W. Schänzer, and M. Thevis, *Immunoaffinity techniques coupled to mass spectrometry for the analysis of human peptide hormones: advances and applications.* Expert Review of Proteomics. 14 (**2017**):799-807.

143. M. Pernemalm and J. Lehtiö, *Mass spectrometry-based plasma proteomics: state of the art and future outlook.* Expert Review of Proteomics. 11 (**2014**):431-48.

144. M. Razavi, L.E. Frick, W.A. Lamarr, M.E. Pope, C.A. Miller, N.L. Anderson, and T.W. Pearson, *High-throughput SISCAPA quantitation of peptides from human plasma digests by ultrafast, liquid chromatography-free mass spectrometry.* Journal of Proteome Research. 11 (**2012**):5642-5649.

145. I. van den Broek, J. Nouta, M. Razavi, R. Yip, M.R. Bladergroen, F.P. Romijn, N.P.M. Smit, O. Drews, R. Paape, D. Suckau, A.M. Deelder, Y.E.M. van Der Burgt, T.W. Pearson, N.L. Anderson, and C.M. Cobbaert, *Quantification of serum apolipoproteins A-I and B-100 in clinical samples using an automated SISCAPA–MALDI-TOF-MS workflow.* Methods. 81 (**2015**):74-85.

146. N.L. Anderson, N.G. Anderson, L.R. Haines, D.B. Hardie, R.W. Olafson, and T.W. Pearson, *Mass spectrometric quantitation of peptides and proteins using Stable Isotope Standards and Capture by Anti-Peptide Antibodies (SISCAPA).* Journal of Proteome Research. 3 (**2004**):235-244.

147. R.M. Schoenherr, L. Zhao, R.G. Ivey, U.J. Voytovich, J. Kennedy, P. Yan, C. Lin, J.R. Whiteaker, and A.G. Paulovich, *Commercially available antibodies can be applied in quantitative multiplexed peptide immunoaffinity enrichment targeted mass spectrometry assays.* Proteomics. 16 (**2016**):2141-2145.

148. N.H. Trier, P.R. Hansen, and G. Houen, *Production and characterization of peptide antibodies.* Methods. 56 (**2012**):136-144.

149. H.K. Hustoft, O.K.M. Brandtzæg, D. Misaghian, M. Røgeberg, S.B. Torsetnes, L. Reubsaet, S.R.H. Wilson, T. Greibrokk, and E. Lundanes, *Integrated enzyme reactor and high resolving chromatography in ''sub-chip'' dimensions for sensitive protein mass spectrometry.* Scientific Reports. 3 (**2013**):3511-3525.

150. S. Olsen, *Evaluation of the hydrazide enrichment method for N-linked glycoproteins in cancer cells by nano liquid chromatography mass spectrometry*. 2013, Master Thesis, Department of Chemistry, University of Oslo

151. B.O. Petritis, W.J. Qian, D.G. Camp Ii, and R.D. Smith, *A simple procedure for effective quenching of trypsin activity and prevention of 18 O-labeling back-exchange.* Journal of Proteome Research. 8 (**2009**):2157-2163.

152. J.R. Wiśniewski, A. Zougman, N. Nagaraj, and M. Mann, *Universal sample preparation method for proteome analysis.* Nature Methods. 6 (**2009**):359-362.

153. A. Shevchenko, H. Tomas, J. Havli, J.V. Olsen, and M. Mann, *In-gel digestion for mass spectrometric characterization of proteins and proteomes.* Nature Protocols. 1 (**2007**):2856-2860.

154. X. Jiang, X. Jiang, G. Han, M. Ye, and H. Zou, *Optimization of filtering criterion for SEQUEST database searching to improve proteome coverage in shotgun proteomics.* BMC Bioinformatics. 8 (**2007**):323-323.

155. S. Rakel, 2017; Personal communication: E-mail from scientific support scientist at Abcam

156. A. Byron, J.D. Humphries, J.A. Askari, S.E. Craig, A.P. Mould, and M.J. Humphries, *Anti-integrin monoclonal antibodies.* Journal of Cell Science. 122 (**2009**):4009-4011.

157. M. Gómez, A. Luque, M.A. Del Pozo, N. Hogg, F. Sánchez-Madrid, and C. Cabañas, *Functional relevance during lymphocyte migration and cellular localization of activated β1 integrins.* European Journal of Immunology. 27 (**1997**):8-16.

158. W. Argraves and H. Tran, *Purification of α5β1 integrin by ligand affinity chromatography.* Journal of Tissue Culture Methods. 16 (**1994**):243-247.

159. H. Daxecker, M. Raab, E. Bernard, M. Devocelle, A. Treumann, and N. Moran, *A peptide affinity column for the identification of integrin α IIb-binding proteins.* Analytical Biochemistry. 374 (**2008**):203-212.

160. J.-F. Charlot, 2017; Personal communication: E-mail from technical service scientist at Merck

161. M. Palmblad and J.S. Vogel, *Quantitation of binding, recovery and desalting efficiency of peptides and proteins in solid phase extraction micropipette tips.* Journal of Chromatography B. 814 (**2005**):309-313.

162. F. Brothier and V. Pichon, *Immobilized antibody on a hybrid organic–inorganic monolith: Capillary immunoextraction coupled on-line to nanoLC-UV for the analysis of microcystin-LR.* Analytica Chimica Acta. 792 (**2013**):52-58.

163. J.S. Hoos, H. Sudergat, J.-P. Hoelck, M. Stahl, J.S.B. de Vlieger, W.M.A. Niessen, H. Lingeman, and H. Irth, *Selective quantitative bioanalysis of proteins in biological fluids by on-line immunoaffinity chromatography–protein digestion–liquid chromatography–mass spectrometry.* Journal of Chromatography B. 830 (**2006**):262-269.

164. D.C. Liebler and A.L. Ham, *Spin filter–based sample preparation for shotgun proteomics.* Nature Methods. 6 (**2009**):785.

165. J.R. Wiśniewski, N. Nagaraj, A. Zougman, F. Gnad, and M. Mann, *Brain phosphoproteome obtained by a FASP-based method reveals plasma membrane protein topology.* Journal of Proteome Research. 9 (**2010**):3280-3289.

166. M. Berna, C. Schmalz, K. Duffin, P. Mitchell, M. Chambers, and B. Ackermann, *Online immunoaffinity liquid chromatography/tandem mass spectrometry determination of a type II collagen peptide biomarker in rat urine: Investigation of the impact of collision-induced dissociation fluctuation on peptide quantitation.* Analytical Biochemistry. 356 (**2006**):235-243.

167. A.J. Borst, Z.M. James, W.N. Zagotta, M. Ginsberg, F.A. Rey, F. Dimaio, M. Backovic, and D. Veesler, *The Therapeutic Antibody LM609 Selectively Inhibits Ligand Binding to Human αVβ3 Integrin via Steric Hindrance.* Structure. 25 (**2017**):1732-1739.

168. A. Wakamatsu, J. Yamamoto, K. Kimura, S. Ishii, K. Watanabe, A. Sugiyama, K. Murakawa, T. Kaida, K. Tsuchiya, Y. Fukuzumi, A. Kumagai, Y. Oishi, S. Yamamoto, Y. Ono, Y. Komori, M. Yamazaki, Y. Kisu, T. Nishikawa, S. Sugano, N. Nomura, and T. Isogai, Unpublished. *NEDO human cDNA sequencing project focused on splicing variants.* 2008 [Accessed 18.03 2018]; Available from: https://www.ncbi.nlm.nih.gov/protein/BAG63819.1?report=genbank&log$=prottop&blast_rank=20&RID=D6N6X916014

169. M. Razavi, N. Leigh Anderson, M.E. Pope, R. Yip, and T.W. Pearson, *High precision quantification of human plasma proteins using the automated SISCAPA Immuno-MS workflow.* New Biotechnology. 33 (**2016**):494-502.
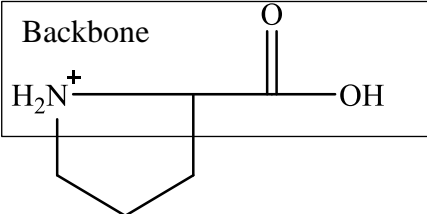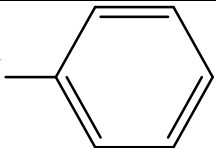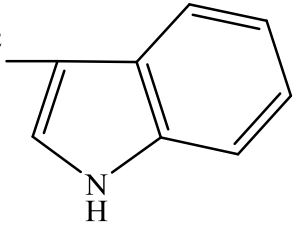
170. O.V. Nemirovskiy, D.R. Dufield, T. Sunyer, P. Aggarwal, D.J. Welsch, and W.R. Mathews, *Discovery and development of a type II collagen neoepitope (TIINE) biomarker for matrix metalloproteinase activity: From in vitro to in vivo.* Analytical Biochemistry. 361 (**2007**):93-101.

171. A.N. Hoofnagle, J.O. Becker, M.H. Wener, and J.W. Heinecke, *Quantification of thyroglobulin, a low-abundance serum protein, by immunoaffinity peptide enrichment and tandem mass spectrometry.* Clinical Chemistry. 54 (**2008**):1796-1804.

172. C. Raska, C. Parker, S. Sunnarborg, R. Pope, D. Lee, G. Glish, and C. Borchers, *Rapid and sensitive identification of epitope-containing peptides by direct matrix-assisted laser desorption/ionization tandem mass spectrometry of peptides affinity-bound to antibody beads.* Journal of the American Society for Mass Spectrometry. 14 (**2003**):1076-1085.

173. M.S. Halquist and H. Karnes, *Quantitative liquid chromatography tandem mass spectrometry analysis of macromolecules using signature peptides in biological fluids.* Biomedical Chromatography. 25 (**2011**):47-58.

174. F. Bleeker, R. Molenaar, and S. Leenstra, *Recent advances in the molecular understanding of glioblastoma.* Journal of Neuro-Oncology. 108 (**2012**):11-27.

175. F. Gritti and G. Guiochon, *Facts and Legends About Columns Packed with Sub-3-µm Core-Shell Particles.* LC GC North America. 3 (**2012**):586-595.

176. O.K.M. Brandtzæg, *Online Sample Preperation Platforms for Targeted Nano Liquid Chromatography Mass Spectrometry Bioanalysis*. 2018, PhD Thesis, Department of Chemistry University of Oslo

177. S. Bekhradnia, K. Lund, K. Bjorseth, F.S. Skottvoll, H.S. Berg, N. Roos, B. Thiede, B. Nystrom, H. Røberg-Larsen, E. Lundanes, and S.R. Wilson, BioRxiv. *Critical comparison of ultracentrifugation and a commercial kit for isolation of exosomes derived from glioblastoma and breast cancer cell lines (preprint)*. BioRxiv 2018; Available from: https://www.biorxiv.org/content/early/2018/03/02/274910.article-metrics

178. P.K. Smith, R.I. Krohn, G.T. Hermanson, A.K. Mallia, F.H. Gartner, M.D. Provenzano, E.K. Fujimoto, N.M. Goeke, B.J. Olson, and D.C. Klenk, *Measurement of protein using bicinchoninic acid.* Analytical Biochemistry. 150 (**1985**):76-85.

179. Abcam, *Anti-Integrin alpha 3 antibody*. [Accessed 02.02 2018]; Available from: http://www.abcam.com/integrin-alpha-3-antibody-ab131055.html

7 Appendix

7.1 Amino acids

Table 11 (p. 87-88) shows all the 20 amino acids commonly found in humans. They are categorized by their polarity and charge. Their 3- and 1-letter code is stated as is the structure of their side chain

Table 11: The amino acids, categorized by their polarity and charge. Their 3- and 1-letter code is stated and the structure of their side chain is shown.

Polarity	Name	3-letter code	1-letter code	Side chain
Non-polar	Glycine	Gly	G	—H
	Alanine	Ala	A	—CH_3
	Valine	Val	V	CH_3 / —CH—CH_3
	Leucine	Leu	L	CH_3 / —C_{H_2}—CH—CH_3
	Isoleucine	Ile	I	CH_3 / —C H—CH_2—CH_3
	Proline	Pro	P	Backbone H_2N^+———C=O—OH
	Phenylalanine	Phe	F	—C_{H_2}— (benzene ring)
	Tryptophan	Trp	W	—C_{H_2}— (indole ring, N–H)
	Methionine	Met	M	—C_{H_2}—C_{H_2}—S—CH_3

	Cysteine	Cys	C	$\overset{H_2}{-C}-SH$
Polar	Serine	Ser	S	$\overset{H_2}{-C}-OH$
	Threonine	Thr	T	$\overset{H}{-C}-OH$ with CH_3 below
	Tyrosine	Tyr	Y	$\overset{H_2}{-C}-$ (benzene ring) $-OH$
	Asparagine	Asn	N	$\overset{H_2}{-C}-\overset{O}{\overset{\|}{C}}-NH_2$
	Glutamine	Gln	Q	$\overset{H_2}{-C}-\overset{H_2}{C}-\overset{O}{\overset{\|}{C}}-NH_2$
Negative Charge	Aspartic acid	Asp	D	$\overset{H_2}{-C}-\overset{O}{\overset{\|}{C}}-\overset{-}{O}$
	Glutamic acid	Glu	E	$\overset{H_2}{-C}-\overset{H_2}{C}-\overset{O}{\overset{\|}{C}}-\overset{-}{O}$
Positive charge	Histedine	His	H	$\overset{H_2}{-C}-$ (imidazole ring with NH and $\overset{+}{N}H$)
	Arginine	Arg	R	$\overset{H_2}{-C}-\overset{H_2}{C}-\overset{H_2}{C}-\overset{H}{N}-\overset{\overset{+}{NH_2}}{\overset{\|}{C}}-NH_2$
	Lysine	Lys	K	$\overset{H_2}{-C}-\overset{H_2}{C}-\overset{H_2}{C}-\overset{H_2}{C}-\overset{+}{N}H_3$

7.2 Chromatography

The distribution of a compound between the SP and the MP in a column is described by the retention factor, k, and is given in Equation A1. Two compounds that interact differently with the SP will have different k values and elute at different times.

$$k = \frac{n_s}{n_m} \qquad\qquad (A1)$$

Where n_s is the number of molecules in the SP, and n_m is the number of molecules in the MP. The retention factor is a measure how much time a compound will use through a column. A detector is connected at the column outlet measuring the intensity of the eluent band as a function of time. The time passed from a compound is introduced onto a column until it elutes is its t_R. The relation between k and t_R is given by Equation A2.

$$k = \frac{t_R - t_M}{t_M} \qquad\qquad (A2)$$

Where t_M is the time a component would elute if it has no interaction with the SP.

Efficiency is a measure of how well two or more compounds from one sample are separated from each other. Two factors that play a role in the separation is the difference in t_R and band broadening. Physical processes produce band broadening, both inside the column, and outside, in tubing and couplings. This leads to the solute eluting in a Gaussian curve with standard deviation σ, and not a straight band. A columns ability to elute a narrow band can be expressed as the column efficiency, given by number of plates, N, given in Equation A3.

$$N = \left(\frac{t_R}{\sigma}\right)^2 \qquad\qquad (A3)$$

A high value of N is an indication of an efficient column. N is inversely proportional to the plate height, H, which also is a measure of band broadening. Their correlation is given in Equation A4, where L is the column length.

$$N = \frac{L}{H} \qquad\qquad (A4)$$

H can be expressed through the van Deemter equation (Equation A5), which combines the different contributions of band broadening.

$$H = A + \frac{B}{u} + Cu \qquad\qquad \text{(A5)}$$

Where A is eddy dispersion, B is the longitudinal diffusion in the MP, C is a combination of the resistance to mass transfer in the MP and SP, whilst u is the linear flow rate [74]. In **Table 12** each of the three terms in the van Deemter equation (Equation A5) is explained.

Table 12: The name of the terms in the van Deemter equation and how they contribute to band broadening.

Term	Name	Contribution to band broadening *[74]*
A	Eddy dispersion	Arises due to the multiple channels of the particle having different widths and lengths. This means that different molecules of the same species will move at different speeds through the particle – causing the band to broaden
B	Longitudinal diffusion	Compounds in a concentrated band will naturally diffuse to less concentrated areas
C	Resistance to mass transfer	band broadening due to resistance of transfer of a molecule from the SP to the MP or from the MP to the SP

7.2.1 Core shell particles and efficiency

With core shell particles the higher efficiency is due to less eddy dispersion and less longitudinal diffusion arising from the thin porous layer compared to a totally porous particle, giving less band broadening [175].

7.3 Monoliths

In *Figure 44*, the pretreatment of the silica walls with NaOH is shown, which is followed by the covalent bonding of γ-MAPS to the capillary wall. This group creates a covalent bond to the monolith and ensure it stays within the capillary. *Figure 45* shows the formation of the polymer.
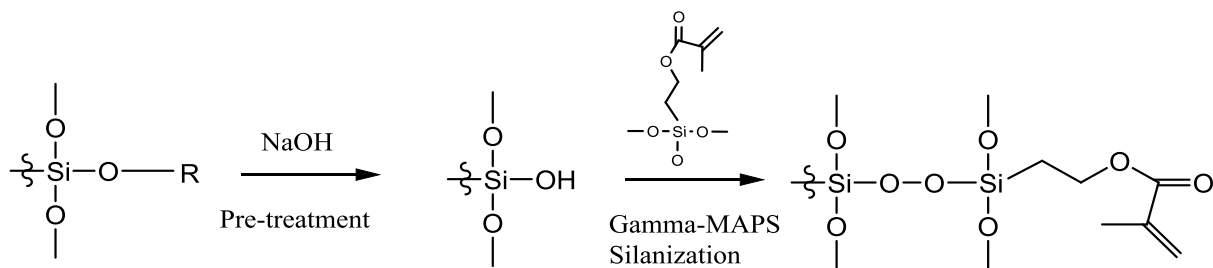
Figure 44: Pretreatment and silanization with γ-MAPS of the silica capillary walls.
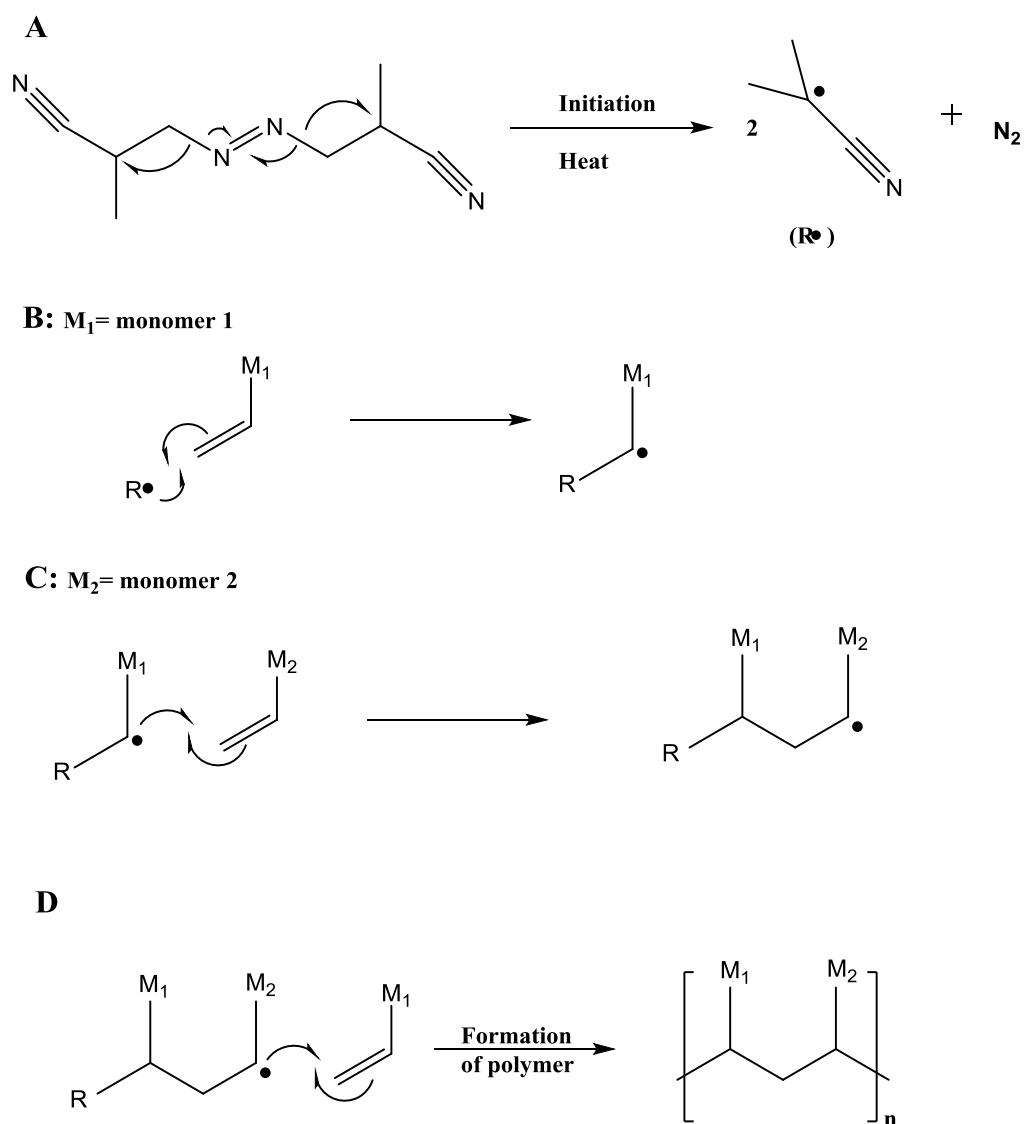
Figure 45: Formation of a polymer. A: the initiator AIBN forms free radicals (R•). B: the free radical reacts with a monomer, creating monomer radicals .C:The monomer radical reacts with monomer 2, creating a dimer radical. D: Polymers are formed. The two monomers in this study was EDMA and VDM. Adapted from [176].

7.3.1 Ethylene dimethacrylate

In *Figure 46* the structure of the monomer EDMA is shown.
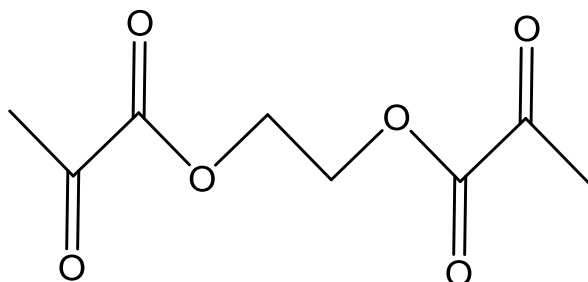
Figure 46: The structure of EDMA

7.3.2 Monolith made in-house

In *Figure 47* a scanning electron microscope (SEM) image of a monolith produced in this study is shown. No ABs are immobilized on it, and the monolith was dry. The image was taken using a FEI Quanta 200 FEG-E scanning electron microscope (Hillsboro, OR, US).

| Det | HV | WD | Mag | 2/15/2017 | ⊢————100.0µm————⊣ |
| SSD | 15.0 kV | 10.3 mm | 400x | 1:15:59 PM | |
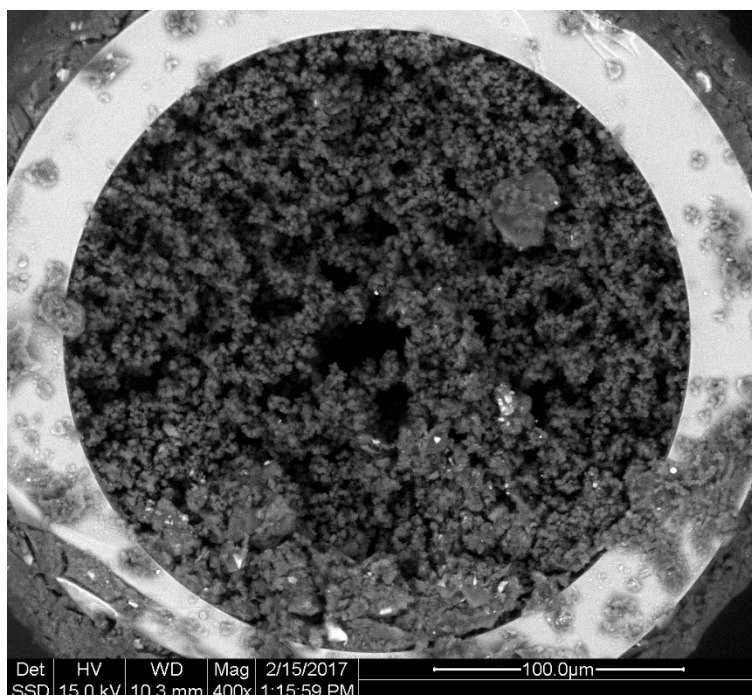
Figure 47: SEM of monolith produced in this study.

7.4 Glioblastoma multiforme cells

7.4.1 Culturing

GBM cells (T1018) were derived from biopsies from a primary GBM tumour. These were obtained by Langemoen lab at Rikshospitalet, Oslo, Norway. The cell culturing was also performed here (see [177] for procedure (note: preprint of the article)).

7.4.2 Glioblastoma cells for in-gel digestion

Figure 48 illustrates how the GBM cells were prepared prior to BCA analysis and for online entrapment on an AB monolith.
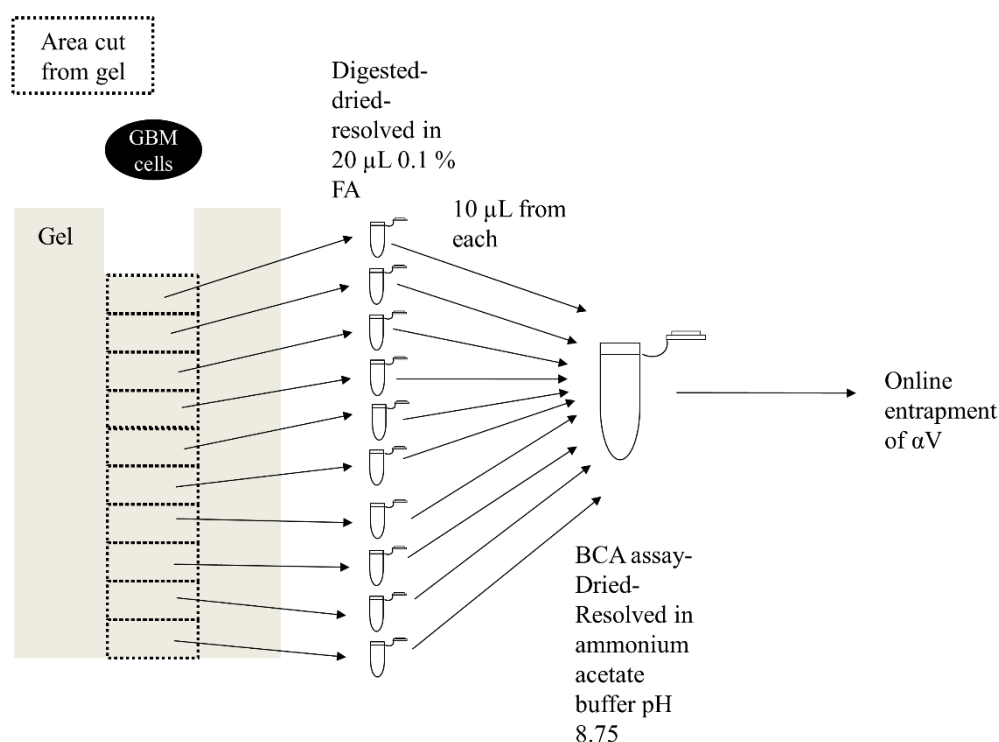
Figure 48*: **Preperation of the GBM cells after GE.** The dotted lines indicate how the gel was cut prior to digestion.*

7.4.3 Bicinchonic acid assay

BCA assay is a method for quantification of total protein content. It is based on the reduction of Cu^{2+} to Cu^+ at alkaline conditions in a protein solution. Cu^+ forms a purple complex with BCA that can be detected with a spectrophotometer. The amount of Cu^+ which is formed is a

function of the protein concentration, the protein content can be determined spectrophotometrically [178].

In *Figure 49*, the calibration curve obtained for the determination of proteins in the GBM cells using a BCA assay. In *Table 13*, the concentrations of proteins in the GBM cells found from the BCA assay is given, with calculations of average and standard deviations.
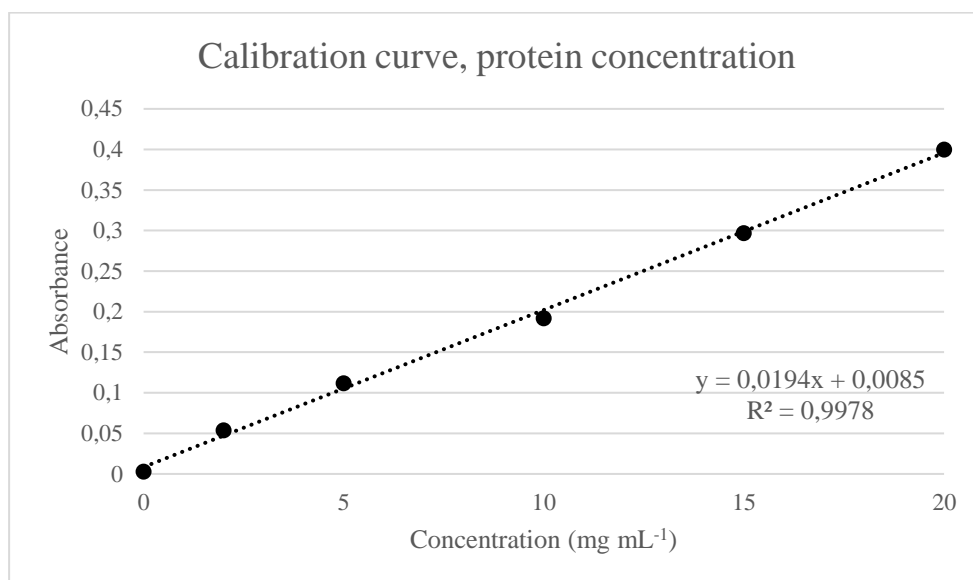
Figure 49: Calibration curve for the protein concentration obtained from BCA assay.

Table 13: the obtained values from the BCA assay of GBM cells.

	Replicates					
	1	2	3	Average	Standard deviation	Relative standard deviation
Protein concentration: (mg mL^{-1})	1.59	1.51	1.50	1.53	0.05	3%

7.5 Integrin standards for in-gel digestion

In *Figure 50* an illustration of what pieces were cut from the gel, to perform in-gel digestion on. The placement of α3 was based on information from [179]. The placement of the other integrin chains was based on WB, and in *Figure 51* the WBs obtained for β5, β1 and αV are shown with images of their respective protein ladders on top.
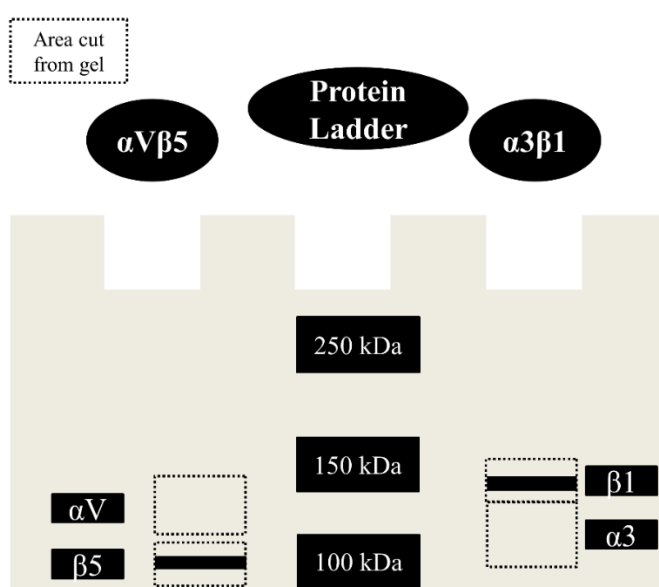
Figure 50: Illustration of the gel pieces that were cut for in-gel digestion. *The dotted lines indicates where the different pieces were cut, and what chain was expected to be there. The black boxes indicates where a band was observed from WB.*
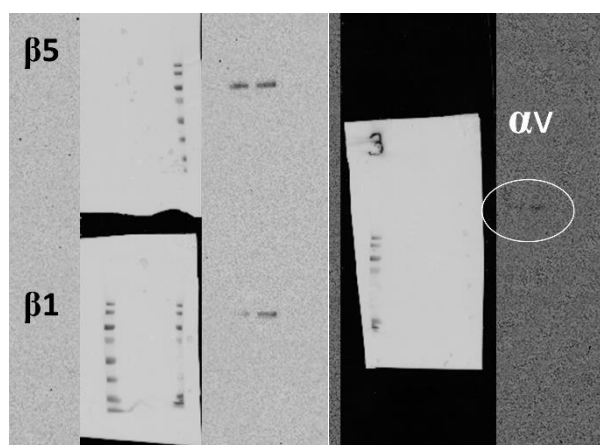
Figure 51: WB and protein ladders to-scale. *Two replicates were done for all three integrin chains.*

7.6 Digestion of epitope range of integrin β1 and β5

In *Table 14* and *Table 15* the peptides from β1 and β5, respectively, that would arise from tryptic digestion of the given epitope range, given no missed cleavages.

Table 14: Epitope range for β1. The peptide sequence and the number (no) of the amino acid sequence in relation to the entire protein.

Sequence	No	Sequence	No
QTDENR	21-27	LKPEDITQIQPQQLVLR	107-123
CLK	28-30	LR	124-125
ANAK	31-34	SGEPQTFTLK	126-135
SCGECIQAGPNCGWCTNSTFLQEG MPTSAR	35-64	FKR	136-138
CDDLEALK(K)(K)	65-72 (73) (74)	AEDYPIDLYYLMDLSYSMKD DLENVK	139-157
GCPPDDIENPR	75-85	SLGTDLMNEMRR	165-175
GSK	86-88	ITSDFR	176-182
DIK(K)	89-91 (92)	IGFGSFVEK	183-191
NK	93-94	TVMPYISTTPAK	192-203
NVTNR	95-99	LR	204-205
SKGTAEK	100-106	NPCTSEQNCTSPFSYK	206-221

Table 15: Epitope range for β5. The peptide sequence and the number (no) of the amino acid sequence in relation to the entire protein.

Sequence	No	Sequence	No
HVFALRPVGFR	441-452	GVLCSGHGECHCGECK	562-577
DSLEVGVTYNCTCGCSVGLEPNSAR	453-477	CHAGYIGDNCNCSTDISTCR	578-597
CNGSGTYVCGLCECSPGYLGTR	478-499	GR	598-599
CECQDGENQSVYQNLCR	500-516	DGQICSER	600-607
EAEGKPLCSGR	517-527	GHCLCGQCQCTEPGAFGEMCEK	608-629
GDCSCNQCSCFESEFGK	528-544	CPTCPDACSTKR	530-640
IYGPFCECDNFSCAR	545-559	DCVECLLLHSGKPDNQTCHSL	641-661
NK	560-561		

7.7 Comparison of digestion of human serum albumin and integrins

The example of the scores and coverages obtained from digestion of HSA and the integrins standards α3β1 and αVβ5 are given in *Table 16* and TICCs from injections using Setup I of HSA, α3β1, αVβ5 and αVβ1 after in-solution digestion are shown in *Figure 52* (TICC from αVβ1 is also included for comparison).

Table 16: score and coverage obtained from injections of HSA, α3β1 and αVβ5 on Setup I, after performing an in-solution digestion.

	Protein	Score	Coverage (%)
	HSA	15454	90.64
Integrin chain	α3	0	0
	β1	0	0
	αv	0	0
	β5	0	0
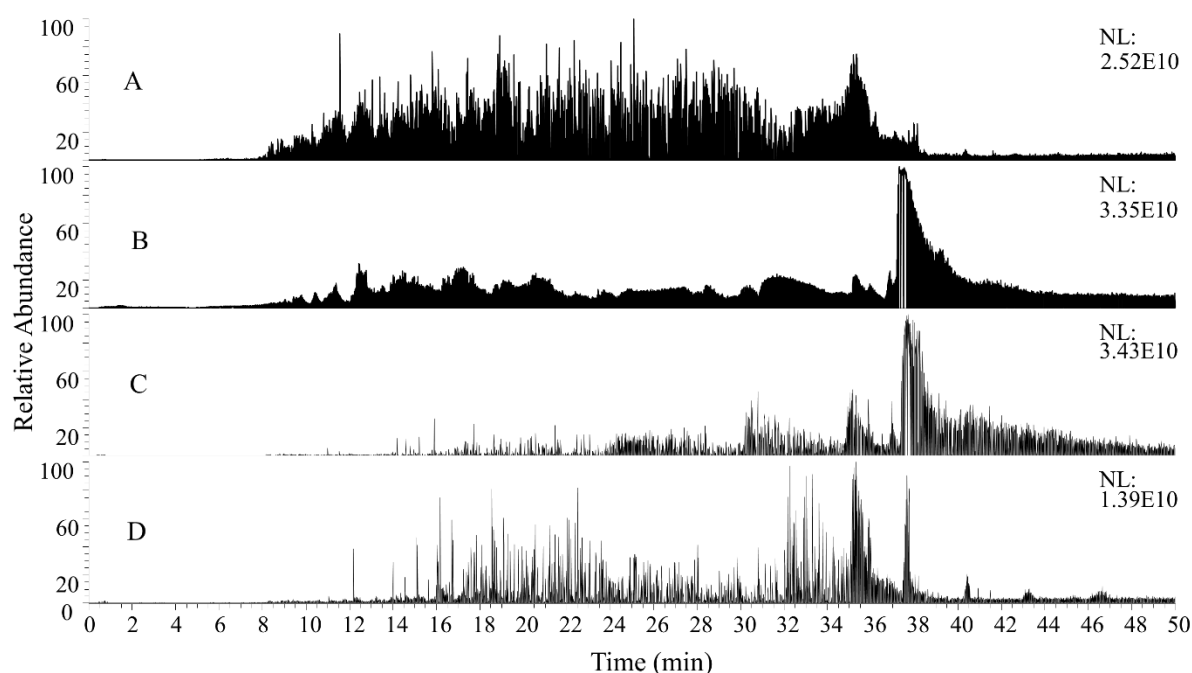
Figure 52: TICC after in-solution digestion. *Integrin concentration was 10 ng µL^{-1} (with HSA the exact concentration is unknown) with 5 µL injection volume on Setup I, with gradient 1. The pre-column was 4.5 cm and the analytical column was 15 cm, A: HSA, B: α3β1, C: αVβ5, D: αVβ1.*

7.8 Fragmentation patterns

7.8.1 Fragmentation after heat

Table 17 shows the obtained values for the correlation score of the peptide SHQWFGASVR from three injections onto an αV AB monolith, using Setup II with the analytical column replaced with fused silica tubing. The MS was in dd/MS/MS mode.

Table 17: The correlation scores from three injections of 100 ng digested αVβ1 standard, on three different αV AB monolithic columns with Setup II (no analytical column). Also the average, the standard deviation and relative standard deviation.

	Injection					
	1	2	3	Average	Standard deviation	Relative standard deviation (%)
Score	1.5	1.5	1.7	1.6	0.1	8

7.8.2 Fragmentation of SHQWFGASVR

In **Table 18** a complete list of s b and y fragments from the peptide SHQWFGASVR is given.

Table 18: b and y fragments from SHQWFGASVR

b_1	S	HQWFGASVR	y_9
b_2	SH	QWFGASVR	y_8
b_3	SHQ	WFGASVR	y_7
b_4	SHQW	FGASVR	y_6
b_5	SHQWF	GASVR	y_5
b_6	SHQWFG	ASVR	y_4
b_7	SHQWFGA	SVR	y_3
b_8	SHQWFGAS	VR	y_2
b_9	SHQWFGASV	R	y_1

7.9   Untargeted detection

7.9.1 No analytical column

In *Table 19* the data found from Proteome Discoverer, from investigations of trapping the epitope-containing peptide from αV, using Setup II with silica capillary replacing the analytical column, is given. In the table, the correlation score for the peptides that could be identified is given (for "other", these are different peptide chains that only could be detected once), the total score of the injection and the coverage obtained. It is also stated which AB monolith was used, and from what injection number the data is from.

Table 19: *The correlation scores for the four peptides identified from several injections (Inj) on different AB monoliths, the total score from the untargeted detection and the coverage obtained. Also, the average, standard deviation and relative standard deviation for the correlation scores for the peptides. "Other" are two different peptides that were only detected once each. Both were from the αV chain.*

AB monolith	Inj	Correlation score for peptides identified					Total score	Coverage (%)
		CQPIEFD ATGNRD YAKDDP LEFK	SHQWFGA SVR	ILACAPLY HWR	RALFLYSR	Others		
AB1	1		2.2	2.2	2.1	1.8	134	12
	2				2.2		2	11
	3		2.2	2.5		1.6	104	12
	4		1.3		3.1		21	7
	5		1.5	2.1			9	3
AB2	1	0.9	1.0				0	5
	2	1.1					0	12
	3	1.4	1.6				3	15
	4		1.1	1.3			8	14
	5	1.1	1.9				10	15
Average		1.1	1.6	2.0	2.5	1.7		
Standard deviation		0.2	0.5	0.5	0.6	0.3*		
Relative standard deviation (%)		18	31	25	24	18*		

* As there were only two peptides, the numbers stated are based on the difference found between the two correlation scores, not the standard deviation.

7.9.2 With analytical column

In *Table 20* the data from Proteome Discoverer, from investigations of trapping the epitope-containing peptide from αV, using Setup II with an analytical column, is found. In the table, the correlation score for the peptides that could be identified is given (for "other", these are different peptide chains that only could be detected once), the total score of the injection and the coverage obtained. It is also stated which AB monolith was used, and from what injection number the data is from.

Table 20: *The correlation scores for the four peptides identified from several injections (Inj) on different AB monoliths, the total score from the untargeted detection and the coverage obtained. Also, the average, standard deviation and relative standard deviation for the correlation scores for the peptides. "Other" are five different peptides that were only detected once each. Both were from the αV chain.*

AB monolith	Inj	Correlation score for peptides identified					Total score	Coverage (%)
		CQPIEFDATGNRDYAKDDPLEFK	SHQWFGASVR	ILACAPLYHWR	RALFLYSR	Others		
AB 2	6		2.3	3.4		1.3	9	5
	7	1.3	2.5	1.8	1.2	2.2	41	12
	8	2.1	2.3	1.0	1.7		40	8
AB 3	1	1.6	2.4	1.9			76	8
	2	1.8	2.1	1.7	1.6	1.2	14	9
	3	1.5	2.2	1.5	3.4	1.5	22	9
AB 4	1	1.0	2.3	3.1	1.9		26	7
AB 5	1		2.3	2.2		1.1	59	8
Average		1.5	2.3	2.1	2.0	1.5		
Standard deviation		0.4	0.1	0.8	0.9	0.4		
Relative standard deviation (%)		24	4	38	45	29		

7.9.3 Comparing β1 detection with and without the use of αV monolith

By comparing the obtained coverage from injections of 100 ng αVβ1 integrin standard with and without an αV AB monolithic column, the effect of the AB monolith can be visualized. In **Figure 53** two areas representing all the amino acids in the integrin β1 chain is shown. Here, the peptides identified by Proteome Discoverer from untargeted MS detection of integrin standard with an αV AB monolith and without such a monolith. This illustrates that β1 peptides were washed away from the αV AB monolith.
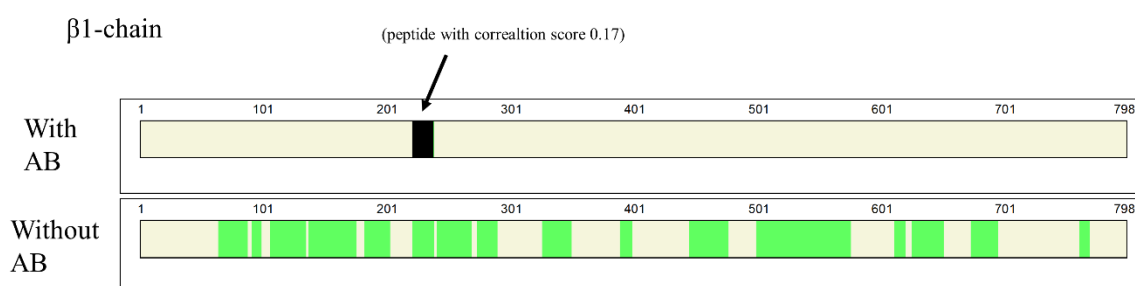
Figure 53: Comparison of peptides identified from β1 with and without an αV AB monolith. Peptides that are detected by Proteome Discoverer are shown in green. On the top shows an injection of 100 ng digested αVβ1 standard onto an online αV AB monolith (Setup II) with untargeted MS detection. The peptide that was considered detected by Proteome Discoverer only had a score of 0.17 and is marked in black, and only 1 fragment was found. The bottom shows the β1 peptides detected after an injection of 100 ng digested αVβ1 standard onto Setup I (no AB monolith) with untargeted MS detection.

The peptide that was considered detected by Proteome Discoverer when using the αV AB monolith only had a correlation score of 0.17 and only 1 fragment was found. So by it does not satisfy the requirements for identification in this study.

7.10 Targeted detection

7.10.1 Identified peptides from injections of 100 ng integrin standard

In *Table 21* the data from Proteome Discoverer, from targeted investigations of trapping the epitope-containing peptide from αV, using Setup II, is found. In the table, the correlation score for the peptides that could be identified is given, the total score of the injection and the coverage obtained. One AB monolith was used for all injections, and 100 ng digested integrin standard was injected.

Table 21: The correlation scores, from a PRM method, for the three peptides identified from several injections on one AB monolith, the total score from the untargeted detection and the coverage obtained. Also, the average, standard deviation and relative standard deviation for the correlation scores for the peptides.

	Correlation score for peptides identified			Total score	Coverage (%)
Injection	SHQWFGASVR	ILACAPLYHWR	RALFLYSR		
1	2.2	0.9		338	6.01
2	2.2	0.9	2.2	357	6.01
3	2.2	1.3	2.9	354	6.01
4	2.3			110	6.01
5	1.9			291	6.01
6	1.9			35	6.01
Average	2.1	1.0	2.6		
Standard deviation	0.2	0.2	0.7*		
Relative standard deviation (%)	8	19	27*		

* As there were only two peptides, the numbers stated are based on the difference found between the two correlation scores, not the standard deviation.

7.10.2 Correlation scores for injection of 50 ng integrin standard

Table 22 shows the obtained values for the correlation score of the peptide SHQWFGASVR from three injections of 50 ng digested integrin αVβ1 standard onto an αV AB monolith, using Setup II and targeted MS mode.

Table 22: *The correlation scores for SHQWFGASVR from three injections of 50 ng digested αVβ1 standard, on one αV AB monolithic column with Setup II and targeted analysis. Also the average, the standard deviation and relative standard deviation.*

	Injection			Average	Standard deviation	Relative standard deviation (%)
	1	2	3			
Score	1.9	1.4	1.4	1.5	0.3	18

7.10.3 Injection of 10 ng integrin standard

In *Figure 54* the TICC and EICs of peptide SHQWFGASVR is shown from injection of 10 ng digested αVβ1 standard on an αV AB monolith.
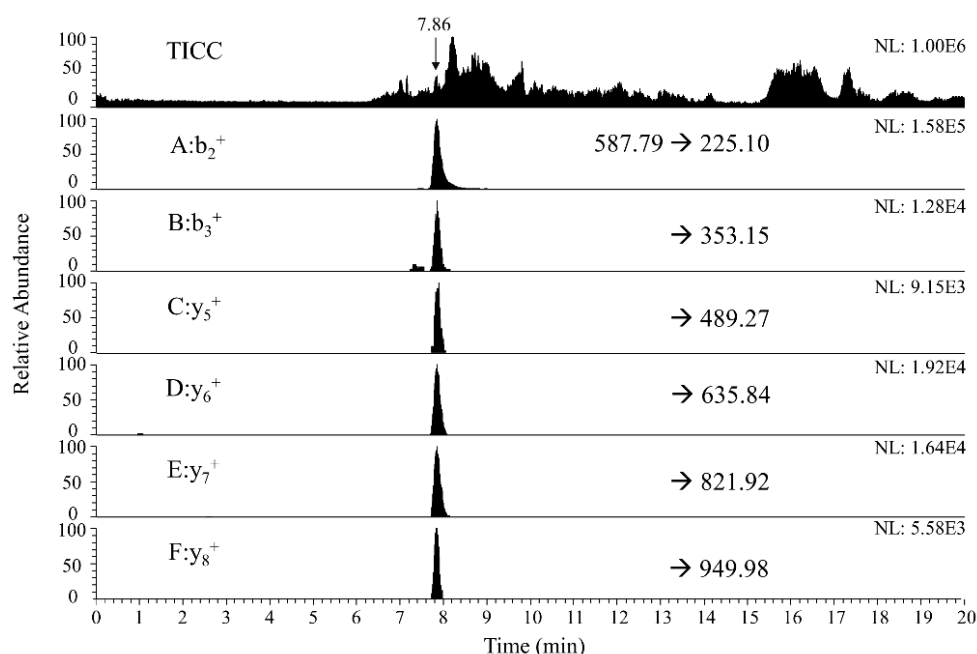
Figure 54: TICC (top) and EIC (A-F) of fragments from peptide SHQWFGASVR (m/z 587.79) identified using setup II with 100 ng standard injected. *Standard concentration was 10 ng μL^{-1} with 1 μL injection onto the online AB monolith, with 10 min flushing and a PRM method. The pre-column was 3 cm and the analytical column was 8 cm. The gradient is given in Table 2 (Gradient 2). The flow was 130 nL min^{-1}. Gaussian smoothing of 15 was applied. A is fragment b_2^+ (m/z 225.10), B is fragment b_3^+ (m/z 353.15), C is fragment y_5^+ (m/z 489.27), D is fragment y_6^+ (m/z 635.84), E is fragment y_7^+ (m/z 821.92), and F is fragment y_8^+ (m/z 949.98).*

7.11 Cell sample

7.11.1 Targeted mode

In *Table 23* the correlation scores obtained for the peptide SHQWFGASVR from 3 injection of digested GBM cells from injection onto an αV AB monolith is given. In *Figure 55* the fragments found from these injections are shown

Table 23. The correlation scores of SHQWFGASVR from three injections of digested GBM cells, onto an αV AB monolithic column with Setup II. Also the average, the standard deviation and relative standard deviation are given.

	Injection					
	1	2	3	Average	Standard deviation	Relative standard deviation (%)
Score	1.7	1.5	1.5	1.6	0.1	6
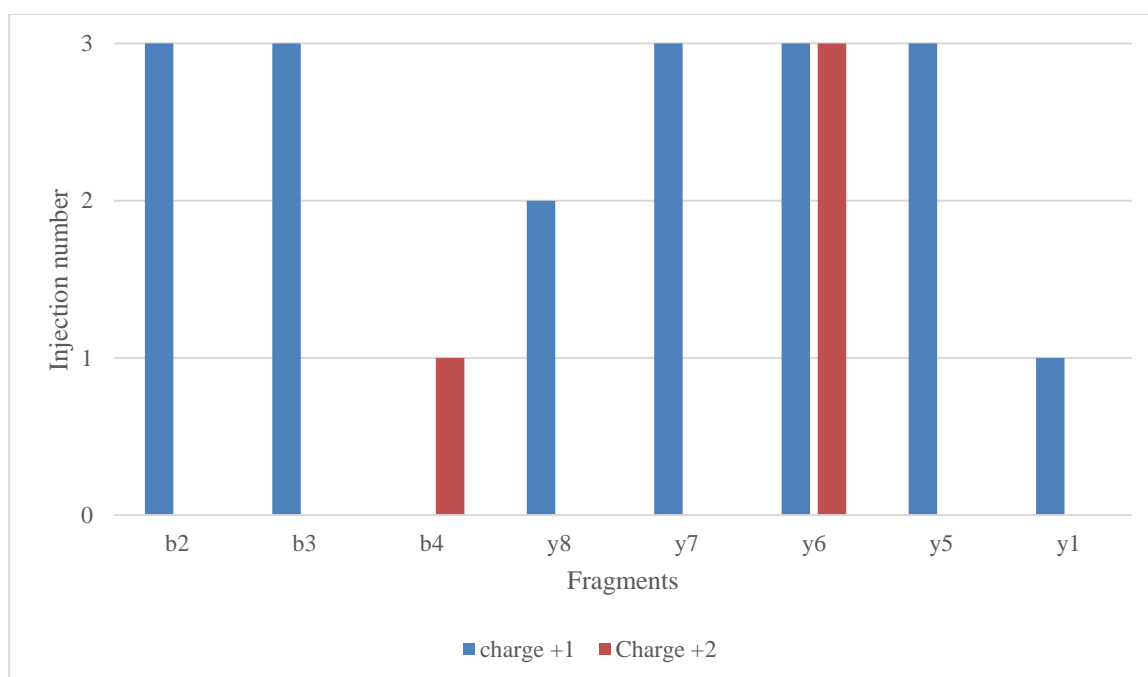
Figure 55: The fragments of SHQWFGASVR. Identified from three injections of 10 µL digested GBM cells with a total protein concentration of 1 µg µL^{-1} onto on αV AB monolith.

7.11.2 Untargeted mode

Proteins identified from digested GBM cells with a 5µL injection onto an αV AB monolith with a total protein concentration of 1 µg µL^{-1} and 10 min flushing is given in **Table 24**. In **Table 25** (p.107-114), the proteins identified from injection of 10 µL digested GBM cells injected onto an αV AB monolith with a total protein concentration of 1 µg µL^{-1} and 1 min flushing is given.

Table 24: *proteins found after a 5µL injection of GBM cells with a protein concentration of 1 µg µL^{-1} and 10 min flushing*

Description	Score	Coverage Factor	Number of proteins
Tubulin beta-4A chain OS=Homo sapiens GN=TUBB4A PE=1 SV=2 - [TBB4A_HUMAN]	13.20	11.49%	8
Elongation factor 1-alpha 1 OS=Homo sapiens GN=EEF1A1 PE=1 SV=1 - [EF1A1_HUMAN]	2.83	8.23%	4
Isoform 4 of Low molecular weight phosphotyrosine protein phosphatase OS=Homo sapiens GN=ACP1 - [PPAC_HUMAN]	2.05	8.93%	2
Peptidyl-prolyl cis-trans isomerase B OS=Homo sapiens GN=PPIB PE=1 SV=2 - [PPIB_HUMAN]	1.65	9.26%	6
Serine/threonine-protein phosphatase 2A 65 kDa regulatory subunit A alpha isoform OS=Homo sapiens GN=PPP2R1A PE=1 SV=4 - [2AAA_HUMAN]	0.00	1.36%	1
Actin, cytoplasmic 1 OS=Homo sapiens GN=ACTB PE=1 SV=1 - [ACTB_HUMAN]	0.00	17.07%	10
40S ribosomal protein S7 OS=Homo sapiens GN=RPS7 PE=1 SV=1 - [RS7_HUMAN]	0.00	4.12%	1
Sideroflexin-1 OS=Homo sapiens GN=SFXN1 PE=1 SV=4 - [SFXN1_HUMAN]	0.00	2.48%	1
Isoform C of Isocitrate dehydrogenase [NAD] subunit beta, mitochondrial OS=Homo sapiens GN=IDH3B - [IDH3B_HUMAN]	0.00	3.86%	3
Isoform 2 of Uroplakin-1a OS=Homo sapiens GN=UPK1A - [UPK1A_HUMAN]	0.00	2.20%	1
Isoform 3 of Alpha-1A adrenergic receptor OS=Homo sapiens GN=ADRA1A - [ADA1A_HUMAN]	0.00	1.40%	4
Isoform 2 of Cytoplasmic FMR1-interacting protein 1 OS=Homo sapiens GN=CYFIP1 - [CYFP1_HUMAN]	0.00	0.85%	4
Isoform 2 of Ephrin type-A receptor 7 OS=Homo sapiens GN=EPHA7 - [EPHA7_HUMAN]	0.00	4.63%	1

Table 25*: proteins found after a 10µL injection of digested GBM cells with a protein concentration of 1 µg µL^{-1} and 1 min flushing*

Description	Score	Coverage factor	Number of proteins
Tubulin beta-2B chain OS=Homo sapiens GN=TUBB2B PE=1 SV=1 - [TBB2B_HUMAN]	227.09	52.13%	4
Tubulin beta-2A chain OS=Homo sapiens GN=TUBB2A PE=1 SV=1 - [TBB2A_HUMAN]	214.86	52.13%	4
Tubulin beta-4B chain OS=Homo sapiens GN=TUBB4B PE=1 SV=1 - [TBB4B_HUMAN]	203.95	42.70%	4
Tubulin beta chain OS=Homo sapiens GN=TUBB PE=1 SV=2 - [TBB5_HUMAN]	203.59	52.25%	4
Actin, cytoplasmic 1 OS=Homo sapiens GN=ACTB PE=1 SV=1 - [ACTB_HUMAN]	128.47	50.13%	8
Isoform 2 of Glyceraldehyde-3-phosphate dehydrogenase OS=Homo sapiens GN=GAPDH - [G3P_HUMAN]	127.30	68.60%	2
Tubulin beta-3 chain OS=Homo sapiens GN=TUBB3 PE=1 SV=2 - [TBB3_HUMAN]	123.63	44.00%	3
Tubulin alpha-1C chain OS=Homo sapiens GN=TUBA1C PE=1 SV=1 - [TBA1C_HUMAN]	108.08	34.97%	10
Isoform 2 of Tubulin alpha-1A chain OS=Homo sapiens GN=TUBA1A - [TBA1A_HUMAN]	105.59	37.74%	7
Actin, alpha cardiac muscle 1 OS=Homo sapiens GN=ACTC1 PE=1 SV=1 - [ACTC_HUMAN]	83.63	28.38%	5
Elongation factor 1-alpha 1 OS=Homo sapiens GN=EEF1A1 PE=1 SV=1 - [EF1A1_HUMAN]	74.26	31.39%	4
Vimentin OS=Homo sapiens GN=VIM PE=1 SV=4 - [VIME_HUMAN]	73.89	40.13%	3
Alpha-enolase OS=Homo sapiens GN=ENO1 PE=1 SV=2 - [ENOA_HUMAN]	52.12	44.70%	4
Isoform 2 of Heat shock cognate 71 kDa protein OS=Homo sapiens GN=HSPA8 - [HSP7C_HUMAN]	47.81	34.08%	8
Isoform 3 of Nucleoside diphosphate kinase B OS=Homo sapiens GN=NME2 - [NDKB_HUMAN]	44.06	52.81%	5
60 kDa heat shock protein, mitochondrial OS=Homo sapiens GN=HSPD1 PE=1 SV=2 - [CH60_HUMAN]	41.15	19.72%	2
Heat shock protein HSP 90-alpha OS=Homo sapiens GN=HSP90AA1 PE=1 SV=5 - [HS90A_HUMAN]	36.86	18.72%	8
Creatine kinase B-type OS=Homo sapiens GN=CKB PE=1 SV=1 - [KCRB_HUMAN]	34.39	46.98%	1
Heat shock protein HSP 90-beta OS=Homo sapiens GN=HSP90AB1 PE=1 SV=4 - [HS90B_HUMAN]	34.35	20.58%	6
78 kDa glucose-regulated protein OS=Homo sapiens GN=HSPA5 PE=1 SV=2 - [GRP78_HUMAN]	31.87	15.75%	1
Annexin A5 OS=Homo sapiens GN=ANXA5 PE=1 SV=2 - [ANXA5_HUMAN]	27.71	26.88%	1
Isoform 2 of Triosephosphate isomerase OS=Homo sapiens GN=TPI1 - [TPIS_HUMAN]	26.07	36.14%	3
Peptidyl-prolyl cis-trans isomerase A OS=Homo sapiens GN=PPIA PE=1 SV=2 - [PPIA_HUMAN]	25.69	30.91%	2
ATP synthase subunit beta, mitochondrial OS=Homo sapiens GN=ATP5B PE=1 SV=3 - [ATPB_HUMAN]	24.40	19.66%	1
Isoform 3 of Protein disulfide-isomerase A6 OS=Homo sapiens GN=PDIA6 - [PDIA6_HUMAN]	23.94	31.81%	5
Malate dehydrogenase, mitochondrial OS=Homo sapiens GN=MDH2 PE=1 SV=3 - [MDHM_HUMAN]	23.01	28.70%	2

Protein disulfide-isomerase A3 OS=Homo sapiens GN=PDIA3 PE=1 SV=4 - [PDIA3_HUMAN]	21.83	20.59%	1
Nestin OS=Homo sapiens GN=NES PE=1 SV=2 - [NEST_HUMAN]	20.18	3.52%	1
Eukaryotic initiation factor 4A-I OS=Homo sapiens GN=EIF4A1 PE=1 SV=1 - [IF4A1_HUMAN]	19.94	17.49%	5
Isoform 2 of Phosphoglycerate kinase 1 OS=Homo sapiens GN=PGK1 - [PGK1_HUMAN]	19.68	17.99%	3
Histone H1.2 OS=Homo sapiens GN=HIST1H1C PE=1 SV=2 - [H12_HUMAN]	17.92	29.11%	5
Serum albumin OS=Homo sapiens GN=ALB PE=1 SV=2 - [ALBU_HUMAN]	17.47	4.93%	3
Isoform A2 of Heterogeneous nuclear ribonucleoproteins A2/B1 OS=Homo sapiens GN=HNRNPA2B1 - [ROA2_HUMAN]	17.42	34.60%	2
Isoform 3 of Heterogeneous nuclear ribonucleoprotein K OS=Homo sapiens GN=HNRNPK - [HNRPK_HUMAN]	16.60	18.64%	3
40S ribosomal protein SA OS=Homo sapiens GN=RPSA PE=1 SV=4 - [RSSA_HUMAN]	16.43	16.27%	1
Transitional endoplasmic reticulum ATPase OS=Homo sapiens GN=VCP PE=1 SV=4 - [TERA_HUMAN]	16.43	11.91%	3
Endoplasmin OS=Homo sapiens GN=HSP90B1 PE=1 SV=1 - [ENPL_HUMAN]	16.20	9.34%	1
Elongation factor 2 OS=Homo sapiens GN=EEF2 PE=1 SV=4 - [EF2_HUMAN]	16.18	13.05%	4
Neutral alpha-glucosidase AB OS=Homo sapiens GN=GANAB PE=1 SV=3 - [GANAB_HUMAN]	15.07	9.00%	2
14-3-3 protein zeta/delta OS=Homo sapiens GN=YWHAZ PE=1 SV=1 - [1433Z_HUMAN]	14.31	23.67%	11
Importin subunit beta-1 OS=Homo sapiens GN=KPNB1 PE=1 SV=2 - [IMB1_HUMAN]	14.27	6.96%	2
L-lactate dehydrogenase A chain OS=Homo sapiens GN=LDHA PE=1 SV=2 - [LDHA_HUMAN]	13.00	24.10%	5
Isoform 2 of Nucleosome assembly protein 1-like 1 OS=Homo sapiens GN=NAP1L1 - [NP1L1_HUMAN]	12.97	6.52%	3
Fructose-bisphosphate aldolase A OS=Homo sapiens GN=ALDOA PE=1 SV=2 - [ALDOA_HUMAN]	12.64	16.76%	2
Fatty acid-binding protein, brain OS=Homo sapiens GN=FABP7 PE=1 SV=3 - [FABP7_HUMAN]	12.11	23.48%	2
Protein disulfide-isomerase A4 OS=Homo sapiens GN=PDIA4 PE=1 SV=2 - [PDIA4_HUMAN]	12.07	8.37%	1
Polyubiquitin-C OS=Homo sapiens GN=UBC PE=1 SV=3 - [UBC_HUMAN]	11.84	60.44%	4
Isoform 2 of Serine/arginine-rich splicing factor 3 OS=Homo sapiens GN=SRSF3 - [SRSF3_HUMAN]	11.46	15.32%	2
Isoform 2 of Aspartate aminotransferase, mitochondrial OS=Homo sapiens GN=GOT2 - [AATM_HUMAN]	11.45	12.66%	2
Isoform 2 of ATP synthase subunit alpha, mitochondrial OS=Homo sapiens GN=ATP5A1 - [ATPA_HUMAN]	11.23	17.50%	3
Phosphoglycerate mutase 2 OS=Homo sapiens GN=PGAM2 PE=1 SV=3 - [PGAM2_HUMAN]	10.91	16.21%	3
Histone H2A type 1-H OS=Homo sapiens GN=HIST1H2AH PE=1 SV=3 - [H2A1H_HUMAN]	10.79	21.88%	18
Eukaryotic translation initiation factor 5A-2 OS=Homo sapiens GN=EIF5A2 PE=1 SV=3 - [IF5A2_HUMAN]	10.68	7.84%	4
Profilin-1 OS=Homo sapiens GN=PFN1 PE=1 SV=2 - [PROF1_HUMAN]	10.05	40.71%	1

Isoform 2 of Reticulon-4 OS=Homo sapiens GN=RTN4 - [RTN4_HUMAN]	9.62	16.62%	6
Cofilin-1 OS=Homo sapiens GN=CFL1 PE=1 SV=3 - [COF1_HUMAN]	9.57	42.17%	3
Poly(rC)-binding protein 1 OS=Homo sapiens GN=PCBP1 PE=1 SV=2 - [PCBP1_HUMAN]	9.32	7.58%	6
Citrate synthase, mitochondrial OS=Homo sapiens GN=CS PE=1 SV=2 - [CISY_HUMAN]	9.21	8.37%	1
Peroxiredoxin-1 OS=Homo sapiens GN=PRDX1 PE=1 SV=1 - [PRDX1_HUMAN]	8.94	21.61%	2
Non-histone chromosomal protein HMG-17 OS=Homo sapiens GN=HMGN2 PE=1 SV=3 - [HMGN2_HUMAN]	8.92	16.67%	1
Protein S100-B OS=Homo sapiens GN=S100B PE=1 SV=2 - [S100B_HUMAN]	8.57	16.30%	1
Isoform 2 of Glucose-6-phosphate isomerase OS=Homo sapiens GN=GPI - [G6PI_HUMAN]	8.43	10.90%	2
Isoform C of Prelamin-A/C OS=Homo sapiens GN=LMNA - [LMNA_HUMAN]	8.42	6.12%	6
10 kDa heat shock protein, mitochondrial OS=Homo sapiens GN=HSPE1 PE=1 SV=2 - [CH10_HUMAN]	8.24	38.24%	1
Isoform 2 of Heterogeneous nuclear ribonucleoprotein M OS=Homo sapiens GN=HNRNPM - [HNRPM_HUMAN]	8.24	6.22%	2
Isoform 4 of Septin-9 OS=Homo sapiens GN=SEPT9 - [SEPT9_HUMAN]	7.75	11.34%	8
Isocitrate dehydrogenase [NADP] cytoplasmic OS=Homo sapiens GN=IDH1 PE=1 SV=2 - [IDHC_HUMAN]	7.65	14.98%	1
Isoform 4 of Heterogeneous nuclear ribonucleoprotein D0 OS=Homo sapiens GN=HNRNPD - [HNRPD_HUMAN]	7.60	12.20%	4
Protein disulfide-isomerase OS=Homo sapiens GN=P4HB PE=1 SV=3 - [PDIA1_HUMAN]	7.46	14.96%	1
Leucine-rich repeat-containing protein 59 OS=Homo sapiens GN=LRRC59 PE=1 SV=1 - [LRC59_HUMAN]	7.36	13.03%	1
Histone H1.5 OS=Homo sapiens GN=HIST1H1B PE=1 SV=3 - [H15_HUMAN]	7.31	20.80%	1
Rab GDP dissociation inhibitor beta OS=Homo sapiens GN=GDI2 PE=1 SV=2 - [GDIB_HUMAN]	7.31	6.52%	3
Isoform 2 of Heterogeneous nuclear ribonucleoprotein A1 OS=Homo sapiens GN=HNRNPA1 - [ROA1_HUMAN]	7.31	28.46%	3
Isoform 4 of Heterogeneous nuclear ribonucleoproteins C1/C2 OS=Homo sapiens GN=HNRNPC - [HNRPC_HUMAN]	7.09	12.40%	7
Polyadenylate-binding protein 3 OS=Homo sapiens GN=PABPC3 PE=1 SV=2 - [PABP3_HUMAN]	7.03	7.61%	6
Small nuclear ribonucleoprotein E OS=Homo sapiens GN=SNRPE PE=1 SV=1 - [RUXE_HUMAN]	7.03	11.96%	1
Isoform 3 of Elongation factor 1-delta OS=Homo sapiens GN=EEF1D - [EF1D_HUMAN]	7.02	14.79%	4
Glutathione S-transferase P OS=Homo sapiens GN=GSTP1 PE=1 SV=2 - [GSTP1_HUMAN]	6.88	9.52%	1
Interleukin enhancer-binding factor 2 OS=Homo sapiens GN=ILF2 PE=1 SV=2 - [ILF2_HUMAN]	6.72	7.44%	1
Isoform 4 of Catenin alpha-2 OS=Homo sapiens GN=CTNNA2 - [CTNA2_HUMAN]	6.66	3.91%	6
Peptidyl-prolyl cis-trans isomerase B OS=Homo sapiens GN=PPIB PE=1 SV=2 - [PPIB_HUMAN]	6.59	18.98%	1
KH domain-containing, RNA-binding, signal transduction-associated protein 1 OS=Homo sapiens GN=KHDRBS1 PE=1 SV=1 - [KHDR1_HUMAN]	6.53	13.77%	3

Polypyrimidine tract-binding protein 1 OS=Homo sapiens GN=PTBP1 PE=1 SV=1 - [PTBP1_HUMAN]	6.50	11.68%	3
Aldose reductase OS=Homo sapiens GN=AKR1B1 PE=1 SV=3 - [ALDR_HUMAN]	6.44	3.16%	2
Isoform 2 of X-ray repair cross-complementing protein 6 OS=Homo sapiens GN=XRCC6 - [XRCC6_HUMAN]	6.43	9.86%	2
Microtubule-associated protein RP/EB family member 1 OS=Homo sapiens GN=MAPRE1 PE=1 SV=3 - [MARE1_HUMAN]	6.42	6.72%	1
Voltage-dependent anion-selective channel protein 1 OS=Homo sapiens GN=VDAC1 PE=1 SV=2 - [VDAC1_HUMAN]	6.41	10.60%	3
Stathmin OS=Homo sapiens GN=STMN1 PE=1 SV=3 - [STMN1_HUMAN]	5.97	9.40%	2
ADP/ATP translocase 2 OS=Homo sapiens GN=SLC25A5 PE=1 SV=7 - [ADT2_HUMAN]	5.92	15.77%	4
Spliceosome RNA helicase DDX39B OS=Homo sapiens GN=DDX39B PE=1 SV=1 - [DX39B_HUMAN]	5.86	3.74%	3
Isoform 6 of Poly(rC)-binding protein 2 OS=Homo sapiens GN=PCBP2 - [PCBP2_HUMAN]	5.84	13.85%	13
Isoform 3 of Sorcin OS=Homo sapiens GN=SRI - [SORCN_HUMAN]	5.81	11.11%	3
Prohibitin-2 OS=Homo sapiens GN=PHB2 PE=1 SV=2 - [PHB2_HUMAN]	5.74	18.39%	2
Isoform 3 of Alpha-actinin-4 OS=Homo sapiens GN=ACTN4 - [ACTN4_HUMAN]	5.67	2.30%	7
60S acidic ribosomal protein P2 OS=Homo sapiens GN=RPLP2 PE=1 SV=1 - [RLA2_HUMAN]	5.66	16.52%	1
Peroxiredoxin-2 OS=Homo sapiens GN=PRDX2 PE=1 SV=5 - [PRDX2_HUMAN]	5.60	18.69%	1
Isoform 2 of Ubiquitin-like modifier-activating enzyme 1 OS=Homo sapiens GN=UBA1 - [UBA1_HUMAN]	5.58	2.46%	2
Ezrin OS=Homo sapiens GN=EZR PE=1 SV=4 - [EZRI_HUMAN]	5.56	8.36%	5
Isoform 3 of Microtubule-associated protein 2 OS=Homo sapiens GN=MAP2 - [MTAP2_HUMAN]	5.52	3.13%	4
Cytochrome c OS=Homo sapiens GN=CYCS PE=1 SV=2 - [CYC_HUMAN]	5.50	31.43%	1
Eukaryotic translation initiation factor 4H OS=Homo sapiens GN=EIF4H PE=1 SV=5 - [IF4H_HUMAN]	5.46	14.92%	2
6-phosphogluconolactonase OS=Homo sapiens GN=PGLS PE=1 SV=2 - [6PGL_HUMAN]	5.21	10.47%	1
Mucin-16 OS=Homo sapiens GN=MUC16 PE=1 SV=3 - [MUC16_HUMAN]	5.15	0.30%	1
Isoform 2 of Septin-7 OS=Homo sapiens GN=SEPT7 - [SEPT7_HUMAN]	5.13	11.24%	2
60S ribosomal protein L10 OS=Homo sapiens GN=RPL10 PE=1 SV=4 - [RL10_HUMAN]	5.04	10.75%	2
Far upstream element-binding protein 2 OS=Homo sapiens GN=KHSRP PE=1 SV=4 - [FUBP2_HUMAN]	5.04	4.36%	1
Isoform Short of Splicing factor, proline- and glutamine-rich OS=Homo sapiens GN=SFPQ - [SFPQ_HUMAN]	5.02	10.31%	2
Ras-related C3 botulinum toxin substrate 1 OS=Homo sapiens GN=RAC1 PE=1 SV=1 - [RAC1_HUMAN]	4.99	13.02%	2
High mobility group protein B1 OS=Homo sapiens GN=HMGB1 PE=1 SV=3 - [HMGB1_HUMAN]	4.91	13.95%	2
Stress-70 protein, mitochondrial OS=Homo sapiens GN=HSPA9 PE=1 SV=2 - [GRP75_HUMAN]	4.79	7.36%	1

110

Isoform 3 of Obg-like ATPase 1 OS=Homo sapiens GN=OLA1 - [OLA1_HUMAN]	4.60	9.35%	2
Zyxin OS=Homo sapiens GN=ZYX PE=1 SV=1 - [ZYX_HUMAN]	4.58	4.37%	2
40S ribosomal protein S13 OS=Homo sapiens GN=RPS13 PE=1 SV=2 - [RS13_HUMAN]	4.53	17.88%	1
Isoform 2 of FERM domain-containing protein 6 OS=Homo sapiens GN=FRMD6 - [FRMD6_HUMAN]	4.48	2.28%	2
Importin-5 OS=Homo sapiens GN=IPO5 PE=1 SV=4 - [IPO5_HUMAN]	4.46	2.64%	4
Isoform 3 of Serine/arginine-rich splicing factor 7 OS=Homo sapiens GN=SRSF7 - [SRSF7_HUMAN]	4.42	15.15%	4
Endoplasmic reticulum resident protein 29 OS=Homo sapiens GN=ERP29 PE=1 SV=4 - [ERP29_HUMAN]	4.39	3.83%	1
Platelet-activating factor acetylhydrolase IB subunit gamma OS=Homo sapiens GN=PAFAH1B3 PE=1 SV=1 - [PA1B3_HUMAN]	4.37	3.90%	1
Isoform 2 of Probable ATP-dependent RNA helicase DDX5 OS=Homo sapiens GN=DDX5 - [DDX5_HUMAN]	4.36	6.73 %	6
Fascin OS=Homo sapiens GN=FSCN1 PE=1 SV=3 - [FSCN1_HUMAN]	4.31	6.69%	1
Epidermal growth factor receptor kinase substrate 8-like protein 2 OS=Homo sapiens GN=EPS8L2 PE=1 SV=2 - [ES8L2_HUMAN]	4.19	2.52%	2
Isoform 2 of Cytosol aminopeptidase OS=Homo sapiens GN=LAP3 - [AMPL_HUMAN]	4.18	2.46%	2
Peroxiredoxin-6 OS=Homo sapiens GN=PRDX6 PE=1 SV=3 - [PRDX6_HUMAN]	4.17	9.38%	1
Platelet-activating factor acetylhydrolase IB subunit beta OS=Homo sapiens GN=PAFAH1B2 PE=1 SV=1 - [PA1B2_HUMAN]	4.16	3.93%	1
60S acidic ribosomal protein P1 OS=Homo sapiens GN=RPLP1 PE=1 SV=1 - [RLA1_HUMAN]	4.11	14.04%	1
3-hydroxyisobutyrate dehydrogenase, mitochondrial OS=Homo sapiens GN=HIBADH PE=1 SV=2 - [3HIDH_HUMAN]	3.99	4.17%	1
Lysosomal Pro-X carboxypeptidase OS=Homo sapiens GN=PRCP PE=1 SV=1 - [PCP_HUMAN]	3.95	3.83%	2
40S ribosomal protein S10 OS=Homo sapiens GN=RPS10 PE=1 SV=1 - [RS10_HUMAN]	3.93	5.45%	1
40S ribosomal protein S14 OS=Homo sapiens GN=RPS14 PE=1 SV=3 - [RS14_HUMAN]	3.85	8.61%	1
Protein DJ-1 OS=Homo sapiens GN=PARK7 PE=1 SV=2 - [PARK7_HUMAN]	3.71	3.70%	1
ATP synthase subunit O, mitochondrial OS=Homo sapiens GN=ATP5O PE=1 SV=1 - [ATPO_HUMAN]	3.69	11.74%	1
Isoform 6 of Ubiquitin-conjugating enzyme E2 variant 1 OS=Homo sapiens GN=UBE2V1 - [UB2V1_HUMAN]	3.67	9.52%	6
Proteasome subunit alpha type-2 OS=Homo sapiens GN=PSMA2 PE=1 SV=2 - [PSA2_HUMAN]	3.62	9.40%	1
60S ribosomal protein L23 OS=Homo sapiens GN=RPL23 PE=1 SV=1 - [RL23_HUMAN]	3.50	24.29%	1
Elongation factor 1-gamma OS=Homo sapiens GN=EEF1G PE=1 SV=3 - [EF1G_HUMAN]	3.49	16.48%	2
T-complex protein 1 subunit gamma OS=Homo sapiens GN=CCT3 PE=1 SV=4 - [TCPG_HUMAN]	3.36	9.17%	2
Isoform 3 of Protein quaking OS=Homo sapiens GN=QKI - [QKI_HUMAN]	3.36	5.05%	6

Isoform 4 of Perilipin-3 OS=Homo sapiens GN=PLIN3 - [PLIN3_HUMAN]	3.33	4.74%	3
Histone H2B type 1-K OS=Homo sapiens GN=HIST1H2BK PE=1 SV=3 - [H2B1K_HUMAN]	3.30	19.05%	15
Microtubule-associated protein 1B OS=Homo sapiens GN=MAP1B PE=1 SV=2 - [MAP1B_HUMAN]	3.27	0.57%	1
Galectin-3 OS=Homo sapiens GN=LGALS3 PE=1 SV=5 - [LEG3_HUMAN]	3.23	11.20%	1
Sodium/potassium-transporting ATPase subunit beta-3 OS=Homo sapiens GN=ATP1B3 PE=1 SV=1 - [AT1B3_HUMAN]	3.17	8.96%	1
tRNA-splicing endonuclease subunit Sen54 OS=Homo sapiens GN=TSEN54 PE=1 SV=3 - [SEN54_HUMAN]	3.17	8.75%	1
Histone H1x OS=Homo sapiens GN=H1FX PE=1 SV=1 - [H1X_HUMAN]	3.15	12.68%	1
Isoform 4 of Microtubule-associated protein 4 OS=Homo sapiens GN=MAP4 - [MAP4_HUMAN]	3.04	5.28%	5
Isoform 2 of Dihydropyrimidinase-related protein 2 OS=Homo sapiens GN=DPYSL2 - [DPYL2_HUMAN]	3.03	7.65%	2
Isoform 2 of Nuclear autoantigenic sperm protein OS=Homo sapiens GN=NASP - [NASP_HUMAN]	3.00	5.12%	3
Matrin-3 OS=Homo sapiens GN=MATR3 PE=1 SV=2 - [MATR3_HUMAN]	2.96	4.49%	2
Poly [ADP-ribose] polymerase 1 OS=Homo sapiens GN=PARP1 PE=1 SV=4 - [PARP1_HUMAN]	2.89	1.87%	1
Ras GTPase-activating protein-binding protein 1 OS=Homo sapiens GN=G3BP1 PE=1 SV=1 - [G3BP1_HUMAN]	2.86	11.16%	1
Isoform 2 of Eukaryotic translation initiation factor 4B OS=Homo sapiens GN=EIF4B - [IF4B_HUMAN]	2.84	2.80%	2
Acetyl-CoA acetyltransferase, cytosolic OS=Homo sapiens GN=ACAT2 PE=1 SV=2 - [THIC_HUMAN]	2.82	7.81%	2
Isoform 3 of Serine hydroxymethyltransferase, mitochondrial OS=Homo sapiens GN=SHMT2 - [GLYM_HUMAN]	2.82	3.73%	3
Isoform 3 of Spectrin alpha chain, non-erythrocytic 1 OS=Homo sapiens GN=SPTAN1 - [SPTN1_HUMAN]	2.80	1.10%	3
Isoform 2 of Translationally-controlled tumor protein OS=Homo sapiens GN=TPT1 - [TCTP_HUMAN]	2.80	14.49%	3
Transgelin-2 OS=Homo sapiens GN=TAGLN2 PE=1 SV=3 - [TAGL2_HUMAN]	2.77	11.06%	2
Annexin A2 OS=Homo sapiens GN=ANXA2 PE=1 SV=2 - [ANXA2_HUMAN]	2.74	9.44%	3
Isoform 2 of Non-POU domain-containing octamer-binding protein OS=Homo sapiens GN=NONO - [NONO_HUMAN]	2.74	3.14%	2
C-1-tetrahydrofolate synthase, cytoplasmic OS=Homo sapiens GN=MTHFD1 PE=1 SV=3 - [C1TC_HUMAN]	2.69	1.18%	1
40S ribosomal protein S16 OS=Homo sapiens GN=RPS16 PE=1 SV=2 - [RS16_HUMAN]	2.68	14.38%	1
Non-histone chromosomal protein HMG-14 OS=Homo sapiens GN=HMGN1 PE=1 SV=3 - [HMGN1_HUMAN]	2.68	14.00%	1
40S ribosomal protein S5 OS=Homo sapiens GN=RPS5 PE=1 SV=4 - [RS5_HUMAN]	2.68	4.90%	1
Lamina-associated polypeptide 2, isoform alpha OS=Homo sapiens GN=TMPO PE=1 SV=2 - [LAP2A_HUMAN]	2.67	3.03%	4
Isoform 2 of Glucosidase 2 subunit beta OS=Homo sapiens GN=PRKCSH - [GLU2B_HUMAN]	2.63	4.95%	2

Isoform 4 of ATP synthase subunit f, mitochondrial OS=Homo sapiens GN=ATP5J2 - [ATPK_HUMAN]	2.62	22.45%	4
Isoform 2 of Alpha-aminoadipic semialdehyde dehydrogenase OS=Homo sapiens GN=ALDH7A1 - [AL7A1_HUMAN]	2.54	3.33%	2
Isoform 2 of Acidic leucine-rich nuclear phosphoprotein 32 family member B OS=Homo sapiens GN=ANP32B - [AN32B_HUMAN]	2.53	20.00%	3
Isoform B of Endothelin B receptor OS=Homo sapiens GN=EDNRB - [EDNRB_HUMAN]	2.53	6.42%	3
Isoform 2 of Cytosolic non-specific dipeptidase OS=Homo sapiens GN=CNDP2 - [CNDP2_HUMAN]	2.52	3.58%	2
Tubulin-specific chaperone A OS=Homo sapiens GN=TBCA PE=1 SV=3 - [TBCA_HUMAN]	2.48	10.19%	2
Membrane-associated progesterone receptor component 1 OS=Homo sapiens GN=PGRMC1 PE=1 SV=3 - [PGRC1_HUMAN]	2.48	7.69%	1
Isoform 2 of High mobility group nucleosome-binding domain-containing protein 3 OS=Homo sapiens GN=HMGN3 - [HMGN3_HUMAN]	2.46	19.48%	2
Isoform 2 of DmX-like protein 2 OS=Homo sapiens GN=DMXL2 - [DMXL2_HUMAN]	2.44	1.21%	3
Isoform 2 of 26S protease regulatory subunit 6B OS=Homo sapiens GN=PSMC4 - [PRS6B_HUMAN]	2.42	10.59%	2
Isoform 2 of RNA-binding motif protein, Y chromosome, family 1 member D OS=Homo sapiens GN=RBMY1D - [RBY1D_HUMAN]	2.42	4.36%	4
Ras-related protein Rab-7a OS=Homo sapiens GN=RAB7A PE=1 SV=1 - [RAB7A_HUMAN]	2.41	4.83%	1
Isoform Alpha-1B-2 of Voltage-dependent N-type calcium channel subunit alpha-1B OS=Homo sapiens GN=CACNA1B - [CAC1B_HUMAN]	2.41	1.21%	2
Isoform 2 of Lysosome-associated membrane glycoprotein 1 OS=Homo sapiens GN=LAMP1 - [LAMP1_HUMAN]	2.41	5.22%	2
Isoform 2 of Heterogeneous nuclear ribonucleoprotein L OS=Homo sapiens GN=HNRNPL - [HNRPL_HUMAN]	2.40	3.07%	2
Aflatoxin B1 aldehyde reductase member 4 OS=Homo sapiens GN=AKR7L PE=2 SV=6 - [ARK74_HUMAN]	2.38	4.53%	2
Isoform 2 of 60S acidic ribosomal protein P0 OS=Homo sapiens GN=RPLP0 - [RLA0_HUMAN]	2.37	7.06%	3
T-complex protein 1 subunit theta OS=Homo sapiens GN=CCT8 PE=1 SV=4 - [TCPQ_HUMAN]	2.36	3.65%	3
Isoform 5 of Methionine adenosyltransferase 2 subunit beta OS=Homo sapiens GN=MAT2B - [MAT2B_HUMAN]	2.33	14.46%	5
40S ribosomal protein S3 OS=Homo sapiens GN=RPS3 PE=1 SV=2 - [RS3_HUMAN]	2.33	5.76%	2
40S ribosomal protein S9 OS=Homo sapiens GN=RPS9 PE=1 SV=3 - [RS9_HUMAN]	2.33	6.19%	1
Isoform 2 of 3-hydroxyacyl-CoA dehydrogenase type-2 OS=Homo sapiens GN=HSD17B10 - [HCD2_HUMAN]	2.31	4.76%	2
Isoform 7 of Calcium/calmodulin-dependent protein kinase type II subunit beta OS=Homo sapiens GN=CAMK2B - [KCC2B_HUMAN]	2.28	2.45%	20
SH3 domain-binding glutamic acid-rich-like protein 3 OS=Homo sapiens GN=SH3BGRL3 PE=1 SV=1 - [SH3L3_HUMAN]	2.24	10.75%	1
Serine/threonine-protein phosphatase 2A 65 kDa regulatory subunit A alpha isoform OS=Homo sapiens GN=PPP2R1A PE=1 SV=4 - [2AAA_HUMAN]	2.23	4.07%	1

Isoform 2 of 4F2 cell-surface antigen heavy chain OS=Homo sapiens GN=SLC3A2 - [4F2_HUMAN]	2.23	6.62%	4
Isoform 2 of Ubiquitin-conjugating enzyme E2 D2 OS=Homo sapiens GN=UBE2D2 - [UB2D2_HUMAN]	2.22	9.32%	5
Spermine synthase OS=Homo sapiens GN=SMS PE=1 SV=2 - [SPSY_HUMAN]	2.19	4.92%	1
Isoform 2 of Sulfatase-modifying factor 2 OS=Homo sapiens GN=SUMF2 - [SUMF2_HUMAN]	2.18	4.69%	3
Isoform 2 of Acetyl-CoA acetyltransferase, mitochondrial OS=Homo sapiens GN=ACAT1 - [THIL_HUMAN]	2.15	10.49%	2
Splicing factor 3B subunit 2 OS=Homo sapiens GN=SF3B2 PE=1 SV=2 - [SF3B2_HUMAN]	2.15	1.23%	1
Proteasome subunit alpha type-1 OS=Homo sapiens GN=PSMA1 PE=1 SV=1 - [PSA1_HUMAN]	2.13	7.22%	2
Heterogeneous nuclear ribonucleoprotein H OS=Homo sapiens GN=HNRNPH1 PE=1 SV=4 - [HNRH1_HUMAN]	2.06	9.13%	2
Peptidyl-prolyl cis-trans isomerase FKBP4 OS=Homo sapiens GN=FKBP4 PE=1 SV=3 - [FKBP4_HUMAN]	2.06	1.96%	1
Lysosome-associated membrane glycoprotein 2 OS=Homo sapiens GN=LAMP2 PE=1 SV=2 - [LAMP2_HUMAN]	2.04	1.95%	3
Isoform 3 of Putative RNA-binding protein Luc7-like 2 OS=Homo sapiens GN=LUC7L2 - [LC7L2_HUMAN]	2.04	2.31%	4
Isoform 3 of Basigin OS=Homo sapiens GN=BSG - [BASI_HUMAN]	2.01	5.11%	4
Isoform ASF-3 of Serine/arginine-rich splicing factor 1 OS=Homo sapiens GN=SRSF1 - [SRSF1_HUMAN]	1.98	3.48%	4
Fibronectin type III and SPRY domain-containing protein 1 OS=Homo sapiens GN=FSD1 PE=1 SV=1 - [FSD1_HUMAN]	1.98	3.43%	1
Actin-related protein 2/3 complex subunit 3 OS=Homo sapiens GN=ARPC3 PE=1 SV=3 - [ARPC3_HUMAN]	1.98	9.55%	1
Neuron-specific calcium-binding protein hippocalcin OS=Homo sapiens GN=HPCA PE=1 SV=2 - [HPCA_HUMAN]	1.97	5.18%	1
Isoform 4 of Histone-binding protein RBBP4 OS=Homo sapiens GN=RBBP4 - [RBBP4_HUMAN]	1.96	4.10%	6
Histone H3.3C OS=Homo sapiens GN=H3F3C PE=1 SV=3 - [H3C_HUMAN]	1.96	11.11%	5
60S ribosomal protein L4 OS=Homo sapiens GN=RPL4 PE=1 SV=5 - [RL4_HUMAN]	0.00	3.75%	1
Isoform 2 of Ubiquitin carboxyl-terminal hydrolase 15 OS=Homo sapiens GN=USP15 - [UBP15_HUMAN]	0.00	1.05%	3
Isoform 2 of Dynein heavy chain 17, axonemal OS=Homo sapiens GN=DNAH17 - [DYH17_HUMAN]	0.00	0.72%	3